University of Dundee

Nonlinear Wave Interaction with a Floating Fish Cage in Two-Dimensions

A thesis submitted in partial fulfilment of the requirements for
the MSc degree in
Marine Hydrodynamics and Ocean Engineering
School of Science and Engineering

Student - Angus Nicoll
Supervisor – Dr Masoud Hayatdavoodi

August 2020

Contents

List of Figures

List of Tables

Abstract

Due to the needs and demands placed on the aquaculture sector, an interest is being taken in more energetic, deeper water sites. This comes with both benefits and challenges that the industry must address particularly in the design and deployment of fish cages as fish farms, and the wave forces they can survive. The interaction of a cage with nonlinear waves is explored in two dimensions through computational fluid dynamics. Analysis is undertaken of 5 different waves of varying height and period interacting with a single cage restricted in various levels of movement. The motions, forces, pressure and velocity fields are reviewed and their pertinence to the fish-farming industry explained. This gives particular insight into the design challenges around aquaculture as well as interesting responses related to the motion restriction of the cage and the potential benefits of multi-cage deployment.

Introduction

Due to the reduction of wild fish stock, greater limits or quotas in place due to overfishing, and an increasing population, the huge demand for seafood (100 Million Tons/year (Anderson Coldebella, 2017)) continues to rise as found by Asche (2015). With such a demand, and reduced natural stock, increasing focus is being given to Marine Aquaculture.

The aquaculture industry is influenced, and constrained by the waves, current, and associated forces at play within the marine environment which affect the motions, lifespan and safety of the fish cages as well as the fish being farmed.
This project seeks to understand the challenges which the fish farming industry faces, and the direction that fin fish aquaculture may take in the future. A focus will be made around the current level of research regarding the motions of the cages and the method of analysis used both around fish cages, and other floating structures. This will be achieved through comprehensive review of literature to develop an understanding of the gaps in research surrounding marine aquaculture, in particular the Fin Fish Farming industry. Interest will also be taken into the tools and further research and tools could undertake done to improve design and understanding of fish cages and their motions.

Classically, fish farm cages are located near shore, in calmer waters, with easy and quick access to infrastructure (boats/harbours/feed deliveries). These sheltered waters are excellent for the safety of the cage, where wave height and current strength are minimal, so forces on the cage are also relatively small. However, without such water activity, there is a risk of "self pollution" (Lumb(1989)) where the accommodating waters, and bed beneath the cage, are of a lower, polluted, quality reducing farm yield according to E. Mantzavrakosa (2007).
There is a widely accepted argument being made with in industry for fish farming to be moved offshore. This is for reasons such as;

- Sediment (i.e uneaten food, faecal matter, undigested medication etc) is dispersed throughout the water body more effectively under strong current (L.D. Wright, 2001)
- Reduced disease/pests – due to the increased current flow the health of the fish increase because of the fresh, oxygenated water filling the cage. The lower temperatures discourage sea lice. This has been trailed as a possible lice-removal treatment (Kathy Overton, 2019)
- Due to the improved water quality and sediment dispersion, fish can be kept in greater numbers per cage, with cages closer together without harm to their health.

As with all industry decisions there are compromises and challenges associated with relocating fish farms offshore away from sheltered water. Namely the motions caused by the increase wave height and current strength.
Waves, in particular extreme waves, can cause fatigue and damage to any floating offshore structure, as a result of airgaps, green water, or the structure slamming (the most likely for fish cages). Large motions of the cage are also undesirable and detrimental for the fish.
Similarly for increased current speed, it was shown by Yun-Peng Zhao et al. (2019) that fatigue and damage can be caused to the floating structure, particularly at the mooring attachment points of the fish cage, and in the mooring lines themselves. These motions can cause the fish to crowd, especially when the cage volume decreases (known as deforming). which may result in a rapid decrease of available dissolved oxygen due to consumption, causing fish mortality (Yun-Peng Zhao et al.(2007)).
Therefore, understanding the wave interaction with floating fish cages is important for the development of the industry – as future successful farms depend on viable and secure cages which are suitable for the offshore environment which would increase their yield.

Chapter 1
Literature Review

This chapter reviews the current state of literature surrounding the problems the aquaculture sector faces in regards to fish cage deployment. Such as the increased current velocities, wave heights, and generally more energetic environments. This is all undertaken in the pursuit of cleaner, cooler, faster water in which a greater farmed yield can be had. Within this chapter multiple means of cage assessment are explored followed by the definition of the project objectives once suitable gaps have been identified.

1. Literature Review

To date, many researchers have investigated fish cages under waves and current to understand the motions and inform design choices. This is usually in pursuit of the same thing, improving the current understanding of aquaculture cages, and how they can be better deployed to harness the benefits of cleaner, colder, faster water whilst mitigating the risks. Useful insight can be found in the current works as to the basics of the problem at hand, namely the forces acting on the cage, how to design something structurally sound enough to survive the environment, but which does not react to the waves in such a way that may harm the fish.

1.1. Experiments and Computations

In review of the literature it is clear there are many approaches to the problem of understanding fish cages as they move further offshore – though these can be split into two main categories. Experimental Testing within a physical wave tank, and Numerical Computations. Where experimental testing consists of a model cage set within a wave tank, actuated by a wave maker. This allows for "real-world" observation of the cage's response to waves (usually at scale) and is ordinarily measured via image processing. Numerical Computations involves a broad use of methods in determining the motions of a fish cage. This includes empirical relations, wave theories, and pressure equations. These computational and experimental methods are explored through literature, below.

1.1.1. Experiments

Lee et Al(2008), whilst performing a dynamic simulation of a fish cage system were particularly interested in the effects of waves and current on the tension of mooring lines, and deformation of the cage. The authors looked at this under wave and current conditions to help inform design choices.

The wave tank set up (Figure 1) shows that a motion capture camera was used, with a wave height meter behind it, this was to determine the motion of the cage's floater and sinker. Loadcells were also used in the experiment to determine mooring line tension, both of these topics are subjects of interest to the industry.

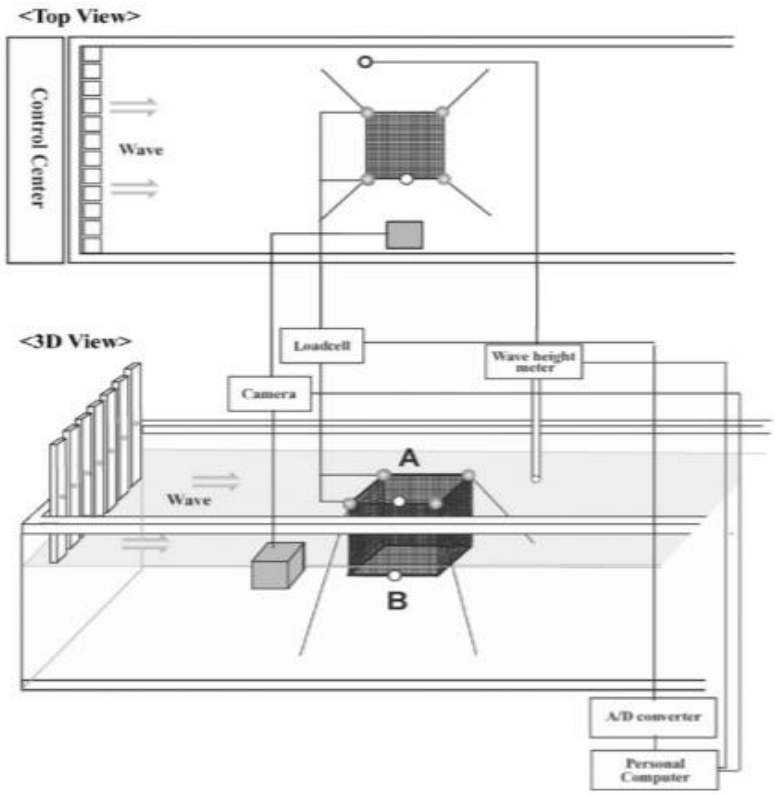

Figure 1 - Wave tank experiment set up. (Chun-Woo Lee, 2008)

The authors tested this cage under two wave conditions. Wave condition (a) – Period of 2.4s and a height of 0.1m, and wave condition (b) Period of 2.4s and a wave height of 0.3m.
As can be expected, the tension in the mooring line was at maximum just as the wave reached the windward side of the cage, i.e. when the cage was lifted to maximum height by the wave. This tension quickly reduced as the wave passed the cage, allowing the floater to drop closer to the bed, relaxing the mooring lines (Figure 2). This relaxation occurs in 1.2 seconds, i.e half a wavelength.

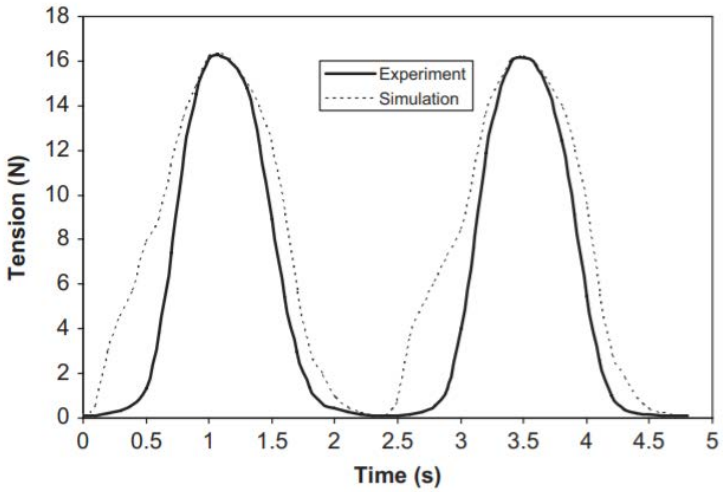

Figure 2 - Mooring line tensions - Wave condition (b) (Chun-Woo Lee, 2008)

This experiment utilised simple linear theory to generate the waves, which is in line with the experimental shape shown above. The above Figure 2 also shows that the mathematical model's

predictions of mooring line tension may require review. Particularly as the wave approaches the cage. This may be due to an over prediction in the steepness of the wave in front of the wave peak and so the expected rise in the floater of the cage is also exaggerated.
The authors review of the cage's motions, however, were more aligned to the experimental data. As shown in Figure 3, the float and sinker followed the peak and trough of the incoming wave as could be expected. In both wave conditions, the float and sinker rise and fall in line with the associated wave heights along with the 2.4second period.

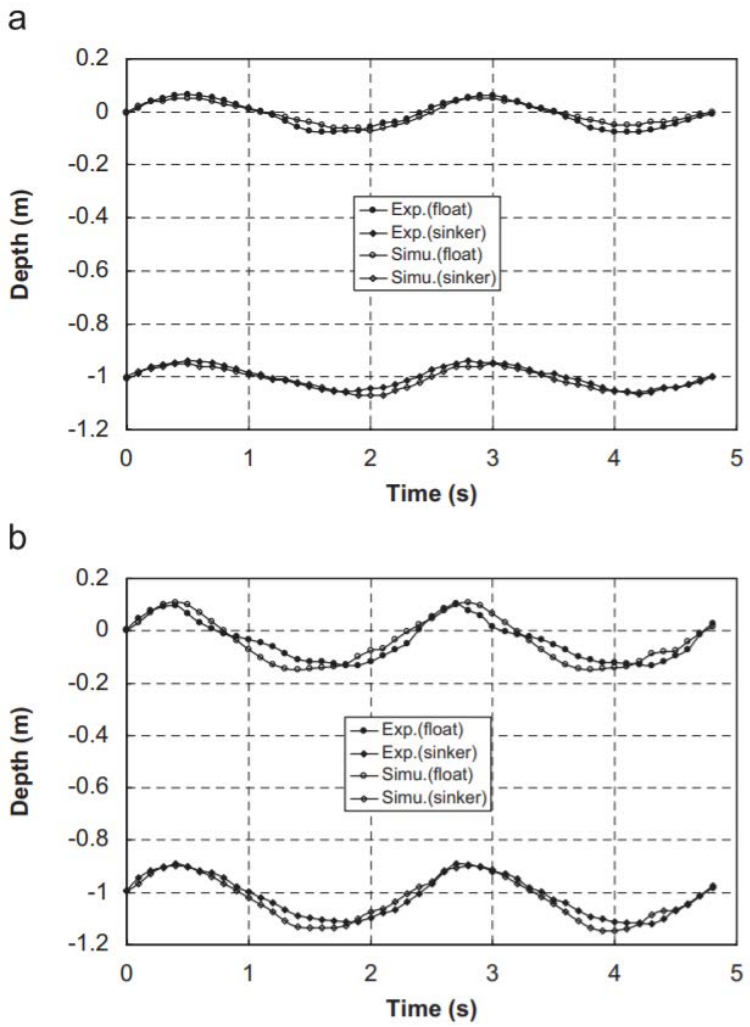

Figure 3 - Floater and Sinker Motion under (a) and (b) (Chun-Woo Lee, 2008)

However, if we re-inspect Figure 1, it becomes obvious that the above data only indicates heave motion. This is because the points used to determine float/sinker depth are placed halfway along the length of the square cage. A position which is arguably the Longitudinal centre of floatation for the structure (i.e only heave is measurable here). This wave tank experiment therefor gives no indication as to the pitch or roll of the cage, important factors in understanding the possibility of slamming/green water etc.
To improve this experiment, more assessment points for motion capture would be beneficial in understanding the full range behaviour which the cage presents.

Some literature involving wave tank experiments have better summarised the motions of their selected cage. Fredriksson et Al(2003), motivated by the industry's recognised need to move offshore due to an increased demand, investigated the motions of a spar type fish cage.This was

because spar-type floating structures are generally more stable due to a lower centre of gravity (COG). Their research involved both numerical and physical models and included field measurements taken from the cage's demonstration site. The set up of their physical experiments was similar to Lee's, measuring mooring loads, the amplitude of the wave, and amplitude of the motions of the cage.

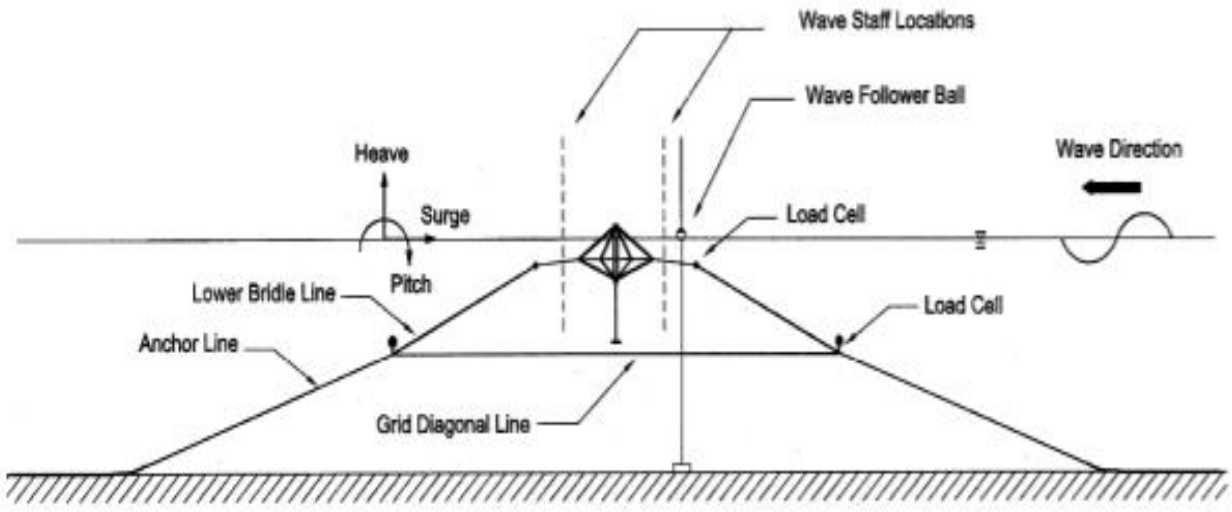

Figure 4 - Wave tank experiment set up (David W. Fredriksson, 2003)

The authors here assessed the cage under regular waves (linear theory), over a frequency range of 0-0.6 Hz. This allowed them to find the Response Amplitude Operator (RAO) of the spar fish cage. These RAO's can then be multiplied by the wave spectrum (from demonstration site) to find short term statistics, i.e response in irregular waves (Tahsin Tezdogan, 2014).
The RAO's are found in the following way;

- Heave : dividing heave amplitude by wave elevation amplitude,
- Surge: dividing surge amplitude by wave excursion amplitude,
- Pitch: dividing pitch amplitude by wave slope amplitude (David W. Fredriksson, 2003).

The RAO's found from both physical and numerical tests are shown below in Figure 5 to Figure 7 .

The RAO graph for heave (Figure 5)shows that the numerical model used here underpredicts the response by almost 50%. Though the graph shape for numerical and physical tests are similar, but slightly out of phase with each other. This suggests that the Fourier transform used (to convert time domain to frequency domain) is not quite accurate enough. There is also no indication of resonant frequency, though the authors suggest it should exist below 0.5Hz. This is in line with the Pitch RAO graph, which indicates pitch resonant frequency lies around the 0.5Hz region, shown by the spike in RAO value.

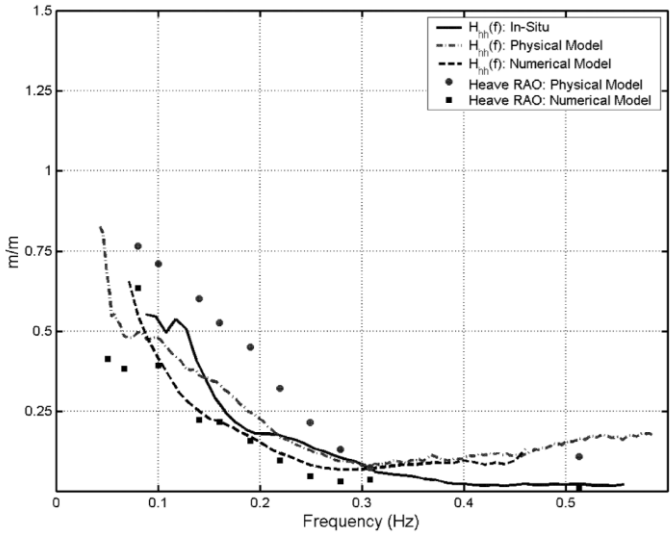

Figure 5 - Heave RAO Graph

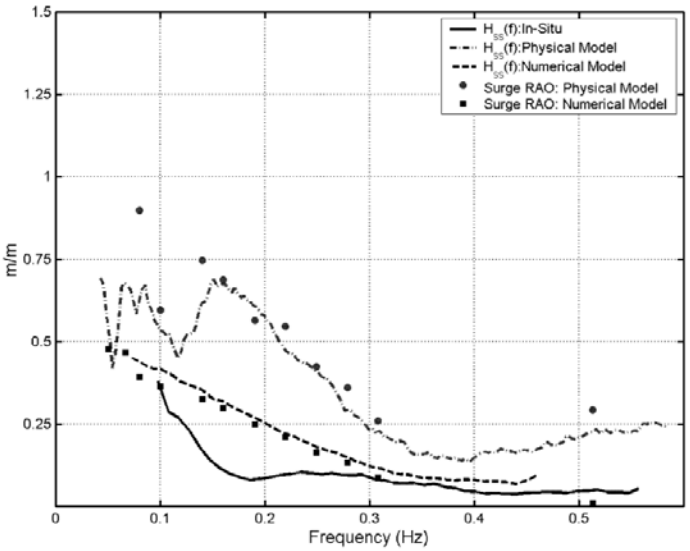

Figure 6 - Surge RAO Graph

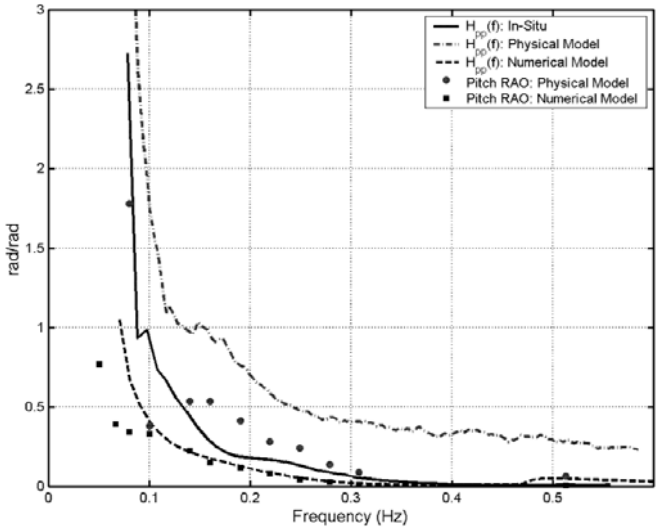

Figure 7 - Pitch RAO Graph

In all cases the value observed in situ at the demonstration site was rarely predicted by either the physical or numerical models. It should be noted that physical tests provided a more conservative estimation of the responses and, for safety sake, are the better values to use for design (Fredrikson(2003)).

It is obvious why physical experimental tests are important and useful to researchers in this field. They can be used to confirm hypothesis, and check methods, however physical tests are not a cover-all to abide by. They, as Fredriksson(2003) showed, don't always perfectly predict the real-world case. The use of validation is an excellent way of ensuring an experiment or computation is accurate or reliable. Many researchers in this field have used experiments to validate the different computation methods utilised in investigating the motions of fish cages. This is a favourable approach as it allows for fine-tuning of the experiments parameters without the expense of changing the model. The computational methods used are discussed below.

1.1.2. Morison's Equation

Some researchers have relied on the use of empirical relations to investigate the motions of fish cages. These relations, in essence, are determined through observation, and experiment, but are not supported by theory necessarily. As such, drifting from the parameters of the experiment they are observed in, can show unreliable results.
The most popular empirical method used in the area of hydrodynamic response research is the Morisons Equation. Morrisons equation defines (sometimes separately) the hydrodynamic inertial forces (Equation 2) and drag forces (Equation 1) which act on an object within a wave's path (Sørensen(2011)).

$$F_d = \frac{1}{2}\rho C_d A u^2 \quad \{1\}$$

$$F_i = \frac{1}{2}\rho C_m A u^2 \quad \{2\}$$

Where;

- A is the cross-sectional area of the object (in plane perpendicular to direction of flow),
- C_d is the coefficient of drag. This is dimensionless and is based on the resistance of the object in water,
- C_m is the coefficient of inertia. C_m is equivalent to $C_a + 1$, where C_a is the coefficient of added mass. Both C_I and C_a are dimensionless,
- u is the incoming velocity of the fluid. Usually taken as u = u(x,y,z,t) (Sørensen, 2011).

These forces can be heavily influenced by the values selected for the coefficients C_d and C_m so accuracy of this method can be flawed. As such, some researches have modified the equation to better suit their scenario.
Whilst investigating the hydrodynamic loads on net cages. Bore et al (2017) used a 'screen model' to better determine the drag and lift coefficients and thus improve the accuracy of the equation. The

authors also modified the equation to better incorporate the effect of the structures movement in relation to the fluid particles, on the inertia and drag forces.

As is shown in the below figures, the unmodified Morison equation does not agree with previous research undertaken by Loland. There is however strong agreement shown by the modified Morison equation. This suggests that without heavy modification of the equation for the direct application, the accurate use of Morisons by itself may be unreliable for fish cage motion assessment.

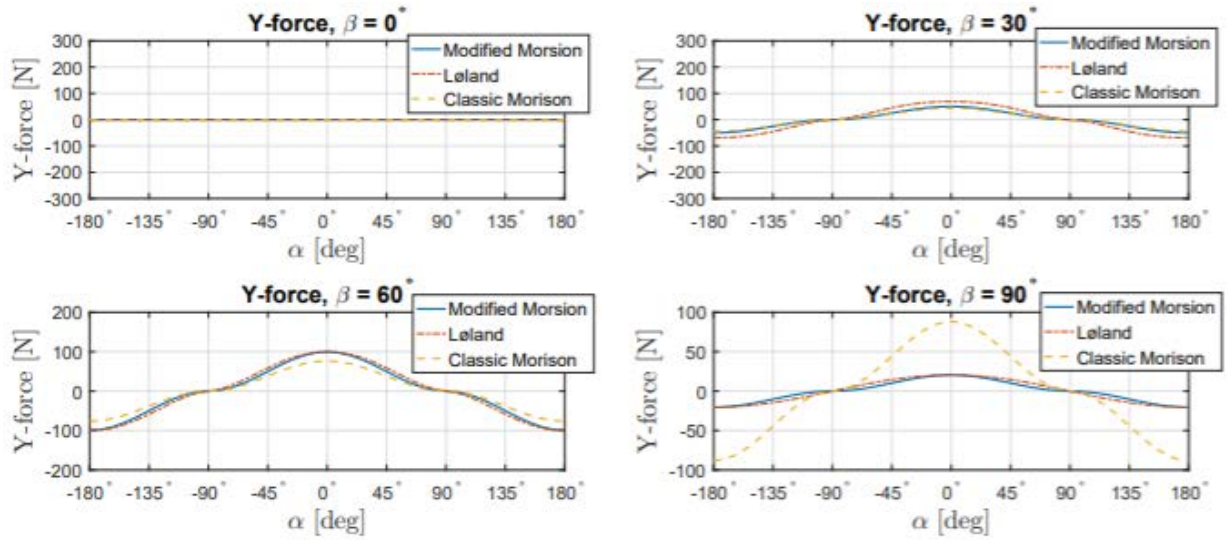

Figure 8 - Force in Y direction - Comparison of Morison Methods (Pal T. Bore, 2017).

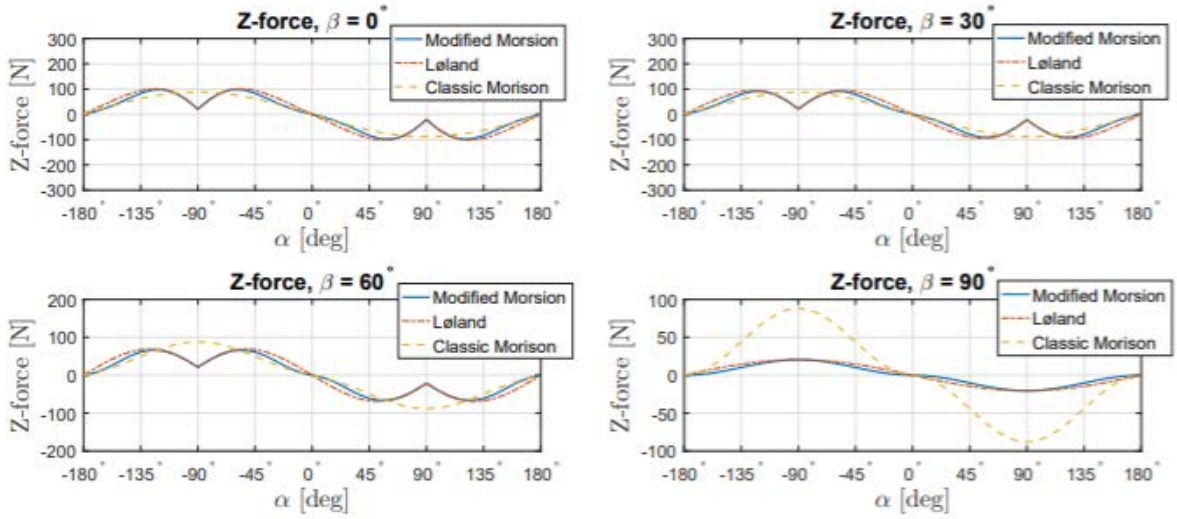

Figure 9 - Force in z Direction - Comparison of Morison Methods (Pal T. Bore, 2017).

As such. Morison's equations are often combined with other methods, such as finite element analysis/spring mass analysis. The hydrodynamic loading found using this relation is then applied to each node individually as in Yun-Peng Zhao(2019). This gives a better indication as to the effect the wave has on the floating structure and so its motions. Whilst Morison's Equation is a useful tool. Its original use applied to upright cylinders in flow, so, without proper modification, may not return accurate results for fish cages.

1.1.3. Potential Flow.

Potential flow is often used by researchers in the investigation of floating offshore motions. Fish cage motion research is no different. The theory determines the hydrodynamic force on the structure through the integration of pressure over the corresponding surface and so the motions of the structure can be found through Newton's second law..

The theory treats all fluid as incompressible, irrotational and inviscid, it ignores all surface tension and viscous effects and is developed purely for unidirectional regular waves but under such conditions it predicts the motions well. Using linear wave theory, Dong et al(2010) found the motions of a gravity cage via their numerical simulation. When checked against wave tank experiments, the potential flow based numerical solution agreed very strongly. This is clearly visible in Figure 10 showing maximum horizontal displacement for varying wave height and periods, and Figure 11 showing maximum vertical displacement for varying wave height and periods.

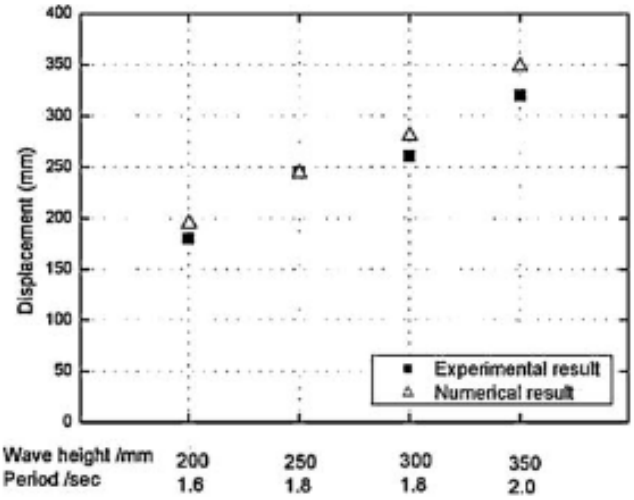

Figure 10 - Maximum Horizontal Displacement (Guo-Hai Dong, 2010)

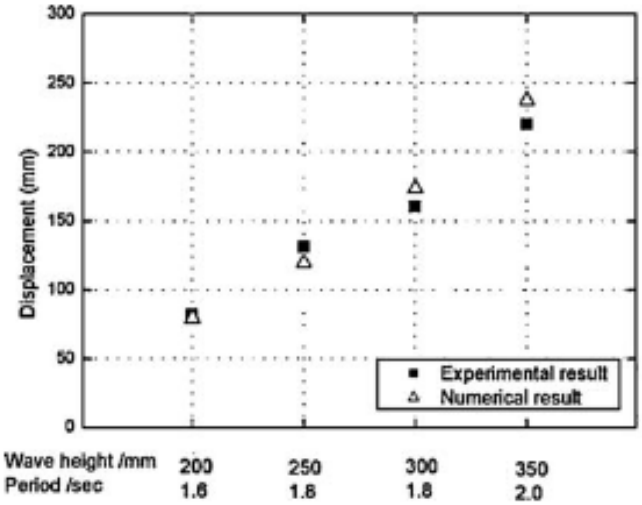

Figure 11 - Maximum Vertical Displacement (Guo-Hai Dong, 2010)

Given the strong agreement with model tests it is clear why potential flow theory is a popular and common method for predicting floating structure motions. However, the limitations of irrotationality, uni-directional waves, and only applying to small amplitude waves does limit the

theory's scalability. This makes full scale predictions less accurate, and as flow speed increases, the rotational effects cannot reasonably be ignored.

It is clear from literature that there is broad acceptance amongst researchers of the benefit of real-world experiments. The literature demonstrates an obvious understanding of the theory behind wave agitated motion and how to apply it to this problem. Also, all researchers appear to acknowledge the shortcomings of their selected method of analysis and take steps to manage these limitations. For example, modifying Morisons Equation.

However, a method of analysis which has been largely under-used by researchers investigating offshore fish cages is Computational Fluid Dynamics. Whilst very little high-quality literature exists on the use of Computational Fluid Dynamics to asses these structures, plenty exists in other offshore fields such as Oil and Gas, or Renewable Energy. This is the computational tool at the heart of this project which draws on the research from other fields to investigate the applicability and effectiveness of CFD in aquaculture.

2. Motivation

The motivation of this project is to raise, discuss and inform the design choices made during cage design by indicating whether or not CFD may be a valuable tool in this sector. Whilst there is an abundance of research into the use of floating fish cages, their design, their motions, and benefits – much of this research is mentioned above. Few academic papers have considered CFD as a cage analysis tool. There is an abundance of literature which shows CFD to be a useful and accurate tool for understanding motions of floating structures. The computation can re-size to full scale or be used to match the setup of the wave tank where the experiments have taken place (model scale). The ability to determine what is happening at a desired time step is also advantageous especially in the design stage where specific problems may need addressed and as such are easier to view by "pausing time". This computational method is without doubt one which should be of interest to all those who are investigating the motions of any floating body, including floating fish cages due to its accuracy and versatility - With the aquaculture industry only set to expand in the coming years as demand grows, understanding the motions of the farming assets is of paramount importance. Thus it is the ambition of this project to show Computational Fluid Dynamics to be both reliable and applicable to the assessment and analysis of floating fish cages with a view for Offshore Fish-Cage Design.

3. Objectives

With CFD an under-used tool within the Aquaculture sector, there is an obvious gap in showing its uses and applicability to the assessment of floating fish cages.

As such. the primary objectives of this project is to: -

- Study wave interaction with Floating Fish cages
- Further inform the discussion around floating fish cages
- Show that CFD is a reliable and useful tool which is applicable to this field.

This will be done by;

- Creating a model within a reliable Numerical Wave Tank that allows wave interaction with floating bodies.
- Comparing the forces acting on a cage as wave height or wave period changes.
- Investigating the motions of a floating cage where wave height and wave period are varied
- Review the reaction of pressure field around the cage as it interacts with waves.
- Review the changes to the velocity field around the cage as it interacts with waves.

Chapter 2
Methodology

This chapter covers the planned use of Computational Fluid Dynamics, the software utilized, and the verification of that software. This chapter lays out the domain in which the simulations will take place and the conditions under which the fish cage will be assessed.

4. Methodology

The planned project procedure to obtain results for discussion, and achieve the outlined objectives for this project can be broken into two work stages. Creation of a Numerical wave tank which is tested and shown to be reliable. Analysis of a floating object under non-linear waves and a discussion as to how this can be applied to design within the aquaculture sector. This will all take place within computational fluid dynamics software.

The CFD simulation involved utilising the opensource software OpenFoam which is a CFD software based around Linux. This allows the solution of CFD problems through the application of solvers and (pre and post) processing tools contained within the software. The theory utilised and operation of this software is highlighted below.

4.1. CFD Wave-Modelling Theory

CFD utilises the equations which govern fluid motion – The Navier stokes equations, explained below - to provide insight and predictions into situations which may otherwise be impractical or impossible to understand. Solving them for a set time step across the length of the simulation. The process used in determining structure motions using these equations is shown in Figure 12.

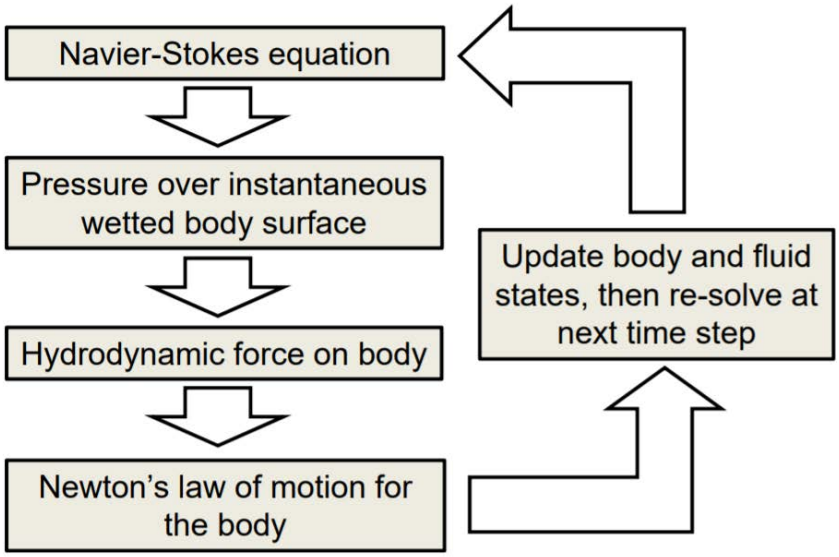

Figure 12 - CFD motion solving process (Josh Davidson, 2015)

Whilst the use of computational fluid dynamics software allows for a hand's off approach to the solving of fluid problems, it is important to understand the theories used. This will allow a better understanding of the solution which is found, whether it is reliable, and what CFD's limitations, if any, may be.

4.1.4. Finite Volume Method

The Finite Volume Method (FVM) is a numerical technique which transforms the partial differential equations that represent the conservation laws into algebraic equations across finite volumes. The approach is similar to finite element, or finite difference methods.
Firstly, a computational mesh is created over the domain in which fluid flow is to be assessed – this

consists of non-overlapping volumes of a finite size – upon which the governing equations are solved. This also determines the positions of points in time and space where the solution is sought. The process can be dissected into two parts -discretization in space, and time as shown by Jasak (1996).

The discretization of time depends simply on the selection of time-step size. This is the value by which time will be marched on from the initial prescribed condition and is set by the user.

The discretization of space requires control volumes (CV) to be set within the domain. They are taken as sharing faces with neighbouring control volumes, though the shape of the CV is not important. This means CV's can be set by a 'mesh' of varying size, which has its benefits (explained below). Such faces can be divided into two groups, internal faces, i.e. faces which control volumes share, and boundary faces, which outline the edge of the computational domain, the boundaries are also further explained later.
Since the unknown variables when using CFD are evaluated at the volume's centroid, it is simple to adjust boundary conditions without directly affecting the calculation method, which makes it perfect for influencing the solution without directly imposing a condition at the node.

4.1.5. Navier-Stokes Equations – Governing Equations

The Navier-Stokes Equations refer collectively to the conservation of mass, and momentum equations. They can be used to understand a broad range of fluid flow which is achieved by describing how the velocity, density and pressure of a moving fluid are related to each other.

The Navier-Stokes equations are defined as;

$$\nabla \mathbf{u} = 0 \qquad \{3\}$$

Which is the continuity equation representing the conservation of mass – i.e. the fluid in the CV does not change in density as it moves through control volumes.

$$\rho \frac{Du}{Dt} = -\nabla p + \mu \nabla^2 u + \rho \boldsymbol{F} \qquad \{4\}$$

Which is the momentum equation. This defines the total derivative (Equation 5) being equal to the sum of the pressure gradient, the diffusive term and the external force term

$$\rho \frac{Du}{Dt} = \rho\left(\frac{\partial \boldsymbol{u}}{\partial t} + (\boldsymbol{u}.\nabla)\mathbf{u}\right) \qquad \{5\}$$

Where u is velocity vector such that $\mathbf{u} = (u_i, v_k, w_j)$, ∇ is the gradient operator, p is pressure, ρ is the density of fluid, μ is the dynamic viscosity of the fluid, **F** is any external force which may occur within the problem, for example, gravity. (Yuanchuan Liu, 2017).

Combining the above equations with the finite volume method, the fluid can be parcelled into numerical 'chunks'. The properties of the fluid (namely velocity and pressure) are assessed at the centre of each cell, as defined by the finite volume method, using Navier-Stokes equations.

4.1.6. Volume of Fluid (VOF) Method

Volume of fluid is a numerical method which allows for the tracking of the free surface – the interface between water and air. It does so by specifying the density of the control volume with Equation 6.

$$\rho = \alpha\rho_w + (1 - \alpha)\rho_a \quad \{6\}$$

Where - ρ_w is the density of water, ρ_a is the density of air, α is the amount of water in the cell where 1 = filled with water, and 0 = filled with air.
As such the density is a mixture of air and water within each cell, if the cell density is less than that of water, it forms part of the free surface. This is visually represented in Figure 13, below.

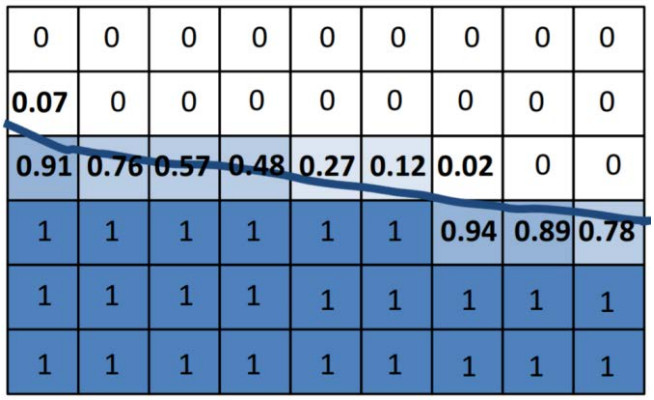

Figure 13 - Visual representation of the VOF method which captures the free surface location. The blue line here represents the free surface, and the numbers show the fraction of water in each cell (Josh Davidson, 2015)

'Wave gauges' can be combined with this method to record the value of the free-surface at a specified location within the domain. This is useful for checking the proper implementation of wave theory, and the effect of a floating object on the wave height, down wave.

4.2. OpenFoam

Given that computer simulation in analysing the hydrodynamic responses of fish cages is in its infancy, it is useful to utilise a tool designed to handle these fluid-related problems computationally which has a proven record of accuracy.
There are many powerful CFD tools available for use – Ansys Fluent, Star CCM, Autodesk CFD to name a few – all with excellent pre and post processing capabilities which allow a truly professional presentation of the results, there is one main problem with them. They operate as "black box" computation. This means the commercial user of the software, despite the expense of purchase, does not have access to the inner workings of the CFD solver's code. As such, no understanding can be taken as to the process which produces the solution, which in turn prevents modification of the software to better suit the problem to which it is being applied should the user have the expertise to do so.
This is where OpenFoam fits in. Being open source, the adaptability and applicability of the software and the numerical solvers depends entirely upon the users - who have full access to the internal workings. This combined with the free 'price-tag' makes OpenFoam quite desirable however there are caveats to its use. There is a very steep learning curve to OpenFoam, as there is no commercial backing, it suffers from a lack of GUI (Graphical User Interface) thus appearing very complicated to beginners due to the multitude of choices which can be made.

Despite this, the benefit of understanding of, and having access to, the internal workings outweighs the disadvantage of the learning curve. Therefore, OpenFoam has been selected for use as the CFD software in this project.

4.2.7. OpenFoam Operation

The flow of information within OpenFOAM can be split into three main stages – Pre-processing, simulation, and Post-Processing. These stages are further explained below, and the overall OpenFOAM simulation process is visually outlined in Figure 14.

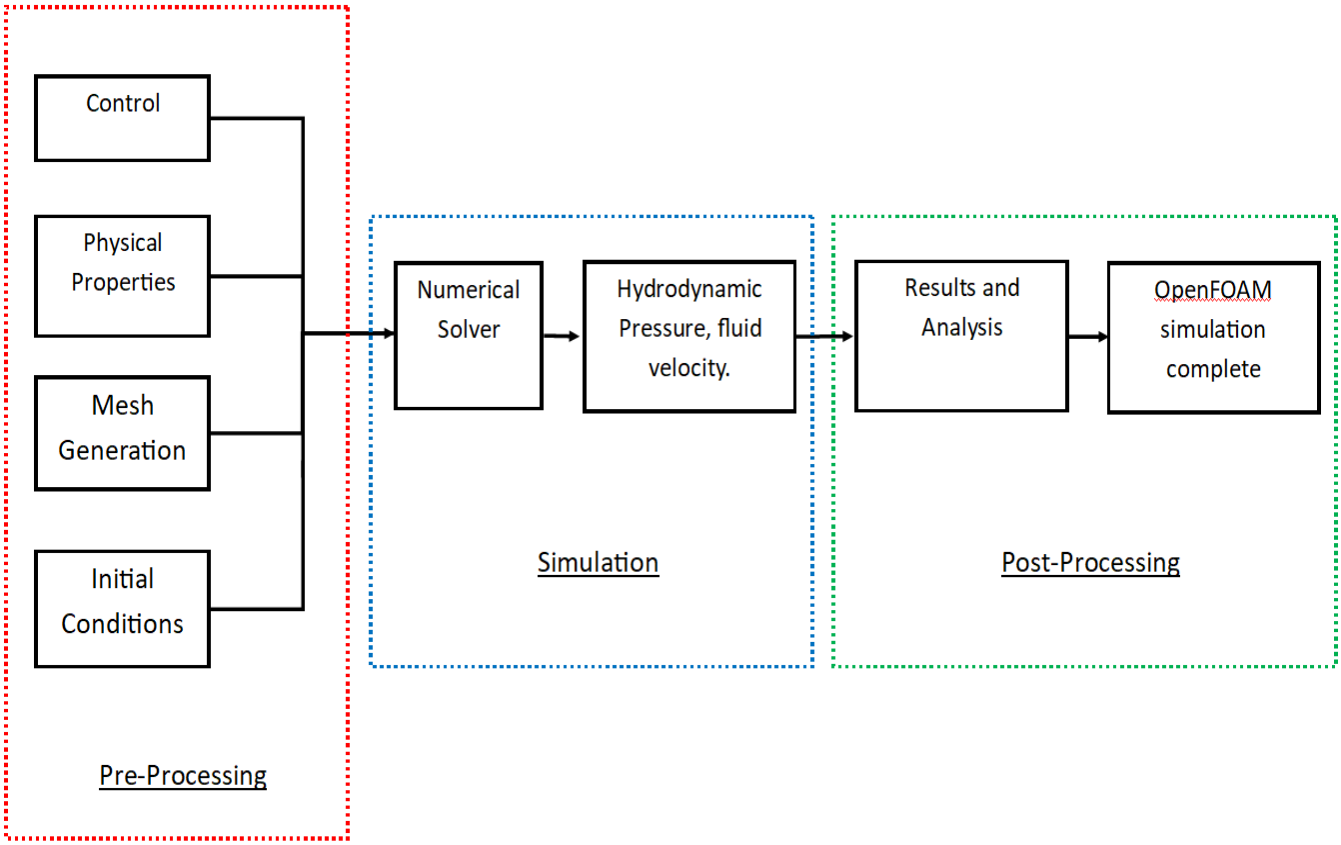

Figure 14 - Flow of information through OpenFOAM software.

4.2.8. Pre-Processing

Pre-processing can be split into a number of sub processes. These are where the problem is defined;

- Mesh Generation – Where the item is spatial discretized into control volumes. A mesh can be considered 'coarse' or 'fine', where the 'finer' the mesh, the more control volumes specified. It can be said that accuracy increases as mesh becomes finer, this is because the mesh coheads more closely to the object/domain shape- particularly on curves. It also allows a closer examination of the values in the domain, indicating where something occurs in a more accurate location.

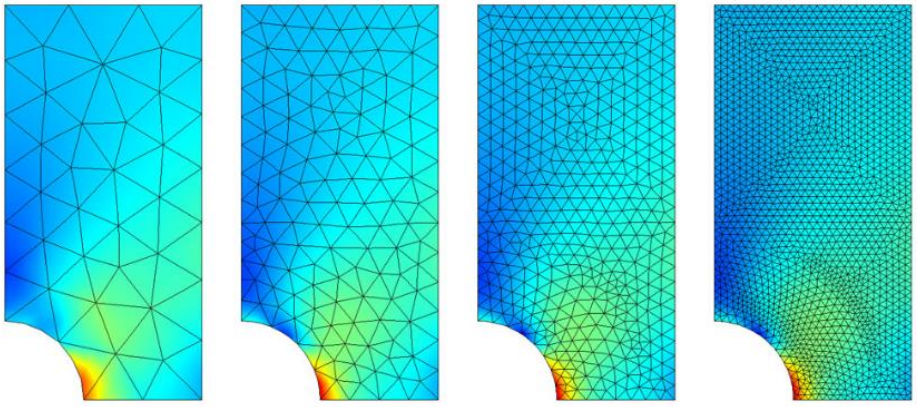

Figure 15 - Meshes of varying refinement (Comsol, 2017)

Figure 15 gives an example of mesh refinement. Moving from Coarse on the left, to fine on the right. As is visually obvious, a more accurate location for the indication of variables etc can be found using a finer mesh. There is however a fine balance to the mesh as the more control volumes present in the domain, the greater the computation power required and the longer the execution time. There are two approaches to handling this. Firstly, checking the change in results, as mesh is refined. The stopping point is ordinarily chosen by the user, where they decide the change in results does not justify the increased computation expense. Secondly, a graduated mesh. This allows for the focus to be placed on specific areas of interest, allowing areas with little to no interest to be evaluated with less computing power. Mesh refinement, rather than graduation was chosen in this project for simplicity and ease/speed of use as it proved to be more stable within OpenFoam.

- Control – This is where the time step, the time at which the simulation data is recorded, and the point at which the simulation should stop are defined. It also defines how often the data is written and in what format. There are also options for defining what data should be recorded. As standard data relating directly to the fluid is recorded, though sampling forces on an object, or wave gauge sampling can be controlled here. Various time steps should be considered to ensure a smooth and accurate solution is obtained. This at times may require a convergence type approach, like the Mesh Generation above.
- Physical Properties – This is where the physical properties of the fluids involved in the simulation is defined. This includes the density and viscosity of the fluids – here the water and air densities are defined.
- Initial Conditions – The starting point for the simulation is defined here. What the initial velocities and pressures are, i.e. what the fluid is doing before the simulation begins. This is occasionally taken as a flow into a stagnant domain which avoids the interference of original conditions. Hideaki Miyata(1997) presents this clearly. – In the case of this project, stagnant fluid, with a wave input is used here.
- Boundary Conditions – This defines how the boundaries, i.e the edges of the computation influence the calculation. This can range from no-slip conditions - where the fluid ‘sticks’ to the boundary, having a velocity equal to the boundary – to pressure conditions – where a pressure can be defined into, or out of the fluid affecting the conditions in which the simulation occurs.

4.2.9. Simulation

Within OpenFoam there are three popular algorithms for approaching simulation.

These solvers, for incompressible fluid, include SimpleFOAM, PisoFOAM and interFoam. These are the Semi-Implicit-Method-for-Pressure-Linked-Equations (SIMPLE) and the Pressure-Implicit with Splitting of Operations (PISO) algorithms – Inter is not considered to be an abbreviation.

Simple is very widely used, and has a had adaptions to directly apply the algorithm to more specific cases. It solves steady-state problems iteratively by assessment of the Navier-Stokes Equations, adjusting the pressure after velocity is found, to ensure continuity is satisfied (Hideaki Miyata, 1997). PISO is one of the adaptions of Simple. It solves the Navier-Stokes equations without iteration and with large time steps. It was originally developed for unsteady compressible flow, but has since been modified to appropriately model steady-state problems.

Both Simple and PISO are well developed and useful solvers, as they have the ability to solve the Navier-Stokes equations across a steady-state incompressible problem domain – however they are predominantly used for single-fluid problems. Interfoam, based on SimpleFOAM is a solver for two incompressible fluids which may occupy the same control volume. This is what allows the Volume of Fluid (VOF) method to operate correctly and is the basis for the solvers used here, waveFoam, waveDyMFoam and sixDofMotion. These are clarified below.

4.2.10. Post-Processing

Thankfully, though OpenFoam does not possess a user GUI, the post processing can be done in a visual manner, within Paraview. Paraview is a programme which collects the solution data of the simulation and displays it graphically to allow a better understanding of the data. Not only can users view the also problem's simulation as an animation, but at each time step which allows anomalies to be spotted more easily. Paraview allows the data to be plotted into appropriate graphs and tables which makes it well suited for the post-processing of the data leading to analysis of the problem. However, for the handling and manipulation of large data sets, MatLAB was used. Being a commercial software, the ability to process large sets of data is well refined in this program. This also leads to a clearer and more uniform presentation of data in graphs/figures.

In either case, should the post processing find the solution to be inadequate in some way, the simulation can be adapted and re-run where time allows.

Whilst OpenFOAM is a widely used, and broadly accepted software for the assessment of fluid dynamic problems, it is important to asses its operation. This is to ensure that the components of the problem are being accurately reproduced, eliminating software, or user error.

These components include;

- Reproduction of wave conditions – Does the software produce waves in-line with the appropriate wave theory – is it accurate enough?
- Forces on a fixed/floating object – Are the forces acting on a floating object within the wave field reliable?
- Motion of floating object – Do floating objects which interact with waves respond in a way that can be observed experimentally/in the real world.

All of these components are essential in analysing, and ultimately designing a floating structure. If any of these components are inaccurate, then any solution found cannot be relied upon. Any inaccuracies found were explored and explained.

4.3. Creating a Numerical Wave Tank

It is common practice when undertaking CFD involving waves to construct a “wave-tank” in which the computation can be solved (Christian Windt, 2019). Such a Numerical Wave Tank (NWT) is effectively replicating an experimental (real-world) wave tank. This is the approach which was taken within this project. The layout of such a tank can be seen in Figure 16.

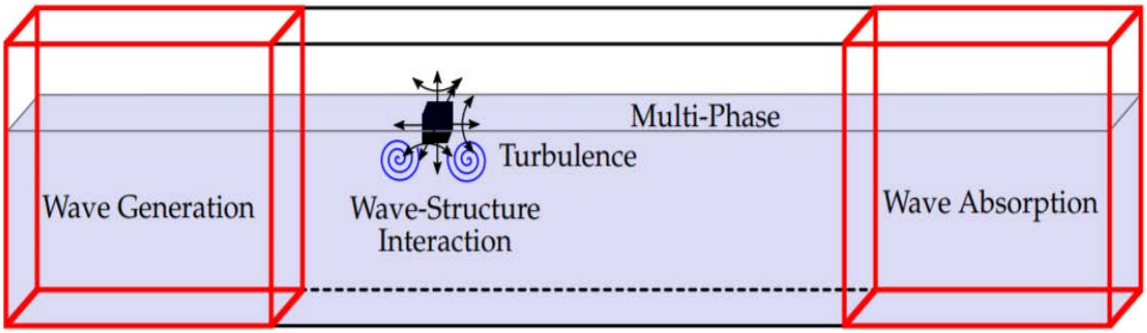

Figure 16 - Generic CFD-based numerical wave tank schematic, depicting the main features to be (Christian Windt, 2019)

The Numerical Wave Tank consists of 3 areas, a Wave Generation zone, a Structure Interaction area, (henceforth referred to as computation zone), and the wave absorption zone. These three areas allow for the generation, transmission, and absorption of the waves across the computational domain.

The first area is often referred to as the “Inlet” where the wave is created in accordance to a selected wave theory. This wave passes through the second area where the structure of interest will interact with the wave. This is where forces acting on a body are computed. Finally, the third zone, usually referred to as the “outlet” deconstructs the wave. This is done to prevent the wave reflecting back toward the structure and changing the parameters under which the floating object is being assessed.

The accuracy of the wave generation, and the minimisation of wave reflection are further explored below to improve the confidence in future simulations.

4.3.11. Co-Ordinate System

This project utilises a right handed Cartesian Co-ordinate system. This is shown in Figure 17, where;

- the X axis is the horizontal axis, positive to the right,
- the Y axis is the axis perpendicular to the page, positive into the page
- the Z axis is positive upwards, in the vertical direction

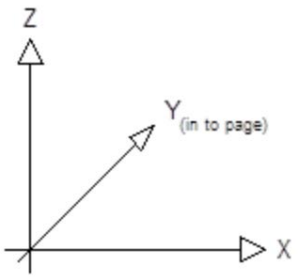

Figure 17 - Right Handed Cartesian Co-Ordinate System

4.3.12. Verification of Wave Generation

The wave generation of three main wave theories were assessed using a two-Dimensional wave-tank of arbitrary length. As can be seen in Figure 18, it has been shown by Le Mehaute(1969) that some wave-theories apply only in certain conditions. Thus, where possible, water depth remained constant across all tests at 0.4m, whilst period and height were varied.

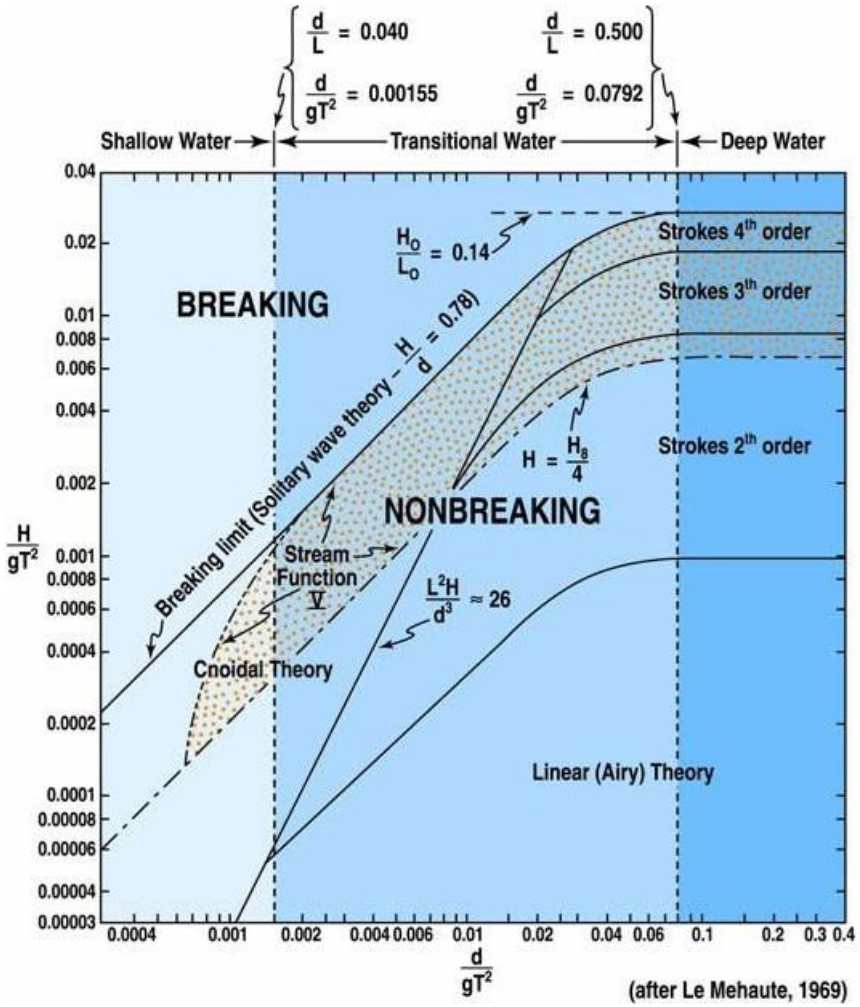

Figure 18 - Le Mehaute Chart characterising various wave types dependent upon Wave Period, Height and Water Depth

The behaviour and reliability of the flat-bottomed wave tank was checked by comparing results from simulation with the expected theoretical result. This was done by measuring the simulation's surface elevation using a numerical wave gauge - for known wave parameter input. The "ideal" surface elevation for the same wave parameters was calculated using the relevant wave theory. Contrasting these would confirm whether OpenFoam is suitable for modelling waves using the tested wave-theories.

In showing CFD as an effective tool for fish cage design, shallow, transitional, and deep water waves may be needed. The Cnoidal, Linear, and Stokes Second Order wave theories apply to these wave types dependent on the wave parameters, as such shall all three types will be assessed and checked for accuracy. The wave parameters used are listed below in Table 1.

Table 1 - Wave Particulars of test waves for 3 scenarios

Wave Particulars for 3 Wave Theories			
	Linear Wave Theory	Stokes 2nd Order Wave Theory	Cnoidal Wave Theory
Wave Period (s)	2	1.158	2.3
Wave Frequency (rad/s)	3.14	5.426	2.73182
Wave Number	1.701	3.001	2.29
Wave Length (m)	3.7	2.09	2.07
Wave Height (m)	0.1	0.07	0.15

4.3.13. Linear Wave Theory

Linear wave theory is used to assess the transitional and deep water-depth waves. It is sometimes referred to as Airy wave theory and is the simplest of the wave types assessed, being linear. The theory describes the propagation of gravity waves, linearly, on the free surface. This theory takes the assumptions that flow is inviscid, incompressible, and irrotational within a fluid that is homogeneous with a uniform depth. As such is useful within the flat-bottom tanked utilised here. Though not as accurate as higher-order theories, often taken as high-enough accuracy for most purposes.

The surface elevation of a wave described by this theory is given by the surface elevation equation (equation 7), the wave number equation (Equation 8), the wave frequency (Equation 9).;

$$\eta = A\cos(kx - \omega t) \quad \{7\}$$

$$k = 2\pi/\lambda \quad \{8\}$$

$$\omega = \pi/T \quad \{9\}$$

Where η is surface elevation in regards to the still-water-line (SWL), A is wave height amplitude, k is wave number, x is position along the wave(in metres), ω is wave frequency (rad/s),t is time in seconds, T is wave period in seconds, and λ is wavelength in metres.

Comparing this surface elevation, to the output of gauge 1 yields the graph shown in (Figure 19), below. It is clear that the linear-wave theory utilised within the software is sufficiently accurate showing no distinguishable error. Thus, it can be relied upon to produce small amplitude waves for the “transitional” and deep-water region when assessing any model or problem in the software.

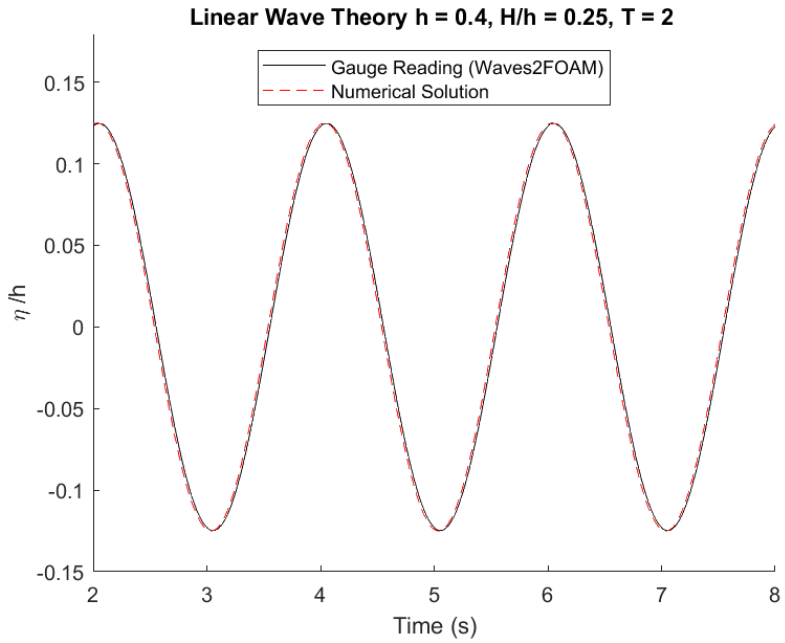

Figure 19 - Linear Theory against Numerical Simulation within OpenFoam

4.3.14. Stokes Second Order Wave Theory

Stokes Second Order Wave Theory is non-linear and is also used for the modelling and assessment of free surface, periodic, regular waves. These waves are not applicable in shallow water, or with smaller waves in transitional or deep-water as Figure 18 shows. This is a higher order theory than Linear-wave-theory, and is more representative of "real-world" waves. There are higher orders of Stokes wave theory, though second order is generally taken as suitably accurate for most use cases.

The theory takes surface elevation as;

$$\eta = \frac{H}{2}\cos(kx - \omega t) + \frac{H^2 k}{16}\frac{\cosh kh}{\sinh^3 kh}(2 + \cosh 2kh)\cos 2(kx - \omega t)$$

{10}

This equation was used to verify that the surface elevation recorded by a wave gauge in the numerical wave tank agreed with the analytical values for Stokes second order waves. Their comparison is shown below in Figure 20.

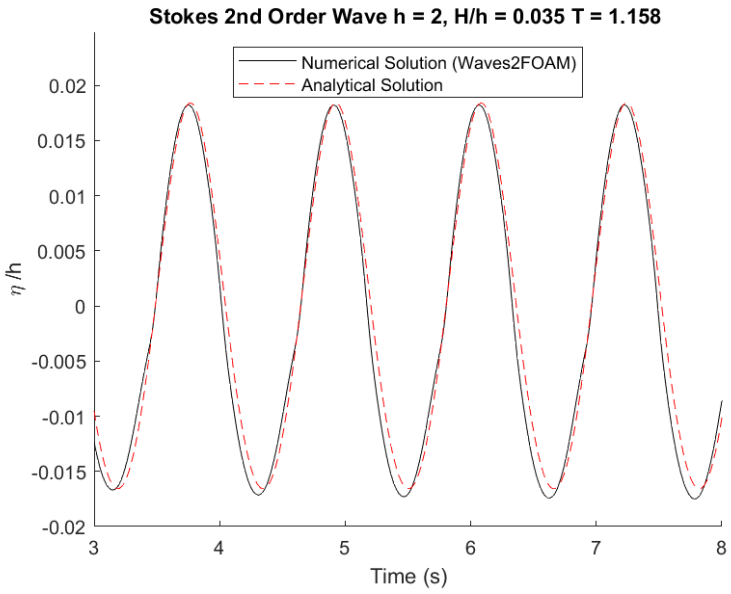

Figure 20 - Stokes 2nd Order Wave Theory against Numerical Simulation within OpenFoam

As can be seen above, the Stokes Second Order wave implemented by the software closely matches the expected surface according to Figure 20. There is a slight underprediction of the trough amplitude in comparison to the theoretical results, though this may be improved by a finer computational mesh, or adaption of acceleration damping parameters. The mesh optimization is explored below. Despite this, the strong agreement shows that OpenFoam can be relied upon to provide accurate deep and transitional water, Stokes Second order waves for test cases.

4.3.15. Cnoidal wave theory

Cnoidal waves are used to assess the waves in a shallow water depth (relative to the waves). It is a non-linear theory, suitable for waves progressing in around one-tenth water depth of their wavelength (Wiegel, 1959). Within OpenFoaam, the surface elevation is generated by the equation below (Equation 11)

$$\eta = H\left[\frac{1}{m}\left(1 - \frac{E(m)}{K(m)} - 1 + cn^2\left(2K(m)\frac{x-ct}{\lambda}\right)\right)\right]$$

{11}

Where, λ is wavelength, m is the eliptic parameter defined by wave characteristics, K(m) is the complete elliptic integral of the 1st kind, E(m) is the complete eliptici integral of the 2nd kind, cn is Jacobi's eliptic function, c is wave celerity, H is wave height and t is time (in seconds).

Comparing this to relevant literature where Hyatdavooid (2015) assessed cnoidal waves using Green-Naghdi Equations, we can see from Figure 21 that OpenFOAM generates waves under this theory sufficiently accurately. As such use of this wave type in assessing a floating body is clearly possible.

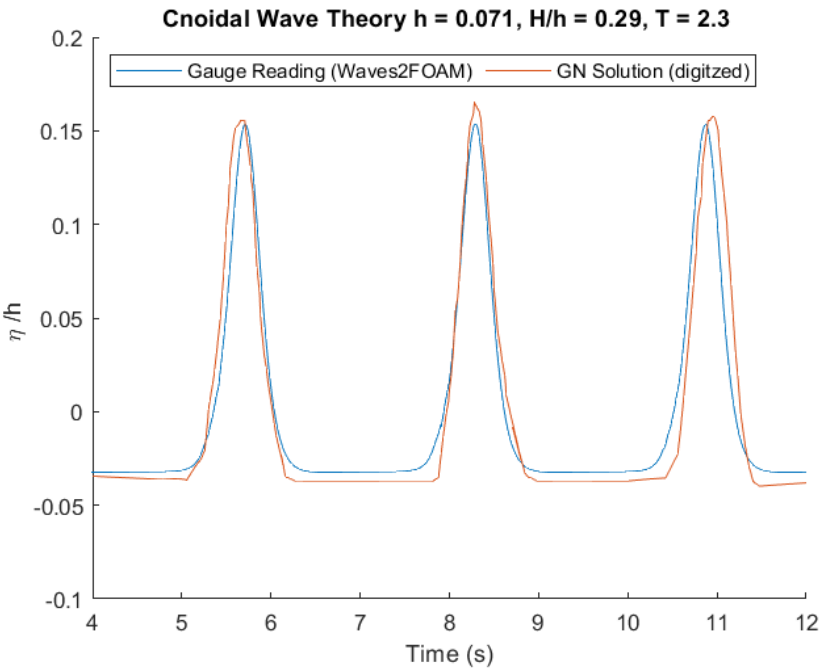

Figure 21 - Cnoidal Wave Theory against Numerical Simulation within OpenFoam

It is therefore taken that OpenFOAM produces suitable and reliable waves for shallow, transitional and deep-waters via the three wave-theories, as above. Any of them could be utilised dependent on the wave parameters/testing conditions required.

4.3.16. Minimization of Reflected Waves at Outlet.

To accurately reproduce waves within the NWT reflection of waves due to the tank should be considered and minimized. This is where waves are reflected back from the outlet towards the structure/object of interest. This causes a change to the wave interaction with the object and thus changing the conditions under which motions are assessed.

There have been multiple solutions considered within literature to counteract this, including;

- Addition of porous material at the wave outlet boundary to dissipate the wave energy,
- Addition of a "beach" – in essence a second, sloping structure within the outlet zone, upon which wave energy could be absorbed as shown by Morgan(2010).
- Mesh Stretching – Where the cell size within the outlet is gradually increased causing wavelengths smaller than the cell to be filtered out. Though, according to Windt (2019) this requires a very long NWT.

Generally all methods extend the computation time. For simplicity, the Relaxation Zone Method within OpenFOAM was used here. This implements a relaxation function to smoothly reduce the waves' to zero, bringing the free surface to the still water level, and pressure to the hydrostatic value (Adria Moreno Miquel, 2018). Thus mitigating reflections from the down wave boundary.

To determine the rate of reflection within the tank, surface elevation data from numerical wave gauges were assessed to find the reflection coefficient.
The Reflection Coefficient gives an indication as to an object's effect on the wave field, in this case the outlet. It defines, from an incoming wave, how much of the initial amplitude passes "through" the object or boundary, and what amplitude is reflected back toward the wave's origin. With the

gauges measuring only surface elevation, the reflected and initial waves are intertwined in the readings, so use of a Fourier transform is required to split and asses the waves separately. As can be found detailed below.

To determine the reflection coefficient, 2 wave amplitudes are needed. The amplitude of the incoming wave, and the amplitude of the reflected wave. This then allows the reflections coefficient calculation to be undertaken (Equation 12).

$$C_r = \frac{a_r}{a_i}$$

{12}

Where *a* is amplitude, *r* denotes reflection and *i* denotes initial wave.

These amplitudes are obtained via the time records of the surface, via the below Fourier Transform (Equation 13).

$$\hat{\eta}(x) = \frac{\omega}{2\pi} \int_0^{\frac{2\pi}{\omega}} \eta(x,t) \exp(-i\omega t)\, dt$$

{13}

The amplitude of the incoming wave is found using Equation 14;

$$a_i = \frac{1}{|\sin(K\Delta X)|} |\hat{\eta}(X_I) - \hat{\eta}(X_{II}) \exp(-iK\Delta X)|$$

{14}

The amplitude of the reflected wave is found using Equation 15;

$$a_r = \frac{1}{|\sin(K\Delta X)|} |\hat{\eta}(X_I) - \hat{\eta}(X_{II}) \exp(iK\Delta X)|$$

{15}

The transmitted wave can also be found in a similar fashion by using Equation 16;

$$a_t = \frac{1}{|\sin(K\Delta X)|} |\hat{\eta}(X_{III}) - \hat{\eta}(X\_IV) \exp(-iK\Delta X)|$$

{16}

And transmission coefficient through Equation 17;

$$C_t = \frac{a_t}{a_i}$$

{17}

These calculations were undertaken in MatLAB software using time-series data of the surface elevation taken from wave gauges.

To demonstrate the full breadth of CFD, and assess its usefulness toward aquaculture design in the context of a wave-tank, three tanks were tested for reflection. One for each of the wave-theories, Cnoidal, Linear, Stokes 2nd Order, previously discussed. The particulars are displayed in Figure 22. Where the absorption zone, who's length is denoted by X, was varied to determine the change in reflection coefficient. The absorption zone was lengthened from 1 to 2.5 wavelengths, at increments of 0.5 wavelengths. Cell size was fixed consistently across all tests, with simulations undertaken on a single processor.

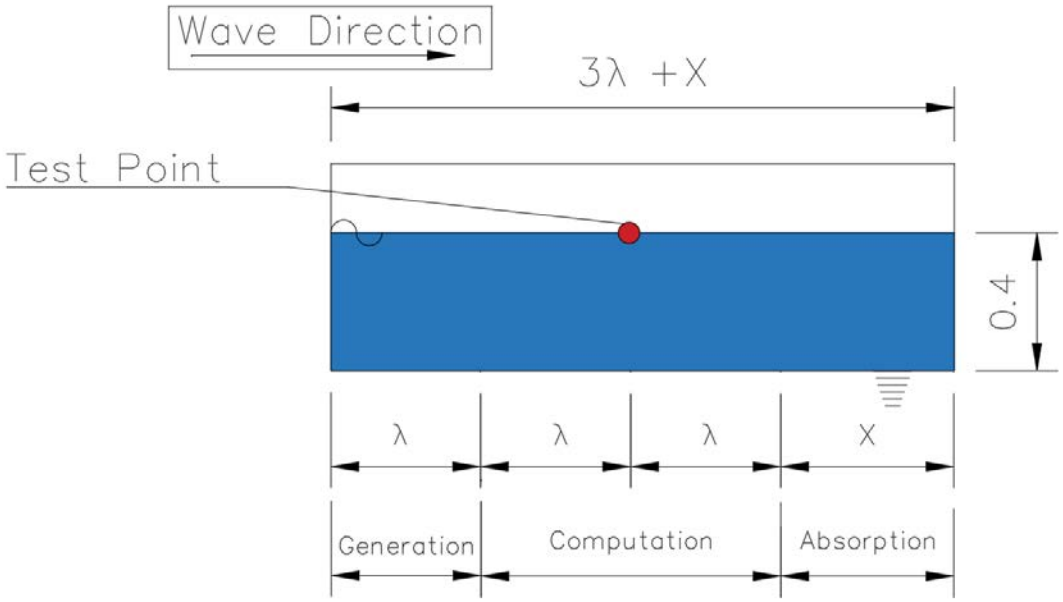

Figure 22 - Wave Tank used to test reflection of the 3 theories.

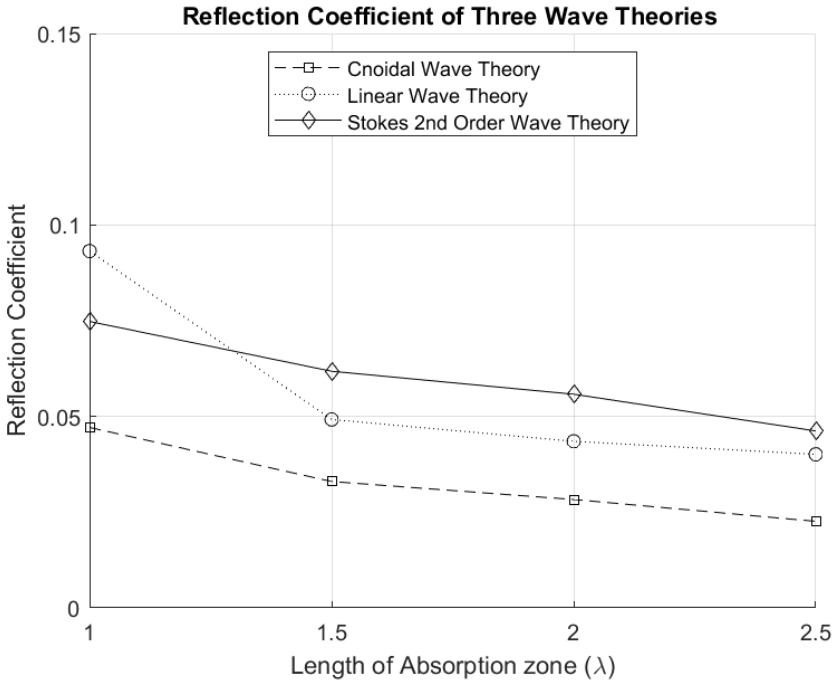

Figure 23 -Plot of Reflection Coefficient as Absorption Zone length increases

As can be seen in Figure 23, reflection coefficient reduces as the absorption zone length increases. Linear Wave Theory saw the greatest reduction in reflection across the 4 tests at 5.1%, whilst Cnoidal Wave Theory showed the smallest reduction of 2.3%. However, Cnoidal Waves were the least reflected wave type regardless of absorption zone length. It is obvious from the above Figure 23 that non-linear theories, such as Cnoidal and Stokes 2nds Order are less effectively absorbed by an increasing relaxation zone such as that used here.

Clearly, if time and resources were no obstacle, a larger absorption zone length could be chosen, however it is also important to consider the effect this has on computational time. An infinitely long wave tank would eliminate reflection, but is not computationally viable, as such, the reflection found should be balanced against the computational expense.

Table 2 - Computational time of simulations when determining reflection within Numerical Wave tank

Computational Time (s)			
	Cnoidal Wave	Linear Wave	Stokes 2nd Order Wave
1 Wavelength	118.91s	236.48s	69.02s
1.5 Wavelengths	466.74s	248.89s	75.3s
2 Wavelengths	616.72s	508.16s	84.51s
2.5 Wavelengths	820.17s	645.19s	101.4s

These were undertaken on an a 16 core Intel Xeon E5-2697A CPUs @2.60GHz using GB of ram.

Comparing computational time with reflection coefficients a balance can be struck. With the aim to reduce both as far as reasonably practicable, a Cnoidal wave tank should have an absorption zone of 0.5 wavelength. Linear and Stokes 2nd Order wave tanks should utilise absorption zones of 2 wavelengths. This will allow for a reasonably un-adulterated computational zone at a minimised computational cost.

4.3.17. Determination and calculation of forces.

To determine the effectiveness of CFD and particularly OpenFOAM, it is important to ensure forces acting on a structure within the wave tank are acceptably accurate. This is because no design of a floating structure can truly be undertaken if the likelihood of the object structurally surviving environmental loading is ambiguous. Thus, the forces recorded in OpenFOAM simulation, are compared to experimental wave tank results.
Ren et al.(2015) investigated the motions and forces of a freely-floating body under non-linear waves using a WCSPH method and real-world experiments (Bing Ren, 2015). These experiments were undertaken in 2D, suitable for the purpose of this project, and their exact set up is indicated below in Figure 24.

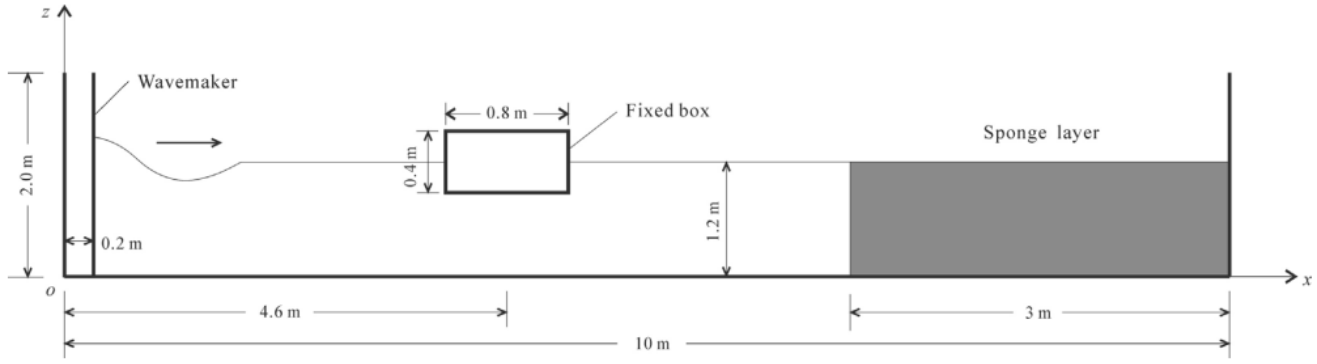

Figure 24 -Experimental set up of 2D fixed box

To understand the accuracy of OpenFOAM's force calculation and recording, this set up was replicated in simulation and the recorded forces compared to those found by Ren et al(2015). A mesh convergence study was undertaken at this point to rule out any possible effects the mesh size could have on the recording of forces, ensuring OpenFoam's use is suitable in determining forces.

This was done by gradually increasing the number of cells present in the wave-tank, and checking the error between the recorded values, and those found by Ren et al. (2015). The mesh sizes are shown in Table 3.Table 3 - Number of Cells within Mesh for Convergence

Table 3 - Number of Cells within Mesh for Convergence

Mesh Number	Cells in X Direction	Cells in Z Direction	Total Cells in Domain.
1	1500	270	405000
2	1750	315	551220
3	2000	360	720000
4	2250	405	911250
5	2500	450	1125000

The change of maximum percentage error between OpenFoam and the forces found in experiments across the varying mesh refinement gives a good indication as to the effect meshing has on the accuracy of calculated values. These are shown in Figure 25. It is clear that finer the mesh, the more accurate the results. The most coarse mesh was found to be over 0.5% less accurate than the finest mesh, Mesh five, which had a maximum error of 3.97%.

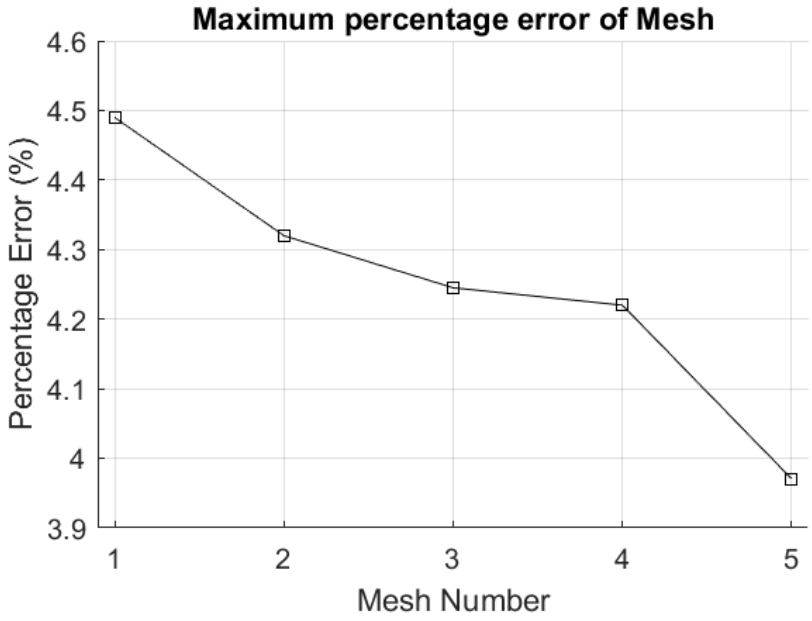

Figure 25 - Maximum Percentage Error as Mesh is refined

In general, the measurements of all meshes tested were reasonably accurate. On average, the coarsest mesh was less than 0.0003% more accurate than the finest when taking the mean error across all force measurements (in the z direction) can be seen in Figure 26.

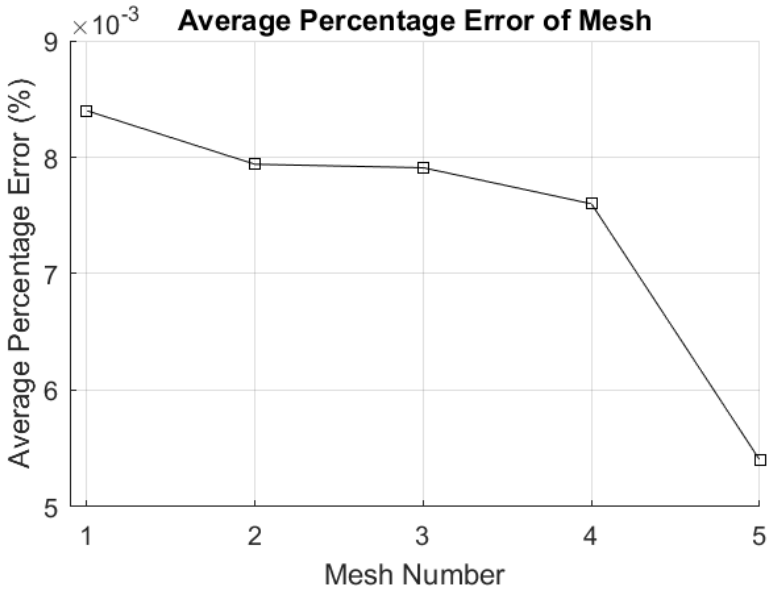

Figure 26 - Average Percentage Error as Mesh is refined

The mesh should be selected in regards to the situation being assessed and the required data. For example, if analysing the maximum force on an object, all meshes would over-predict, however, Mesh 1 would over predict the most. Selecting Mesh 1 for use in analysis could lead to over-engineering. If however a more generic, averaged approach is being undertaken Mesh 1 could be taken, on average, as suitably accurate. The mesh selection is important as a coarser mesh allows for

a lower computational expense, and a faster computational time with the trade-off of accuracy. As can be seen in Figure 27, Mesh 1 is almost 3 times quicker than Mesh 5 whilst undertaking the same simulation. At preliminary stages, is the increase in accuracy of only 0.5% worth the extra 7 hours run time? For a single case, this may be acceptable, but if multiple cases were to be undertaken, varying wave heights, water depth, wave periods, the expense may quickly become too great to justify the benefit.

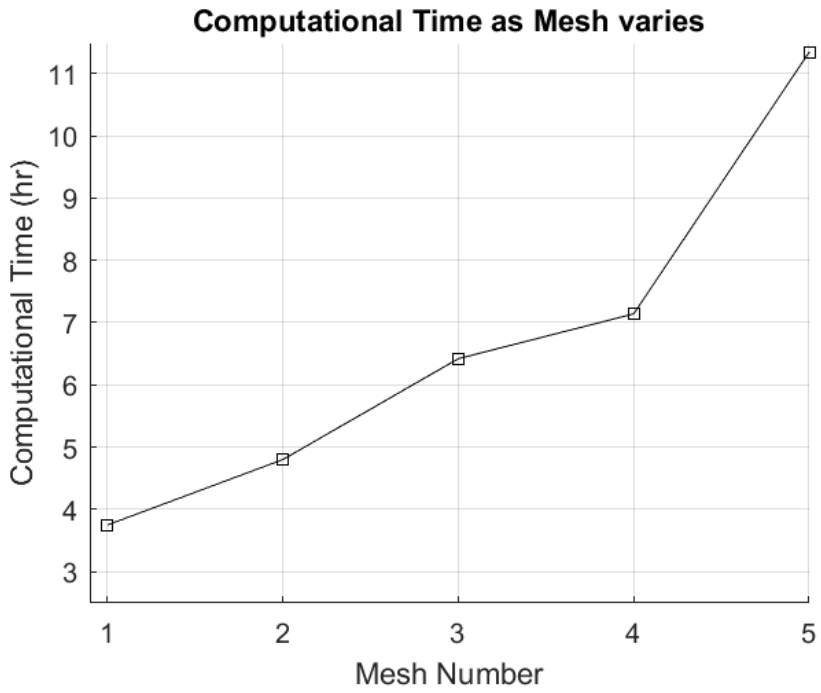

Figure 27 - Computational time as mesh refinement increases

As such, Mesh 2 was settled on. This provided a suitably accurate mesh with a maximum error of 4.32%, an average error of 0.00794% at a computational time of less than 5 hours. As is clear from Figure 28, this mesh allows a reasonably accurate calculation of the vertical forces acting on the fixed object with a slight over-prediction across most peaks.
Figure 29 also shows an accurate prediction of forces, this time in the X-direction. Whilst in places there is a slight calculation error, particularly in the peaks/troughs, this was deemed acceptable. Therefor it can be said that OpenFOAM will reliably predict the forces acting on an object in a wave tank in 2-Dimensions.

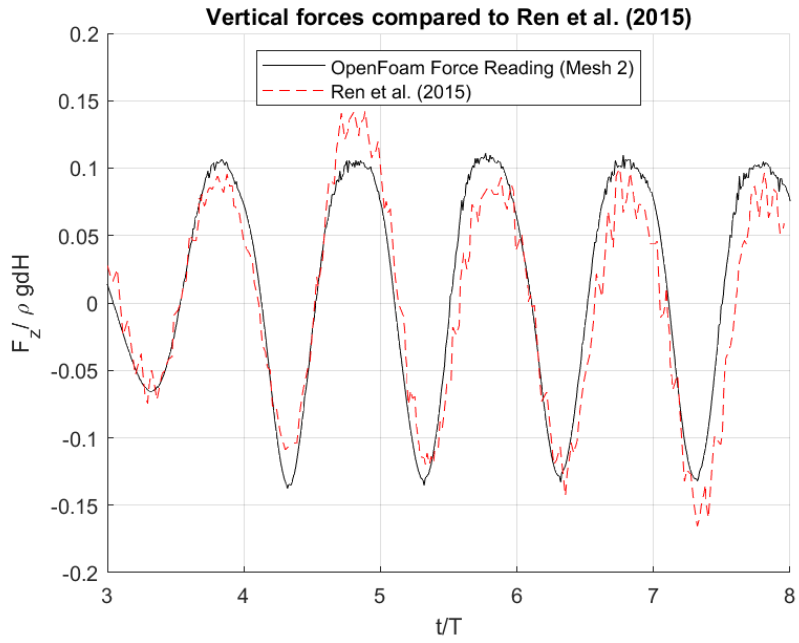

Figure 28 - Vertical Forces on 2D Fixed Box

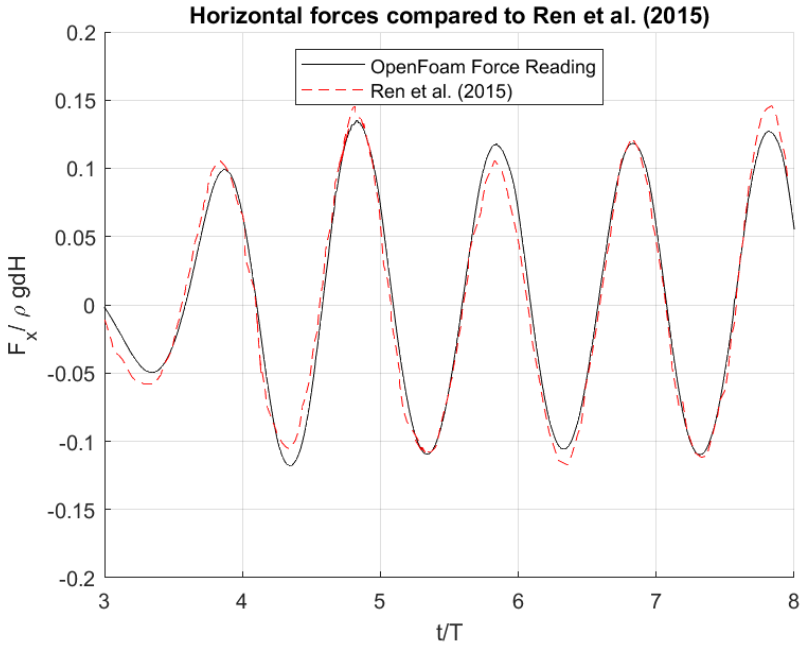

Figure 29 - Horizontal Forces on 2D Fixed Box

4.4. Floating Object Response

The next step in determining the viability and accuracy of the CFD wave-tank is showing hydrodynamic response motions are calculated accurately. Ensuring this confirms that the motions of an object placed within the tank can be reliably found when placed in a wave field. This is

important as extreme motions can stress and crowd the fish within a cage. Such motions also have implications for the structural and fatigue design of any floating object and may require special consideration dependant on the motions' magnitudes.

Firstly, it is important to define what is meant by hydrodynamic response
These refer to the magnitude of motion within the 6 degrees of freedom – Surge, Sway, Heave, Roll, Pitch and Yaw. These are shown more clearly in Figure 30

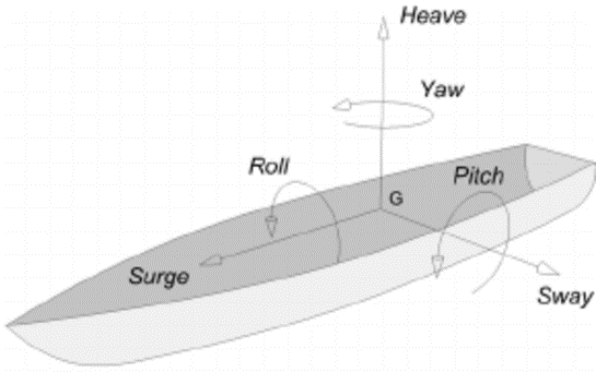

Figure 30 - Degrees of freedom in relation to a floating vessel (Miguel, 2011)

If these magnitudes can be appropriately understood and predicted - safety, viability, and operability of the cage can be more easily defined.

Often these motions are condensed into Response Amplitude Operators (RAO's) which define the response motions in terms of the incoming wave height. Where translation motions are metre of response/ metre of wave height (m/m) and rotational motions are degree of rotation response /metre of wave height (degree/m). These are detailed below in Table 4 It should be noted here, that as all cases are two-dimensional, sway, roll and yaw are restricted and so will not be measured or commented on.

The motions of the cages were recorded with the use of the OpenFOAM solver SixDofMotion combined with wavesDyMFoam, which allows a mesh to flex and move. This occurs by effectively "re-meshing" at every time step, once a solution for the previous step has been calculated. Thus, allowing the object to float and move within the tank, this is more clearly detailed by Figure 31 which shows the flow of the solver as part of the CFD computation process.

Table 4 - Response Motions, corresponding Axis and RAO Units

Translational Motion	Axis	RAO Unit
Surge	X	m/m
Sway	Y	m/m
Heave	Z	m/m
Translational Motion	Axis	RAO Unit
Roll	X	Degree/m
Pitch	Y	Degree/m
Yaw	Z	Degree/m

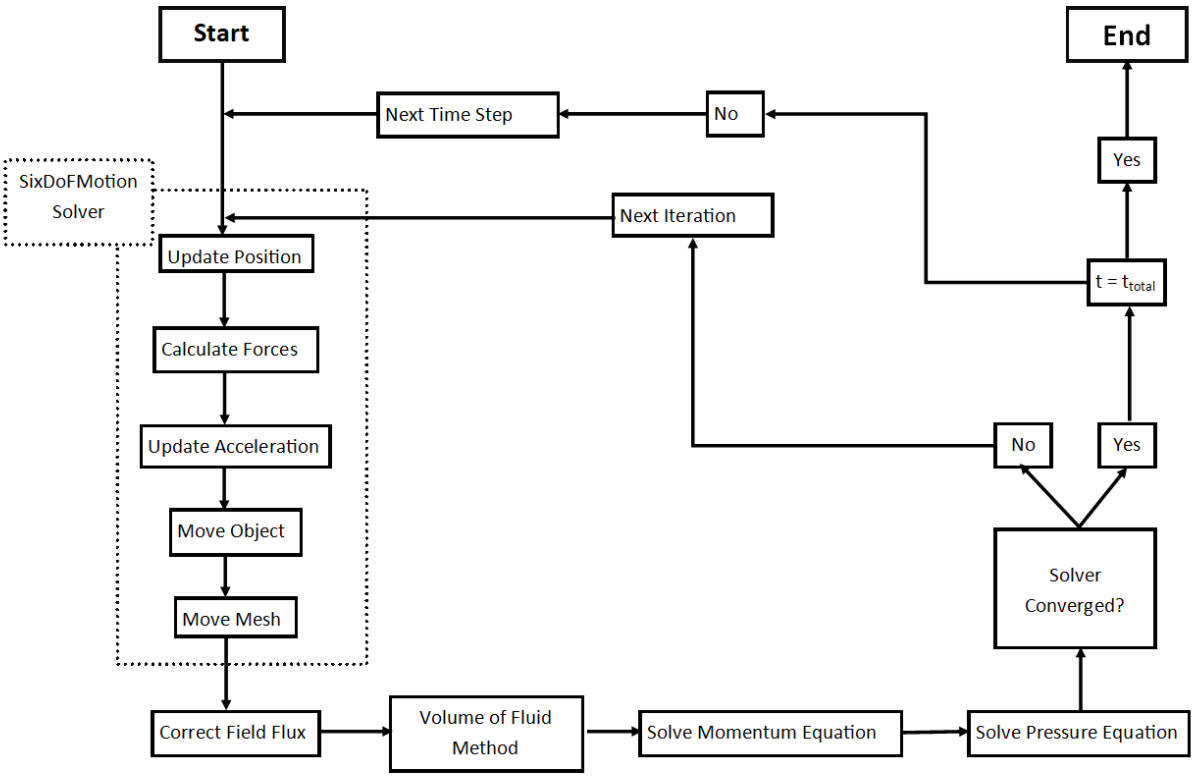

Figure 31 - Re-meshing solvers as part of the CFD computational flow

To have confidence in the motions calculated by OpenFOAM they were compared against physical wave tank experiments. The tank tests were again undertaken by Ren et al(2015) and the set up used is shown in Figure 32. All motions in the experiment were compared. Such a comparison allows verification of the translational (Heave and Surge) and rotational (Pitch) motions, ensuring that the motions of a freely floating 2D case in OpenFOAM are reliably calculated.

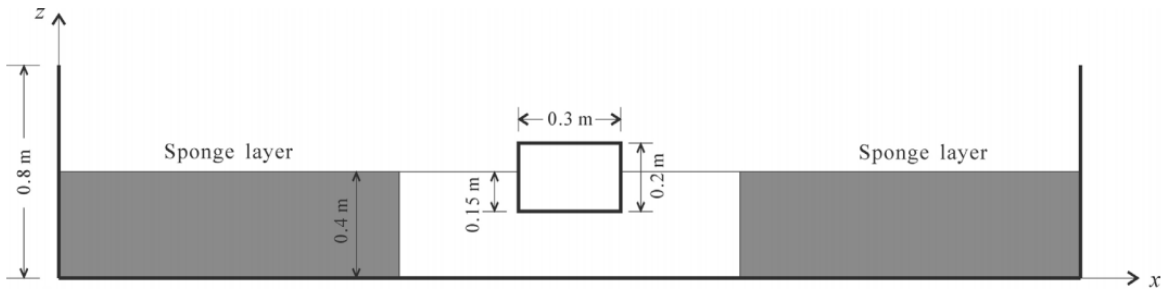

Figure 32 - Wave Tank Experiments Ren et al. (2015)

Mimicking the water depth (0.4m), block size (as shown) and wave parameters (T=1.2s, H=0.04m) a comparison could be made of the CFD calculated motions with the motions recorded in experiment.

As can be seen from Figure 33, the vertical (heave) motion showed very strong agreement with only a slight under prediction at peaks and troughs, in line with the error found during mesh convergence of approximately 4%, and the error found when checking wave generation for Stokes 2nd Order Wave Theory.

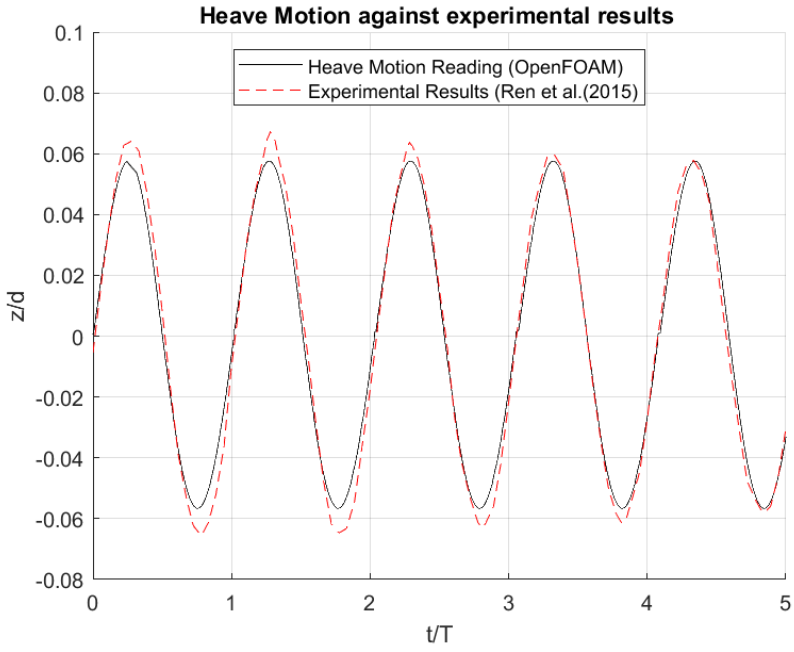

Figure 33 - Validation of Heave motion against experiments (Ren et al. (2015))

Similarly, the other two-dimensional translational motion, surge, was also checked. The agreement between OpenFOAM and the Experimental results showed good agreement in regards to period(See Figure 34). The calculations of surge magnitude showed a weaker agreement, with a maximum

percentage error of 8%. This may be due to an issue with the draught of the box, which initially took time to settle to floating equilibrium. This suggests that the submersion of the box in relation to the density used does not directly match that used by Ren et. Al (2015). Thus, with a change to fore/aft area submerged, the surge motion would increase/decrease, without directly affecting the heave motion.

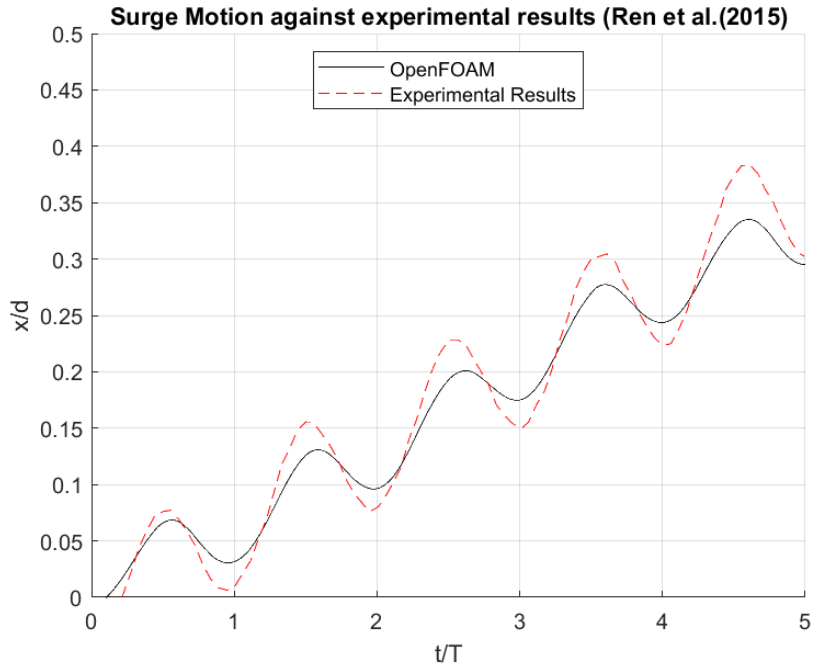

Figure 34 - Surge Motion comparison of Experimental results against those calculated in OpenFoam

The two-dimensional rotational motion, pitch, also showed reasonable agreement. Again, the periodicity showed strong agreement, with the magnitudes showing reasonable agreement despite a maximum error of 10.2%. This difference may arise from the box being treated as a single homogenous material within OpenFOAM, with centre of mass at centre of geometry. There is not indication as to the centre of mass of the box used during the experiment by Ren et al.(2015) despite an average of 500kg/m^3 being given.

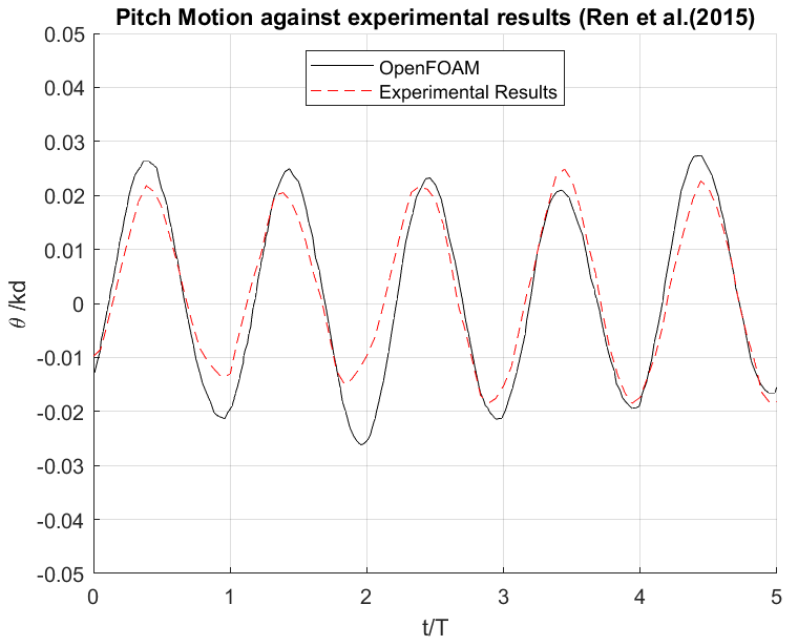

Figure 35 - Pitch Motion comparison of Experimental results against those calculated in OpenFoam

It is clear from the above that through the creation of a CFD Numerical Wave tank, a reliable model can be made.
Accurate wave input can be generated regardless of the theory, whether its Cnoidal, Linear, or Stokes 2nd Order wave theory.
Reflection, ordinarily present within a physical wave tank can be significantly reduced and with enough fine-tuning could be almost eliminated, something not economically possible when using a physical tank.
Following a mesh-convergence to foster accuracy, forces can be reliably recorded, giving insight into the mooring and structural design required for the object in question.
Finally, utilising specialist solvers, an object can be made to flow, and allowed to move freely within the wave tank. This floating object's motions can be recorded and done so with accuracy.
Ultimately this all lends itself to a quicker, more reliable, more economic, and dependent on size, safer method of analysing a floating structure. However, how can this be used within the realms of floating fish cages as a tool for design in the aquaculture sector?

4.5. Application of CFD toward fish-cage design and assessment.

To demonstrate the applicability of CFD as a tool to design and analyse floating fish cages, attempted testing of a sample cage was undertaken. The selected cage is currently situated offshore in the west of Scotland, near the coast of Colonsay. The cage is currently operated by MOWI (formerly known as Marine Harvest). This cage was selected due to it's larger operational water depth of 15m, the availability of technical drawings indicating exact dimensions and the recent challenges which the cages have faced. In January 2020, during the rough weather and seas caused by storm Brendan, these cages suffered a failure, releasing over 73000 salmon at great economic and ecological cost (Coastal Communities Network Scotland, 2020).
As such, there is obvious interest in understanding how the cage behaves when placed under various wave conditions which could give insight into the cause of failure.

The cage measures 40.75m across, and 2.7m in draught. These measurements are visually shown in Figure 36 and Figure 37. The dimensions for the cage used on this site are taken from the local planning department for Argyll and Bute Council (MOWI, 2019). The original planning documents outlining the cage are available in Appendix 1.

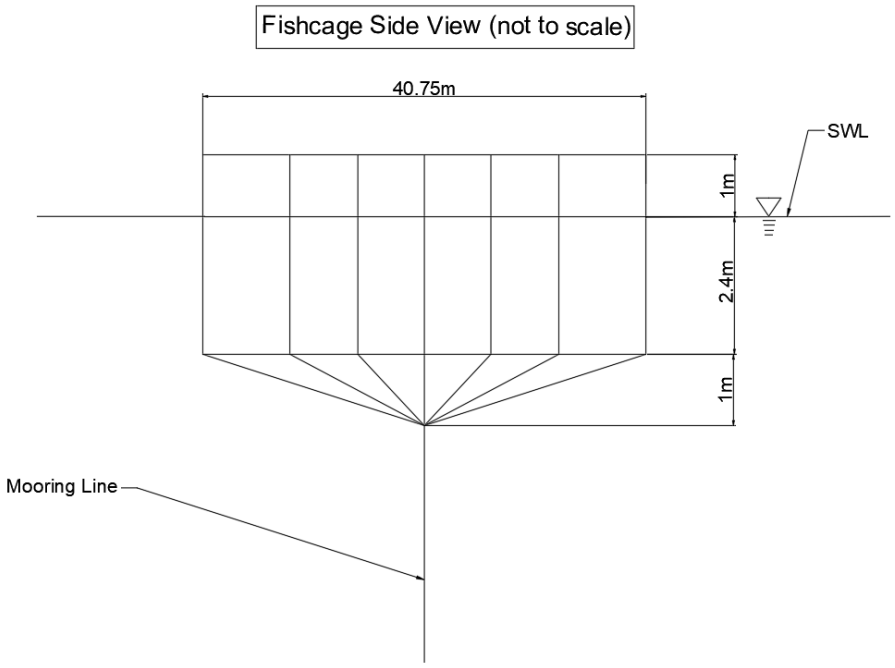

Figure 36 - Side Elevation of MOWI fish cage (Colonsay)

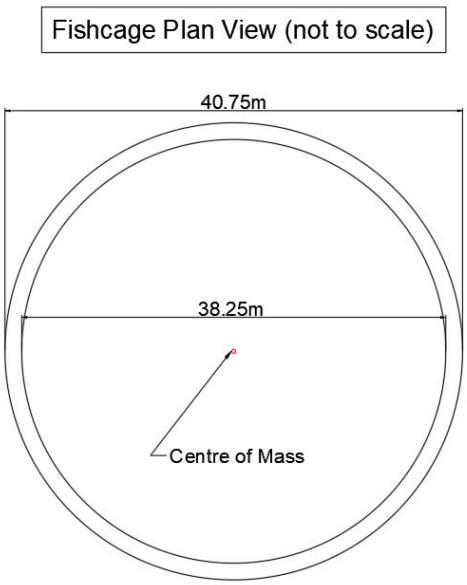

Figure 37 - Plan View of Mowi fish cage (Colonsay)

Due to issues with the dynamic-meshing, this geometry unfortunately had to be abandoned. This was down to time constraints however given enough time these issues could be ironed out, and this exact geometry used. As a replacement, a similarly shaped object was used. Representative of the length and depth of the depth of the industry cage mentioned above, with a sloping shape below the waterline. This will allow a full assessment of a cage like object under multiple conditions to give an indication as to the changing forces acting on and motions of a cage. It will also allow exploration of how a cage affects the fluid filed surrounding it. The cage shape used is shown in Figure 38.

Figure 38 - Selected Cage geometry within OpenFoam

4.6. Cage Assessment Wave Conditions.

In order to achieve a strong understanding as to the behaviour of an object when interacting with waves, a total of multiple cases were undertaken, all within a consistent waterdepth, but various wave heights and periods. Ideally, when assessing the behaviour of a cage, waves which are found at the deployment site should be used – this would give a direct indication of how a specific cage would fare in a specific site. However, due to the required cage modification, this was no longer relevant. As such the below waves were chosen to give a broad spectrum of assessment.

The waves used in these cases were selected to explore the impact a change in height, and a change in period have on interactions between the cage and the wave/fluid. The heights and periods were chosen in accordance to the previously mentioned Le Mehaute's Chart, this allowed for Cnoidal, Linear, and Stokes 2nd Order wave theories to be used across the cases.

To isolate and properly understand the effect of a change in wave height, the period, waterdepth and cage geometry were consistent as wave height was changed. Similarly, when investigating wave period, all other variables remained the same as period was modified, thus isolating the effects of a change in period.

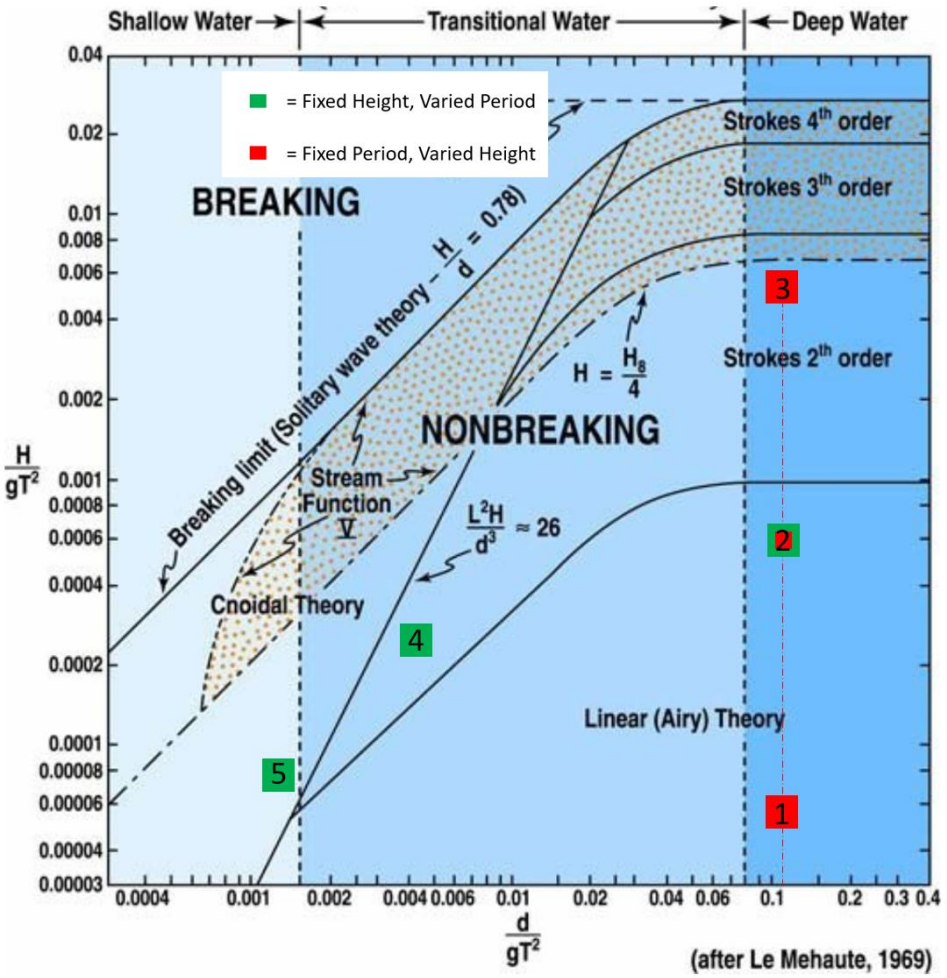

Figure 39 - Selected waves' locations relevant to Le Mehaute Chart

In Figure 39 the locations of the waves selected can be seen. Those where only height was changed are shown by red squares. Those where only period was changed are indicated by green squares. The numbers within these squares correspond to the number of the wave as shown in Table 5.

Table 5 - Wave particulars used in Simulations

Number of Wave	Height (m)	Period (s)	Depth (m)	Wave Theory
Wave 1	0.0002	0.6	0.4	Linear
Wave 2	0.002	0.6	0.4	Linear
Wave 3	0.02	0.6	0.4	Stokes 2nd Order
Wave 4	0.002	2.9	0.4	Stokes 2nd Order
Wave 5	0.002	5.2	0.4	Cnoidal

It should be noted that Wave 2 acts as base point from which the other waves were decided. This was done to allow for a clearer understanding of how a wave, and cage behaviour changes as either parameter is moved from a single common point.

The cases incorporate a fixed object, a freely floating object, and a moored object of identical geometries which allowed investigation into the changes caused by securing an object differently. These three securing types, combined with the five waves, meant 15 cases were required.

Table 6 - Case number, cage condition, and corresponding wave

Case Number	Fixed, Free Floating, or Moored Condition	Selected Wave
Case 1	Fixed	Wave 1
Case 2	Floating	Wave 1
Case 3	Moored	Wave 1
Case 4	Fixed	Wave 2
Case 5	Floating	Wave 2
Case 6	Moored	Wave 2
Case 7	Fixed	Wave 3
Case 8	Floating	Wave 3
Case 9	Moored	Wave 3
Case 10	Fixed	Wave 4
Case 11	Floating	Wave 4
Case 12	Moored	Wave 4
Case 13	Fixed	Wave 5
Case 14	Floating	Wave 5
Case 15	Moored	Wave 5

4.7. Tank Dimensions

The wave tank was kept identical wherever possible, both for comparability of results, and ease of operation. This helped ensure stability of the cases within the timeframe due to using a tank shown to work. The mesh size was consistent across all cases, using Mesh 3 from SECTION. The wave relaxation zone was varied dependant on the wave theory used. As per SECTION, 2 wavelengths were used to reduce the reflection at the object, and avoid incidental modification of the wave conditions due to said reflection. This ensured the reflection due to the tank was, at most, 6% or incidental wave. The exact particulars of the tank can be found in Figure 40.

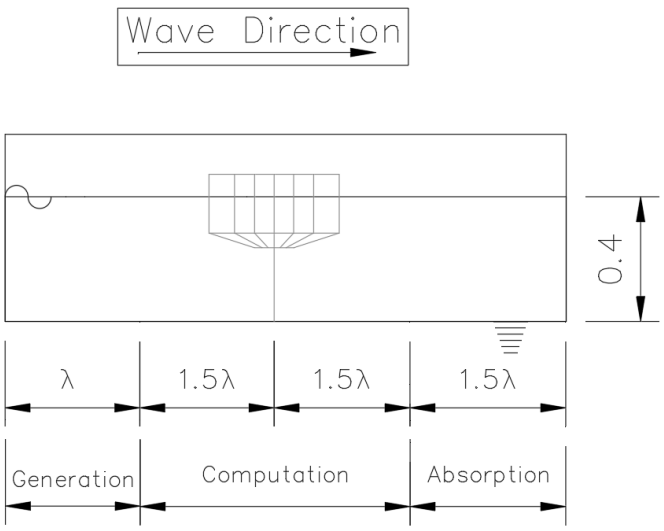

Figure 40 - Numerical Wave Tank with location of cage specified

4.8. Initial Conditions

The CFD simulations within this project are undertaken in two-dimensions, with incompressible and homogenous water at a constant temperature, where the density of water, ρ, is 1.025 x 10^3 kg/m^3. The water is set to have no current flow, i.e stagnant until waves are introduced. The air is set to 1.2 kg/m^3 and is also treated as homogeneous throughout the simulation

4.9. Boundary Conditions

The conditions for the boundaries within the tank are shown in Table 7 and Table 8. These define how a fluid behaves in regards to interaction with the boundary. The location of the boundaries are shown in Figure 41.

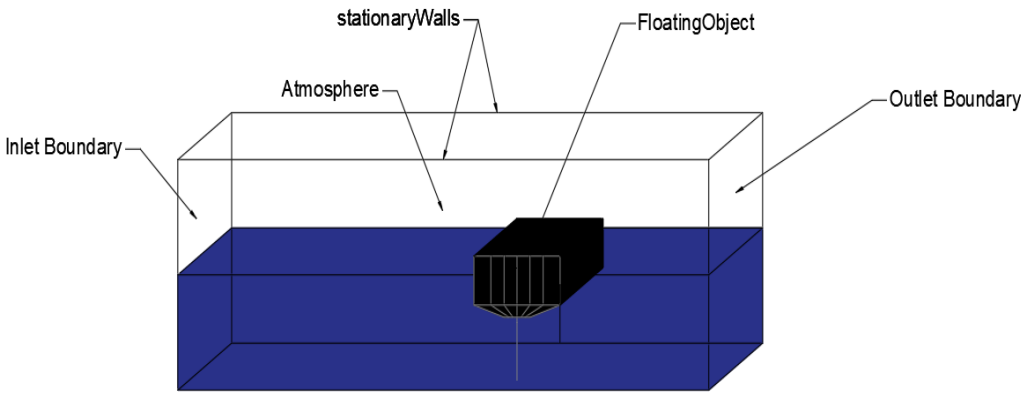

Figure 41 - Location of Boundaries of NWT with Cage in place

Table 7- Velocity Boundary Conditions

Boundary	Boundary Type
Inlet	waveVelocity
stationary Walls	noSlip
Outlet	fixedValue
Atmosphere	pressureInletOutletVelocity
floating Object	movingWallVelocity

Table 8 - Pressure Boundary Conditions

Boundary	Boundary Type
Inlet	zeroGradient
stationary Walls	fixedFluxPressure
Outlet	zeroGradient
Atmosphere	totalPressure
floating Object	fixedFluxPressure

Where:

- waveVelocity – The water velocity at this boundary is defined by the incoming wave, but is otherwise zero i.e stagnant.
- noSlip – fixes the velocity to zero at the boundary.
- fixedValue – The fluid is moving at a constant, fixed value, here specified to be 0 m/s.
- pressureInletOutletVelocity – Applies gradient to all components, here, zero gradient was specified.
- movingWallVelocity – provides a velocity condition for cases with moving walls.
- zeroGradient – Pressure gradient is equal to zero perpendicular to the wall.
- fixedFluxPressure – sets the pressure gradient to value so the flux at boundary is set by the velocity boundary condition.
- totalPressure – calculates the pressure based on velocity and total pressure (set to zero in this case).

4.10. Moored Cases

There was one modification made to the fixed/free floating cases for all moored cases. The mooring was applied using a linear spring attached at the lowest point of the cage, in the middle of its length (see Figure 42). The mooring was attached to the 'sea bed' directly below this point on the bottom boundary of the tank .

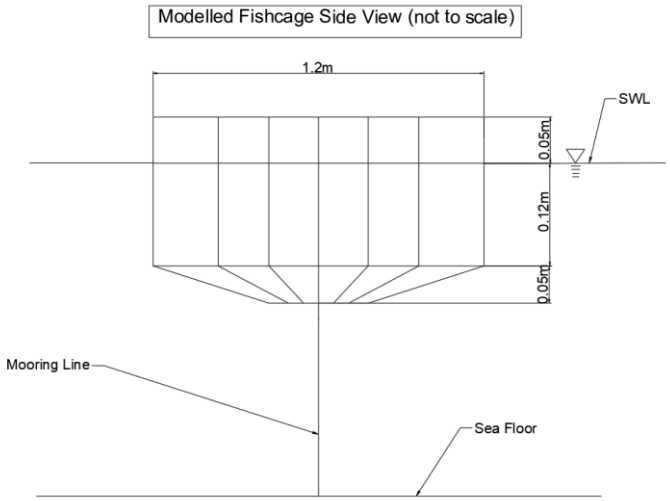

Figure 42- Schematic of modelled cage with exact dimensions as used in OpenFoam

The strength of this spring was determined by using the spring force equation (Equation 18) solving for the spring constant.

$$F = kx \tag{18}$$

Where F is the force of the spring, x is the stretch of the spring, and k is the spring constant. The stretch of the spring, x, was taken as 50% of the maximum positive heave motion from Case 5.

Similarly, spring force, F, was taken as 50% of the force caused by the incoming wave in Case 5. Case 5 was selected as the wave used in that case is a common point of the two areas of investigation. Change in wavelength and change in wave height. The values involved in this calculation are shown in Table 9.

Table 9 - Values used in the calculation of spring constant

Spring Force Calculation Values	
Component	Value
F	5.7N
X	0.0015m
K	3800 N/m

Thus, using the above NWT, wave particulars, and cage conditions, all 15 cases were simulated. The results of which are explored and discussed below.

Chapter 3

Results, Discussion and Project Conclusions

This chapter will review the outcomes of the simulations undertaken in regards to nonlinear wave interaction with a floating fish cage. This chapter covers computational times, forces, hydrodynamic motions, pressure and velocity fields accompanied by discussion and culminates in conclusions on the project as a whole highlighting the achievements and shortcomings in relation to the objectives defined in Chapter 1.

5. Results and Discussion

Before reviewing the cage's interactions with the wave field, the execution times for each case should be noted. All cases were run for 10 wave periods, this allowed time for the wave to be generated, reach the cage, and have 6 waves pass the cage before the simulation was terminated. All cases were run on one node within the University of Dundee Mathematics computing cluster. Each node comprises of a pair of Intel Xeon E5-2697A CPUs @2.60GHz, each has 16 physical cores, hyper-threading for 32 logical cores (so 64 logical cores per node), The nodes each have 64GB RAM (2GB per physical core). The time-step was consistent for all simulations at 0.0002s, with saving of values every 0.1s. The execution times are shown in Table 10.

Table 10 - Execution Time of each case

Case Number	Computation time (hrs)
Case 1	1.593836
Case 2	3.2818
Case 3	3.790806
Case 4	1.206706
Case 5	5.655344
Case 6	3.792222
Case 7	2.165833
Case 8	5.891111
Case 9	3.022086
Case 10	2.062797
Case 11	5.441111
Case 12	5.42667
Case 13	1.954697
Case 14	4.9745
Case 15	5.404

As is to be expected, cases where the cage was not moving were completed in significantly less time, this is because no meshing is required between each time-step to allow the object to move and float. Whilst there was a jump between freely floating and moored cases in terms of execution time, this difference is insignificant when compared to the total runtime, however this does show that the more complex a case, the longer it will take to run.

5.1. Forces

The forces acting on the cage were measured in both the Horizontal (X) direction, and the Vertical (Z) direction for all cases. This allows a comparison not only between how a change to the wave height or period affects the cage, but also the effect changing the constraint condition has on the forces acting on the cage. Though maximums are looked at in-depth here, full time-series plots of the forces can be found in Appendix 2.

5.1.18. Change in Wave Height

As can be seen be seen below in Figure 43, a total of 9 cases were run to compare how a change in wave height affects forces acting on the cage. The upper plot displays the maximum (magnitude) of force felt by the cage across the entirety of the simulation in the horizontal direction. The lower shows the maximum of all vertical forces. The wave height increases from left to right by a factor of ten each time.

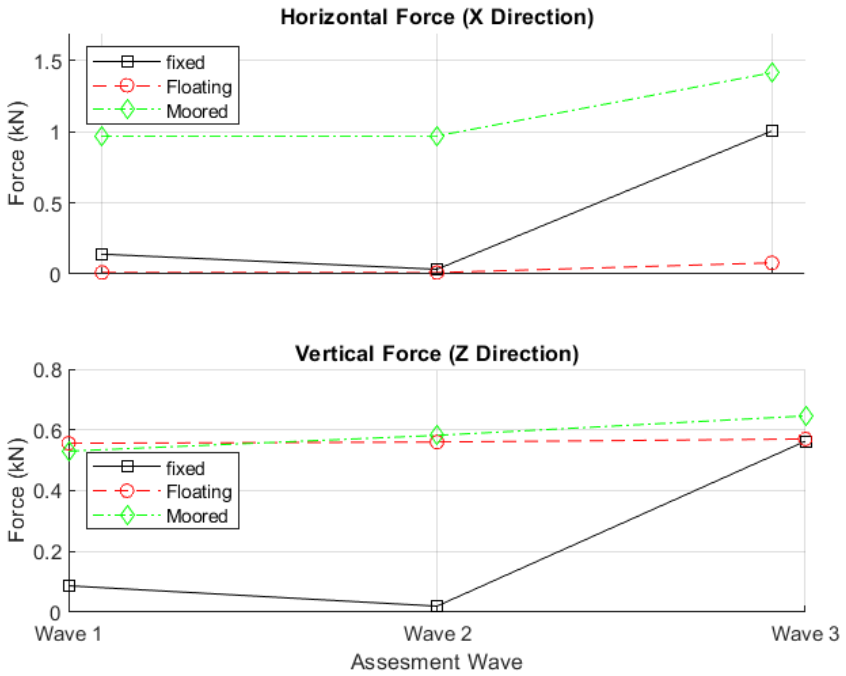

Figure 43 - Forces in acting on the cage as wave height changes, assessing 3 cage conditions

As can be seen from the above figure, there are two major trends present. Firstly, as wave height increases, forces in both directions generally increase. There is however a smaller increase between waves 1 and 2, compared to waves 2 and 3. This indicates that the wave height relative to the cage may be an important factor in the level of force applied to the cage. Secondly, the moored cage fares the worst in terms of forces applied. We see in the horizontal direction that both fixed and floating cages felt comparatively little force which indicates that allowing a cage to move places little risk in the horizontal direction, but the addition of mooring (perhaps improperly) causes a spike in the forces felt. Conversely this isn't true in the Z direction, where vertical forces on both floating and moored cages was roughly equal. This suggests that the mooring applied has little to no effect in the vertical direction.

5.1.19. Change in Wave Period

As can be seen be seen below in Figure 43, again a total of 9 cases were run to compare how a change in wave period affects forces acting on the cage. As above, the upper plot displays the maximum (magnitude) of force felt by the cage across the entirety of the simulation in the horizontal direction. The lower shows the maximum of all vertical forces. The wave period increases from left to right where wave 2 has a shorter length than the cage, and waves 4 and 5 are longer than the cage.

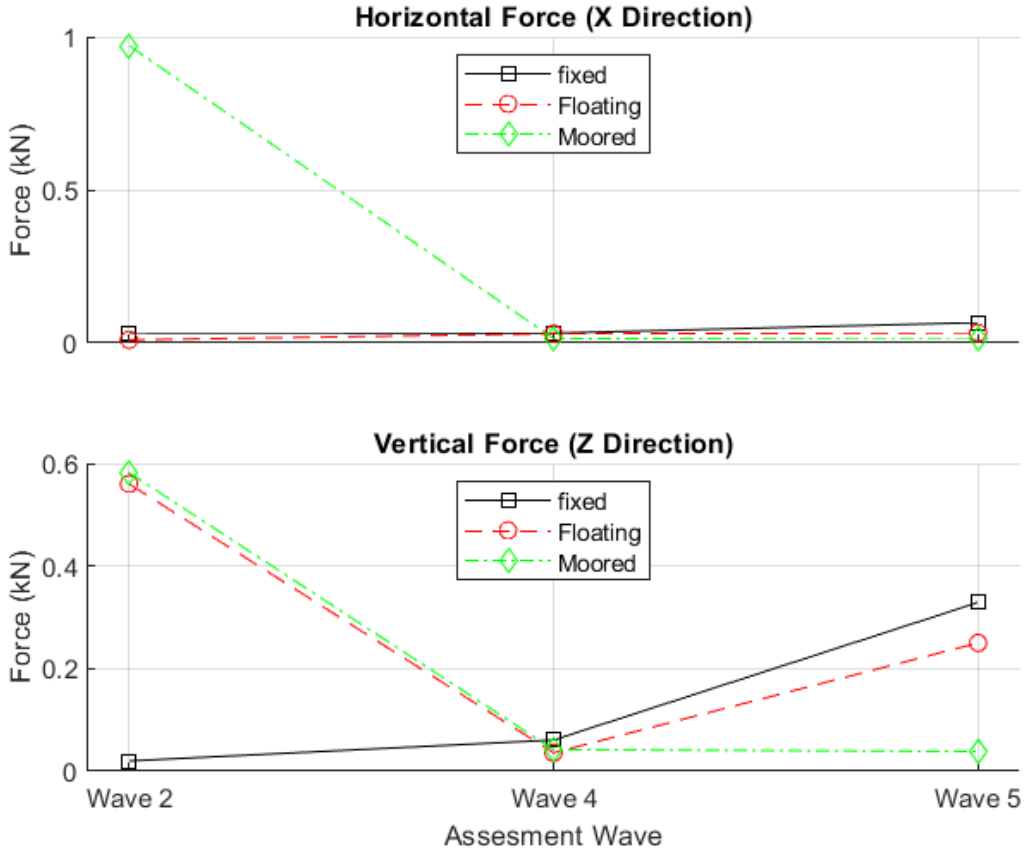

Figure 44 - Forces in acting on the cage as wave period changes, assessing 3 cage conditions

Figure 42 suggests, for both vertical and horizontal forces, a fixed cage will fare best when the wavelength is shorter than the cage. This may be due to a reflection of the wave, preventing little to none of the energy to pass beneath/through the cage as the cage is fixed, limiting the vertical force. However, when the cages are subject to a longer wave, all forces in the horizontal direction drop, though they rise again (marginally) for the longest wave, wave 5. The same is true in the vertical direction where forces on the floating cages drop for a longer wave, and rise again, though to a larger extent, for the longest wave. Where the waves are longer than the cage, the fixed cage has the greatest force acting up on it.

These four plots show useful trends which could be explored when designing a fish cage. For example, if the cage is to be fixed rigidly in place, then it should be much larger than the wave height it is to be deployed in, and longer than the wavelength. This will help reduce the forces acting upon it, and improve the likelihood of survivability of the cage. Conversely, if utilising a floating cage design waves which are shorter than the cage appear to apply less force to it. However, there seems to be a 'sweet spot' in terms of length, as we see in **Error! Reference source not found.** The longer w ave applies the least force to the cage, but under the longest wave, force begins to build. Thus, when designing the cage dimensions, multiple cases could be run to find the ones suitable for the selected site in terms of wave height and length.

That being said, what can we draw from these readings in regards to the cage condition. Taking the average of the maximum forces for fixed, floating and moored cages in the X and Z directions yields some answers (Figure 45)

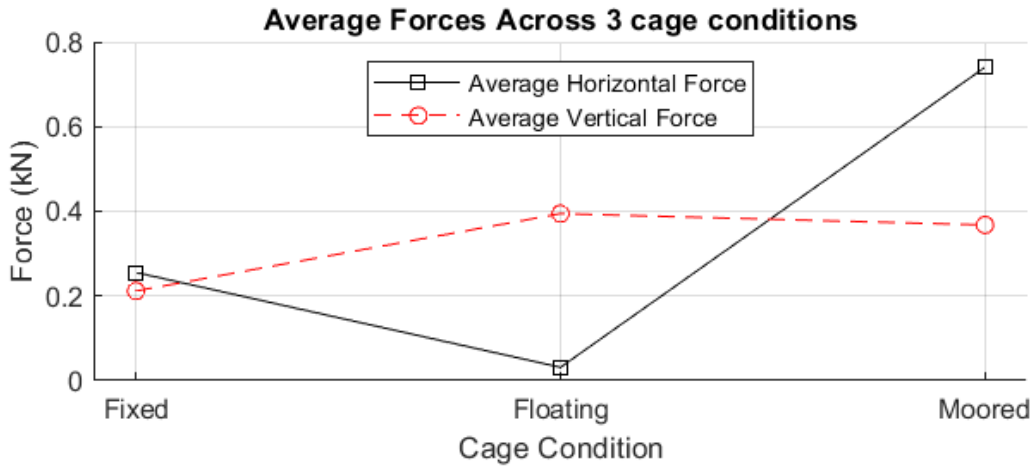

Figure 45 - Average of Maximum forces in x and z direction

It is clear from the above plot that there are trade-offs to be had with each cage restraint condition. Fixing the cage in place allows for the lowest forces acting on the cage on average, but may come with other limiting factors such as water-depth and economic cost. Moving the cage to a freely floating condition reduces the horizontal force, but increases the vertical force by roughly the same amount. If the cage was designed to better withstand vertical forces, this may be the best option (provided it could be secured somehow to prevent it floating away). Lastly, utilising the mooring used her provides a small reduction in vertical force, but a large increase in horizontal force, suggesting that the mooring has little to no effect in the vertical direction. Although, with further research and continued adaption, a suitable mooring configuration could possibly be found which reduces these forces, moving them closer to the levels seen by the freely floating cage.

As with all engineering challenges there are trade-offs. In reducing the forces on a cage. Great expense, or shallower waters are required to fix the cage in place, and mooring the cage requires structural strength in the horizontal direction potentially also at large cost. However failing to moor the cage would probably result in the total loss of the asset. Regardless of this, CFD clearly provides the information a designer would need in order to make these decisions.

5.2. Motions

The motions of the cage are also an important factor in cage design. This demonstrates the effects of various waves on how the cage reacts within the wave field, and is important to understand in this application as excessive motion can stress and harm the health of fish within the cage. These motions may also give insight into harmful behaviors that could be minimized to lengthen the lifespan of the cage.

5.2.20. Heave Motion

Heave motion was assessed for all 15 cases. Comparisons here are made between cases which share wave period, or wave height. Fixed cases are ignored as there is no motion of the cage present within them. All cases have been non-dimensionalised by period along the horizontal axis.

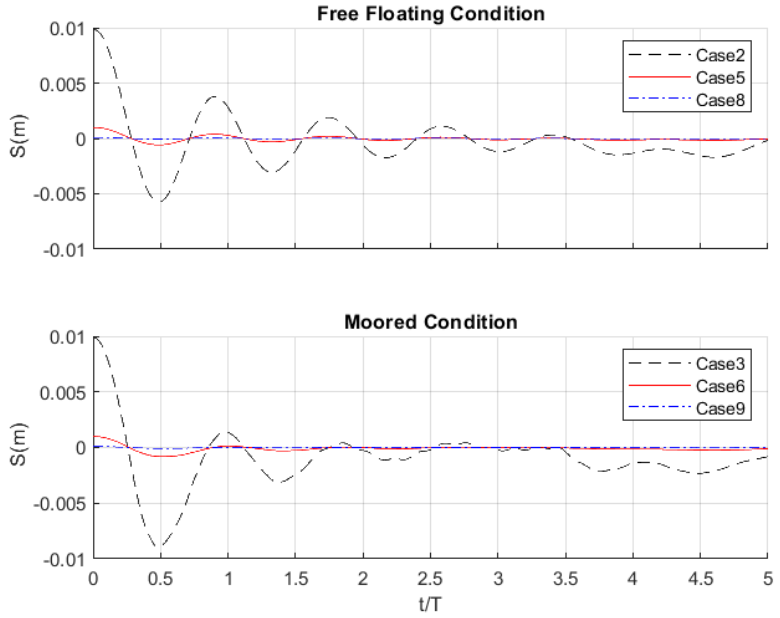

Figure 46 - - Heave motion of Free-Floating (upper) and Moored (lower) cages as wave height changes.

Figure 45 shows the cage's reaction to incoming waves of various heights, increasing in size from case 2, to case 8 for a freely floating cage, and case 3 to case 9 for a moored cage. Interestingly, in the upper plot, the magnitude or the crests are reducing, and the length between them increasing. Toward the end of the plotted data, two waves also occur consistently below the still water line This may show a clear effect the cage has on the waves approaching it. It is believed that as the first wave passes the cage, some of it could be being reflected back toward the incoming wave, reducing the height and modifying the speed of the 2nd incoming wave, this occurs again and again to all approaching waves, resulting in unexpected motions toward the end of the plotted data.

For the moored condition, similar events are believed to be occurring. This is only accelerated by the mooring, which is further reducing the movement of the cage, creating a larger reflection than a freely floating case, it is believed . As such, the waves are reduced in size quicker.

To ensure the motion was a direct response to the correct incoming wave, the waveGauge data, 0.5 wavelengths after the generation zone was plotted, see Figure 47. This shows that the software was behaving as expected and as such the heave motion must be a true response, possibly caused by the geometry of the cage.

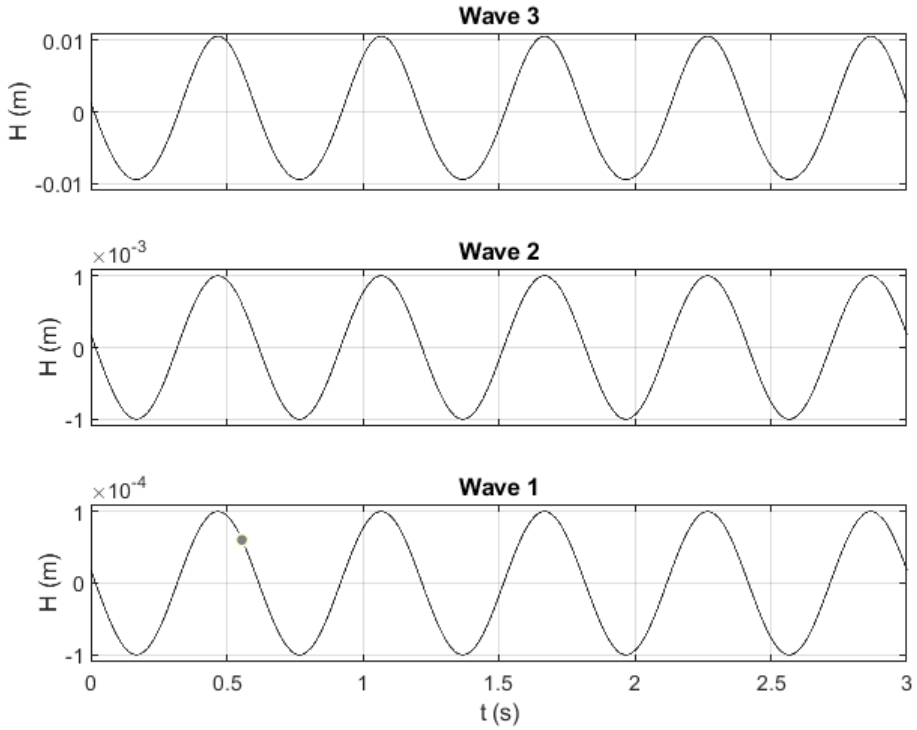

Figure 47 - Wave Gauge data confirming proper wave production.

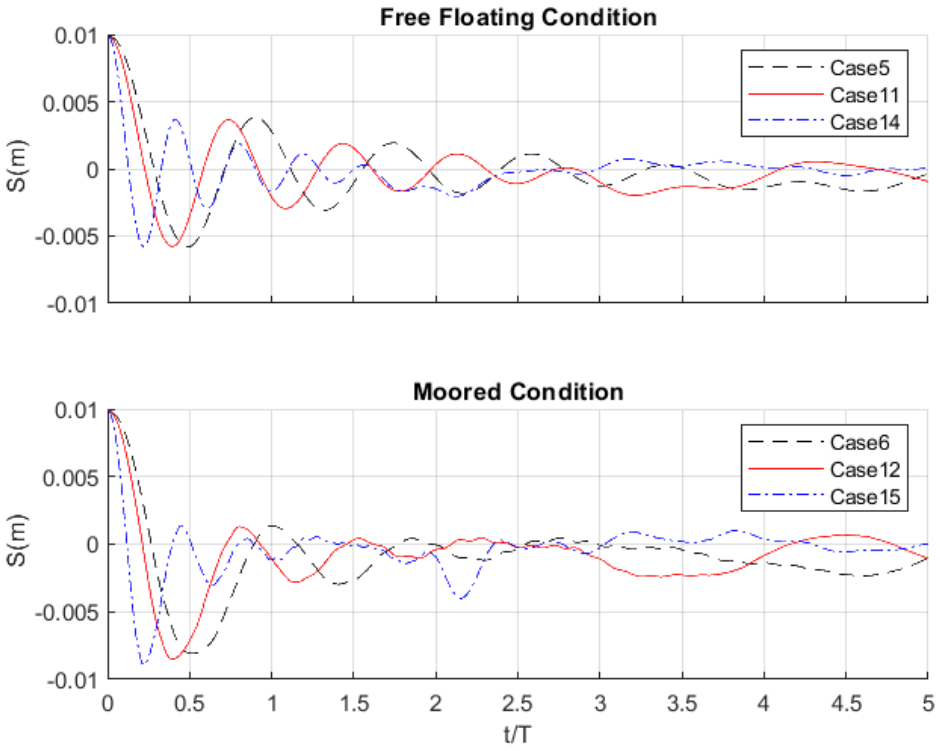

Figure 48 - Heave motion of Free-Floating (upper) and Moored (lower) cages as wave period changes.

The heave motion when period is changed shows a similar trend. The crest of the incoming wave is reduced as more and more waves reach the cage, drastically changing the incoming wave height and length, reducing the overall affect the incoming waves have on the cage. All cases here are modified at different rates, and initial analysis generally suggests that longer waves are reduced in amplitude faster. This trend of reflection can reasonably be expected, with cage design similar to floating breakwaters, where a large, HDPE pipe floating on a surface can be utilized for both structures. Designers may be able to use this to their advantage, by grouping cages. Those closest to the predominant wind/wave direction being designed to withstand greater forces whilst creating less energetic waters for cages in it's shadow. These shaded cages could then be built to withstand more subdued waves, yielding an economic benefit whilst maintaining the benefit of offshore waters. Determination of the reflection/transmission and insights that can be draw from the pressure/velocities are explored below..

Heave motions in relation to the cage are complicated by some effect, believe to be reflection from the cage. This appears to be present in every simulation and will continue to affect the assessment of all motions, however it does meet expectations in regards to the geometry/construction of the cage. The cage handles change in wave height as expected, where magnitude of the incoming wave dictates magnitude of response. This remains true across all cases, regardless of the period change. Further investigation is certainly required to truly clarify the cause these effects, though attempt is made to understand them below.

5.2.21. Surge Motion

Surge motion was also assessed for all 15 cases. Comparisons are again made between waves which have a different height, or waves which have a varying period. The fixed cage cases are ignored as no motion is present within these cases.

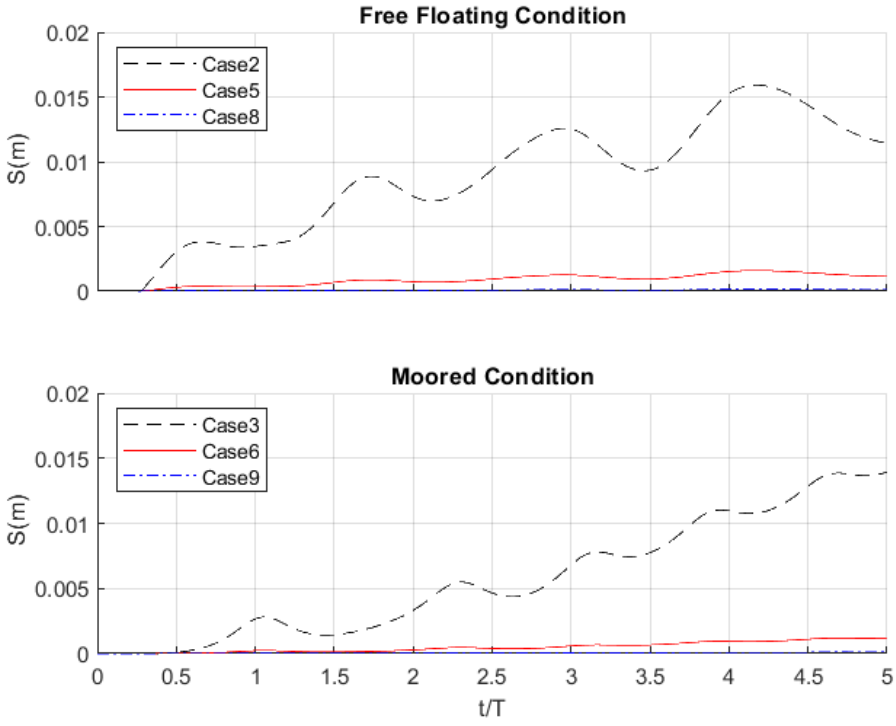

Figure 49 - Surge motion of Free-Floating (upper) and Moored (lower) cages as wave height changes.

As can be seen in Figure 49, the surge response of the cage is drastically affected by a change in wave height. However, there is also a large difference between the free floating and moored conditions where the moored condition shows only a slight difference in the overall magnitudes, but presents a different, smoother oscillation. This suggests that the mooring is too weak, but is having a moderate effect on the response of the cage. The peaks also show a change in magnitude and wavelength, though this is not as dominant as in the heave motions. Further investigation into the exact cause of the unexpected trends in motions would certainly deepen understanding of how best to handle these effects when designing cages.

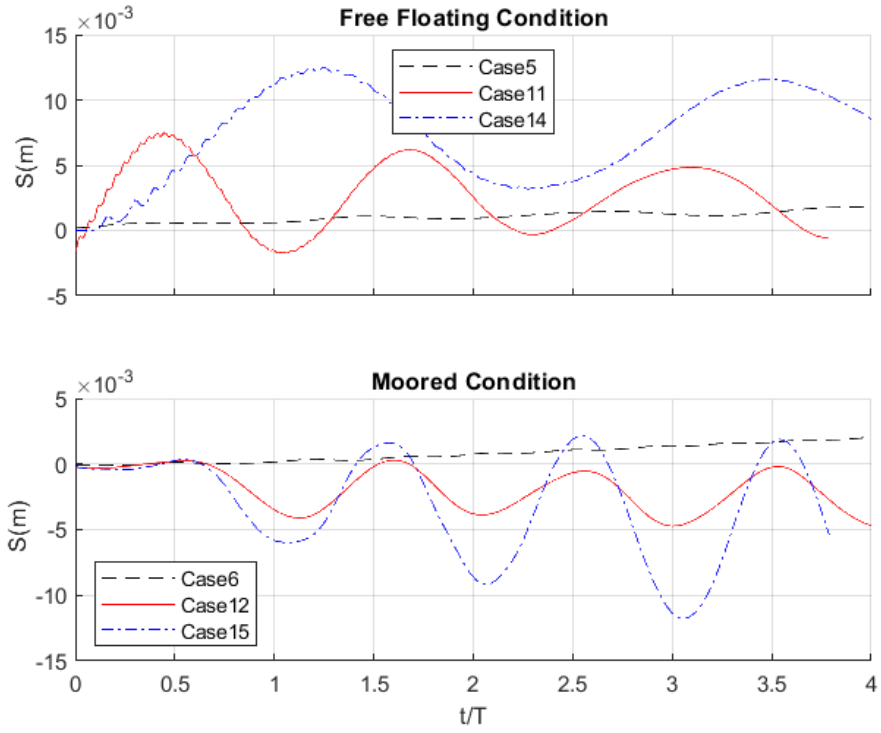

Figure 50 - Surge motion of Free-Floating (upper) and Moored (lower) cages as wave period changes.

Figure 49 continues the trend of a changing wave period/height. Here the magnitude of the motion is reduced by the mooring quite significantly – this is the largest restriction (comparatively) in motion seen across the 15cases when mooring is applied. Interestingly, the difference between the peak and troughs of the motion increases as wavelength increases however the distance from the original point does not increase. This implies that the wave height has a greater effect on the total surge drift of the cage, rather than the wavelength. This is another area which may benefit from further testing, particularly in experiments to confirm or dispute these trends.

5.2.22. Pitch Motion

As with the above, pitch motion was also assessed across all 15 cases. The below figures compare waves which change in height, or period across the two conditions which allow the cage to move, free-floating and moored. This is the only rotational motion assessed due to the two-dimensional nature of the simulations – i.e yaw and roll are not present within these cases.

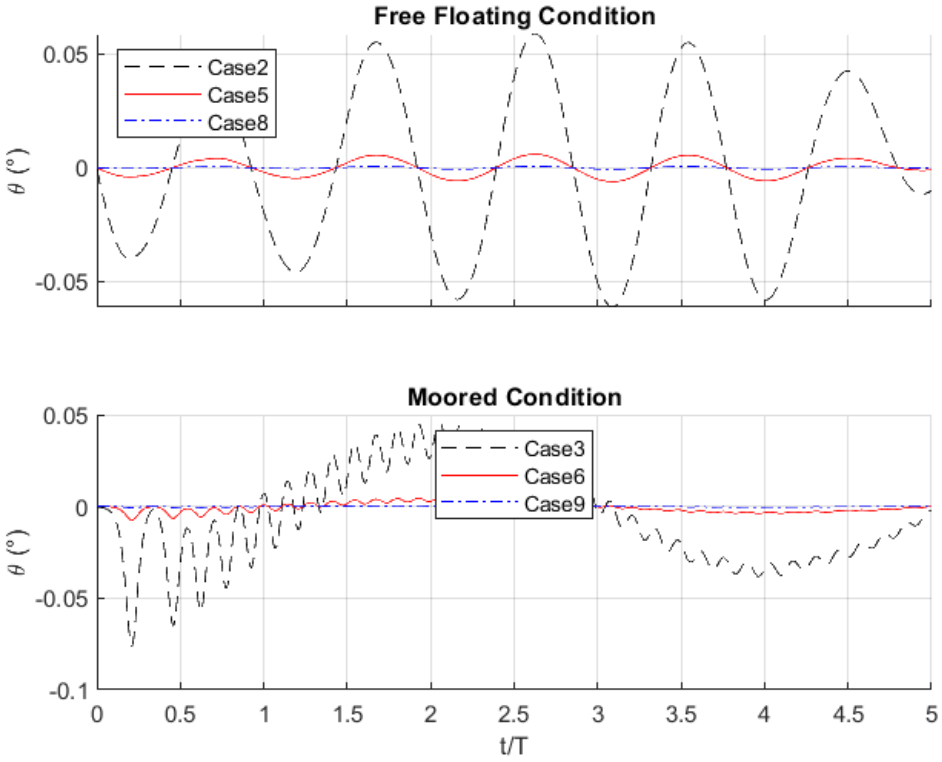

Figure 51 - Pitch motion of Free-Floating (upper) and Moored (lower) cages as wave height changes.

Looking at the upper plot of Figure 51, the cage behaved as expected. Each wave causing a slight pitching of the cage before righting itself as the wave passes by. This is similar to behavior seen on most freely floating structures, and was present when investigating the Ren et al(2015) experiments. The magnitudes vary in-line with the increase in wave height, i.e when height gets larger, the degree to which the cage pitches increases. This is largely due to the steepness of the wave (length/height), where the greater the height of the wave, the steeper the leading edge of the wave is, and so the cage responds with a larger pitching motion around the center of mass.

The lower plot which shows the moored condition for the cage and is not as originally expected, The cage is pitching to a much greater magnitude at almost three times the frequency. This implies that the single point of mooring is having a dramatic effect on how the cage is moving. It is thought that whilst the cage is attempting to pitch around its center of mass, the mooring at the base of the cage is restricting this, and may be pulling the cage back to its original position or otherwise causing this motion. This increased stiffness results in the cage pitching predominantly downward before changing to pitch upward only. It is unlikely that this is a desirable motion as much more frequent pitching places a repeated stress on the cage. This in turn results in a higher chance of failure through fatigue. This motion could perhaps be better constrained by using two mooring lines, secured at equal draughts on opposite ends of the cage. Though further investigation is required, it is thought that this would restrict the motion in a more uniform way, or closer to the center of mass and could prevent the rapid pitching that is seen here. This was not undertaken here due to time constraints.

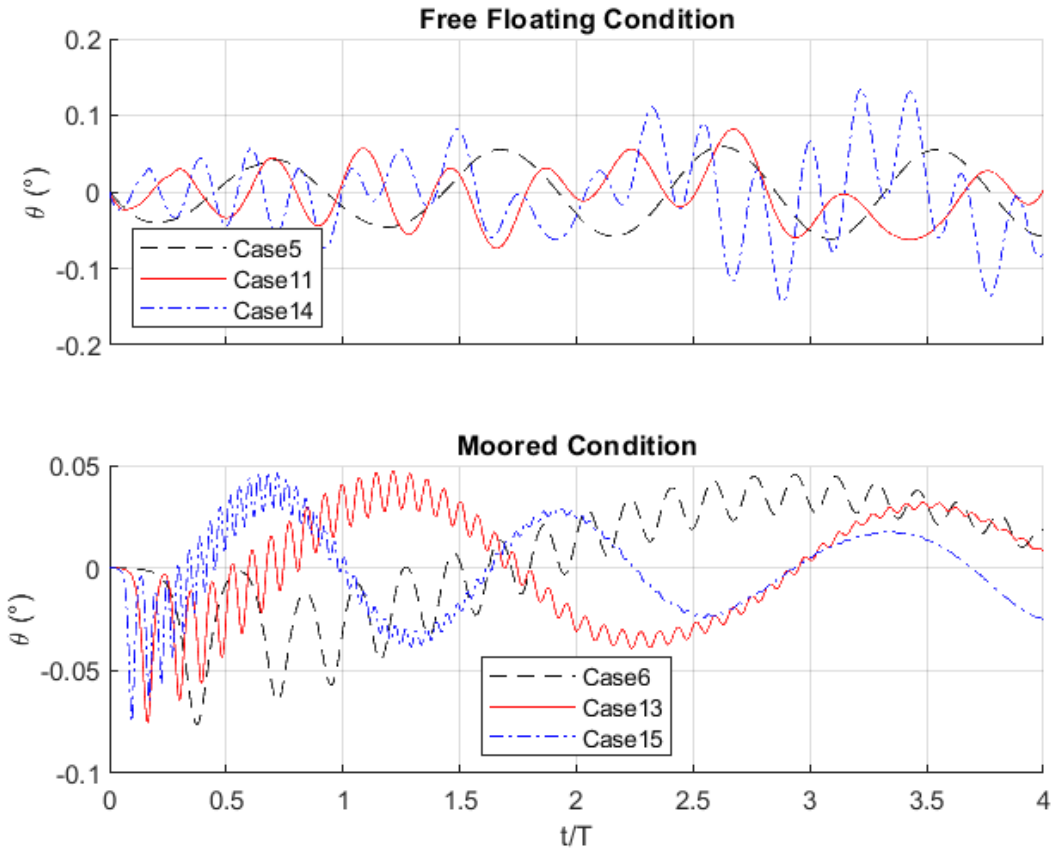

Figure 52 - Pitch motion of Free-Floating (upper) and Moored (lower) cages as wave period changes.

Figure 52 - Pitch motion of Free-Floating (upper) and Moored (lower) cages as wave period changes. Figure 52 shows the cage under 3 waves of varying wave periods but fixed wave height. As in Figure 51 the free-floating condition shows a slightly larger pitch magnitude than the moored condition. It appears here that the longer the wave, the more erratic the pitching will become, particularly un-constrained (freely floating) pitch motion. The increasing wavelength shows an identical increase in pitching frequency compared to the unmoored cases of the same wavelength. It also appears that as wavelength increases so does pitching frequency, though this is an unexpected result. It is believed this is a further consequence of inappropriate mooring and further highlights the need to plan and assess mooring of cages with these motions in mind.

We have seen from the above that usefulness of CFD in terms of cage assessment. The forces under which a cage must operate can be found, and useful insight can be taken from the differences between fixed, floating and moored cages. It has been shown that a totally rigid cage has a greater chance of surviving the tested waves than either of it's floating counterparts due to lower forces acting on it. This was true for both the horizontal and vertical forces but only when the cage is longer than the incoming wavelength. It has also been shown how a change in wave height and period can entirely change the way in which the cage interacts with the waves and the forces which act upon it. In general, smaller, longer waves produce less energetic and violent reactions of the cage so designers should make all attempts to produce cages which are short, relative to their operational site's wavelength. However said designers should also tread carefully around the subject of mooring. It is believed from the cases assessed here that incorrect/insufficient mooring can in fact harm the motions of the cage. This however requires further investigation, perhaps utilizing the same cases with modified mooring and assessing how response changes.

Despite this, it is obvious how CFD could be a useful tool in determining the motions of, and forces acting upon, a floating fish cage.

5.3. Fluid Behavior with Cage Present

The impact of the cage's presence in the fluid and how the fluid responds to the cage's presence is useful and important for a number of reasons. Firstly, by understanding how the fluid behaves with this structure in place, better decisions can be made when modifying or grouping designs. These decisions may stem from wishing to avoid certain levels of pressure, or velocities, or in fact utilizing them to achieve an objective such as faster flow through a cage. Secondly, it indicates the behaviors of the fluid in which the fish must survive. Is the pressure too high? Are velocities greater than those deemed acceptable for healthy fish/fish survivability. Here, the wave reflection, transmission, pressure field, and velocity field surrounding the cage is reviewed to give insight as to the fluid's behavior around the cage.

5.3.23. Reflection and Transmission around Cage

As above (see 4.3.15) the reflection and transmission coefficients can be determined at any point along the cage. This allows review of how the cage is affecting the incoming wave, and the wave height of the wave beyond the cage.

To measure this, 4 gauges were placed within the tank, 0.5 and 1 wavelengths away from the cage, fore and aft. As can be seen from Figure 53 the wave reflection for all cage conditions remained high, reflecting around 90% of the wave when fixed.

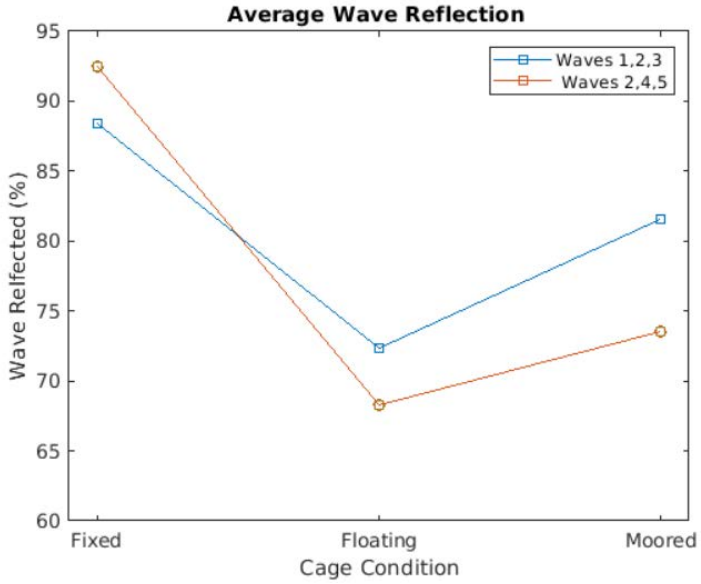

Figure 53 - Average Wave Reflection of the cage in 3 conditions

This explains the low average forces present across all fixed cases as the wave may have been reduced in magnitude by the reflection caused by the cage. Wave reflection reduced as the cage was allowed to move, possibly moving more with the motion of the wave than acting as a barrier to prevent it. This motion was restricted in the moored case and as such reflection again grew. Generally, as wavelength grew, for the fixed condition, wave reflection increased, but decreased in the floating/moored conditions. This is possibly due to a less steep wave, providing a smoother motion which may prevent the cage reflecting more of the wave back. Opposite trends were shown in transmission in Figure 54 where both floating cages allowed more waves to pass. The fixed cages had the lowest wave transmission, this is to be expected, as any fixed object act's more like seawall than a floating fish cage. There were unfortunately inconsistencies within this data, where the sum

of the transmission and reflection percentages were greater than 100. This implies energy is created within this model which cannot be correct. There may be an issue with the way the data is being sampled, or how the calculation is being undertaken though time unfortunately did not allow for this to be checked and corrected.

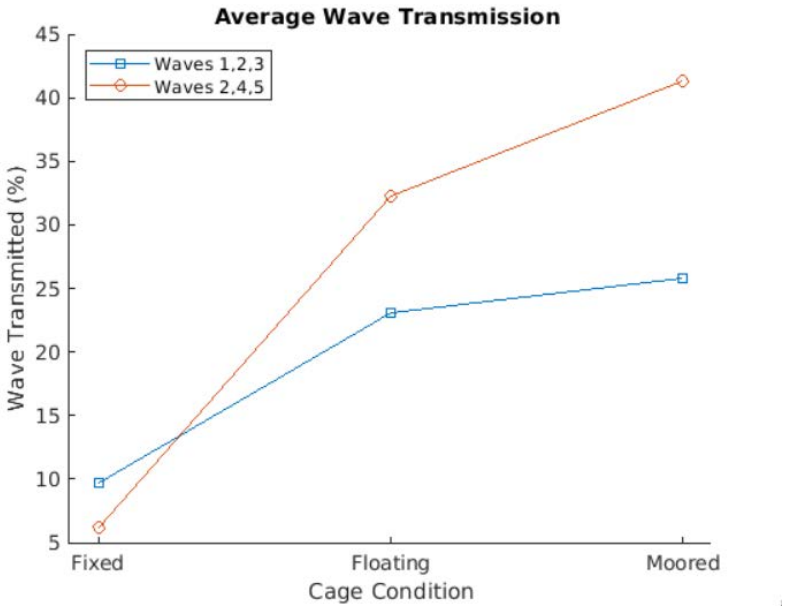

Figure 54 - Average Wave Transmission of the cage in 3 conditions

As such, these values should be treated with caution when determining their usefulness around aquaculture application. Especially where cages are to be grouped as this has an effect on how closely the design may allow them to be situated etc. Though these coefficients may be slightly bloated, it is believed their trends are true. Fixed objects in a wave will reflect more than the same object whilst floating, and when an object meets a wave longer than itself, it is less likely to reflect a larger portion of the wave.

5.3.24. Pressure Field

The pressure field for 3 cases were reviewed. Though there is the capability to review all cases both time, and computing hardware limited this. Throughout this project, emphasis has been placed on computational power and time, but the limitation here is storage. Each folder containing the case files comprised of up to 84gb, thus handling multiple cases became difficult, and results repetitive, so analysis was streamlined.
The cases investigated here were cases 4, 5 and 6 at t = 6.9s-7.4s i.e fixed, floating and moored at a wave height of 0.002m and a wave period of 0.6s. This time range selected was generally arbitrary, but represents one full wave period and was chosen to allow direct comparison between all cases reviewed. The pressure field reviewed has had hydrostatic pressure removed so as to distinguish waves/ wave effects within the plots.

The Pressure field plots for case 4, the fixed case, are shown in Figure 55 where the darker the colour, the greater the pressure in that region.

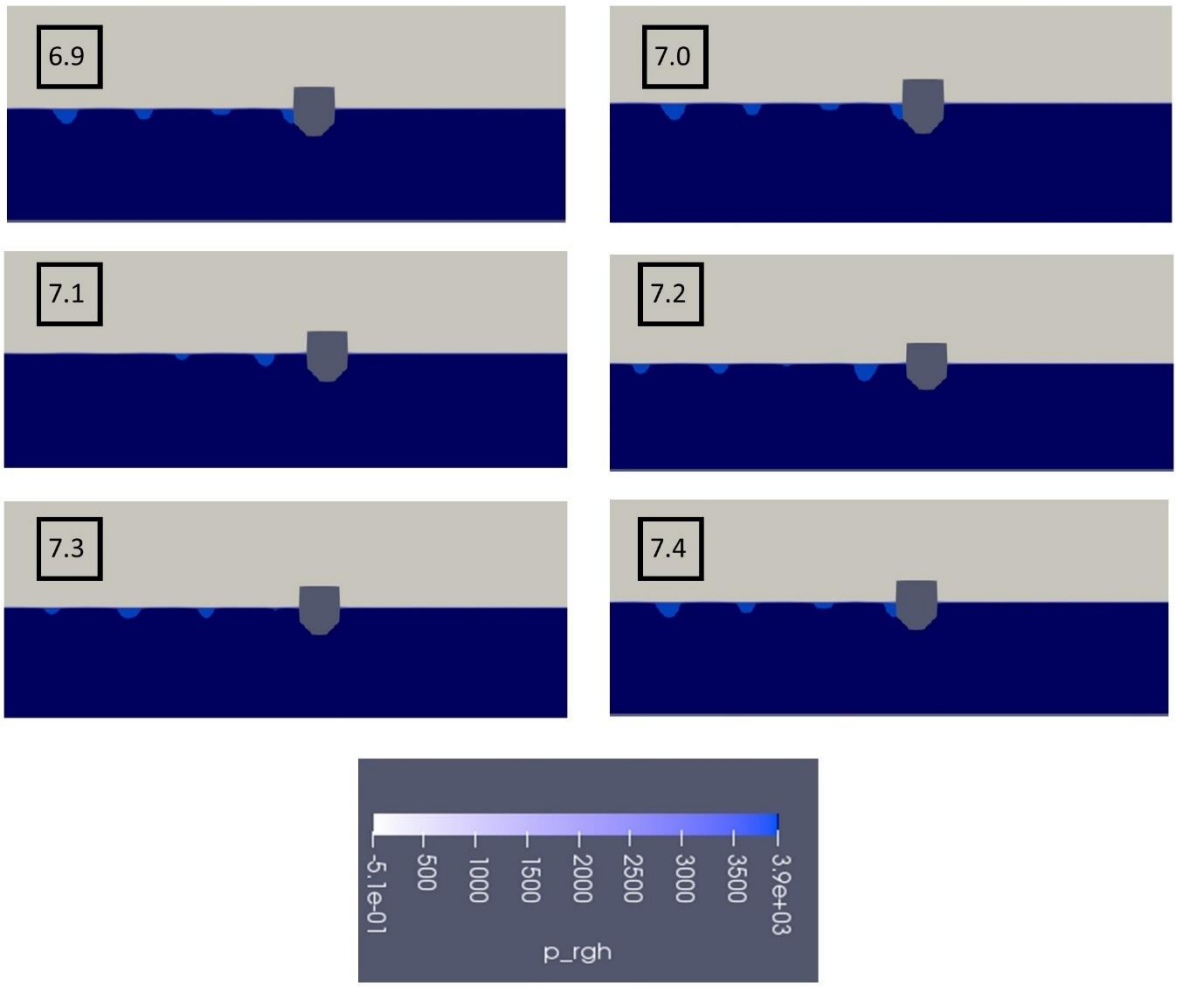

Figure 55 - Pressure Field plot of fish cage in fixed condition

It is obvious from these plots that the cage in the fixed position effectively blocks almost all waves from passing into the second half of the tank. This is shown by the solid darker blue color presenting no noticeable/measured change across the plotted wave period aft of the cage. There is also evidence of the cage reflection reducing the waves as they approach. For example, looking at the low pressure curves shapes (light blue), at t= 7 and t = 7.1, a low pressure area seems to disappear. Moving from 4 low pressure areas to 2 implies that one wave has collided with the cage and a second has been reduced by the reflection. This requires further investigation through a more localized pressure assessment combined with free-surface assessment which may confirm this idea.

Figure 56 shows the pressure field plots for case 5, a floating case with the same wave as that of case 4, again here, the darker colour signifies higher pressure.

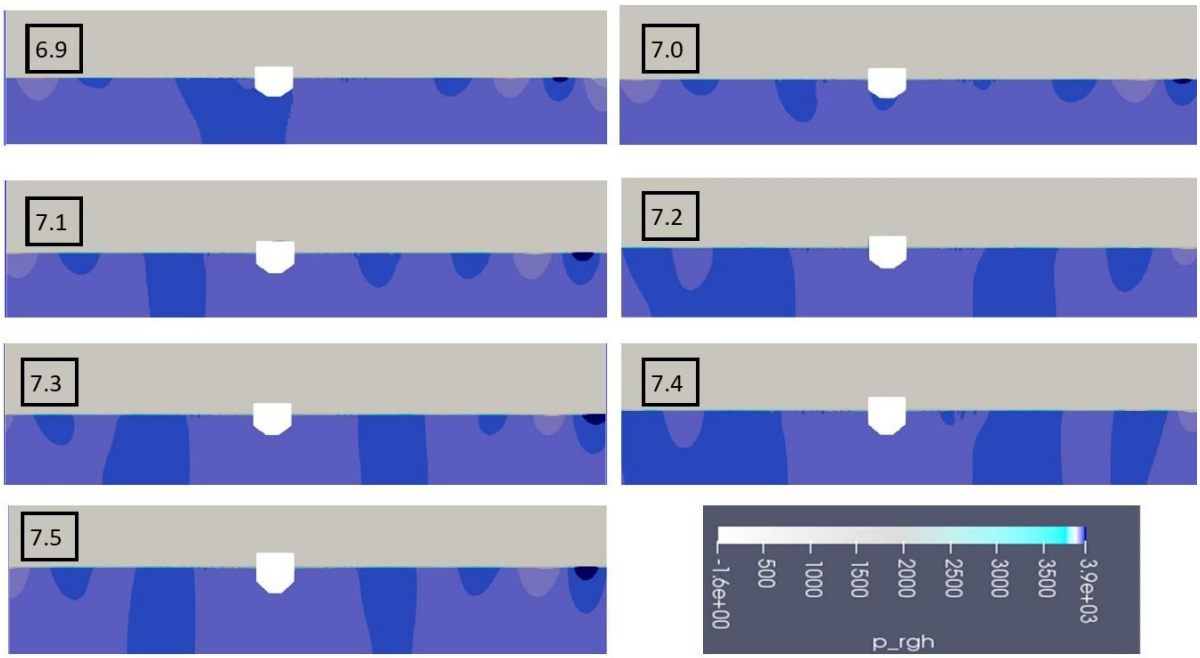

Figure 56 - Pressure Field plot of fish cage in floating condition

There is a dramatic change between case 4 and case 5. Instantly obvious are the varying pressure areas aft (to the right) of the cage. This shows that waves are transmitting past the cage toward the relaxation zone of the tank. Secondly, the pressure areas after the cage are generally smaller than those before it, this shows that although the cage is allowing waves to pass 'through' it, they are being affected and reduced in magnitude. Thirdly, the area around the cage, for the most part is maintaining a relatively constant pressure, particularly 7.1s-7.5s. Further adding to the suspicion that the incoming waves are greatly affected by the reflection of the cage. This constant pressure field may also be tied to the velocity of the water passing under the cage at a near-constant speed. With that being said, the selection of colour scaling may inhibit exact measurements and exact data or trends being smeared out.

Whilst there is evidence to support the trend of large reflection caused by the cage when both fixed and floating, further investigation would only improve understanding. The trends show by the pressure plots could be more accurately checked by focusing on a smaller area adapting the scale to show more exacting, especially when combined with free-surface analysis but due to time, this was not undertaken.

The moored cases also showed waves passing 'through' the cage, as well as a near constant pressure beneath the cage. For the sake of brevity and time management, pressure field plots are not given here due to near-identical data caused by suspected weak mooring.

5.3.25. Velocity Field

The velocity of the fluids (air and water) were investigated in a similar way to the pressure fields. Using paraview, case 4, 5, and 6 were reviewed, here, cases 4 and 5 are given due to indistinguishable differences between floating and moored cases.

Figure 56 shows the velocity of both water and air across 6.9s to 7.5s. Where dark blues are slowest. The white patch in the left of the plots where the air is moving quickly, is believed to be caused by the wave generation, dying out as it reaches the computational zone.

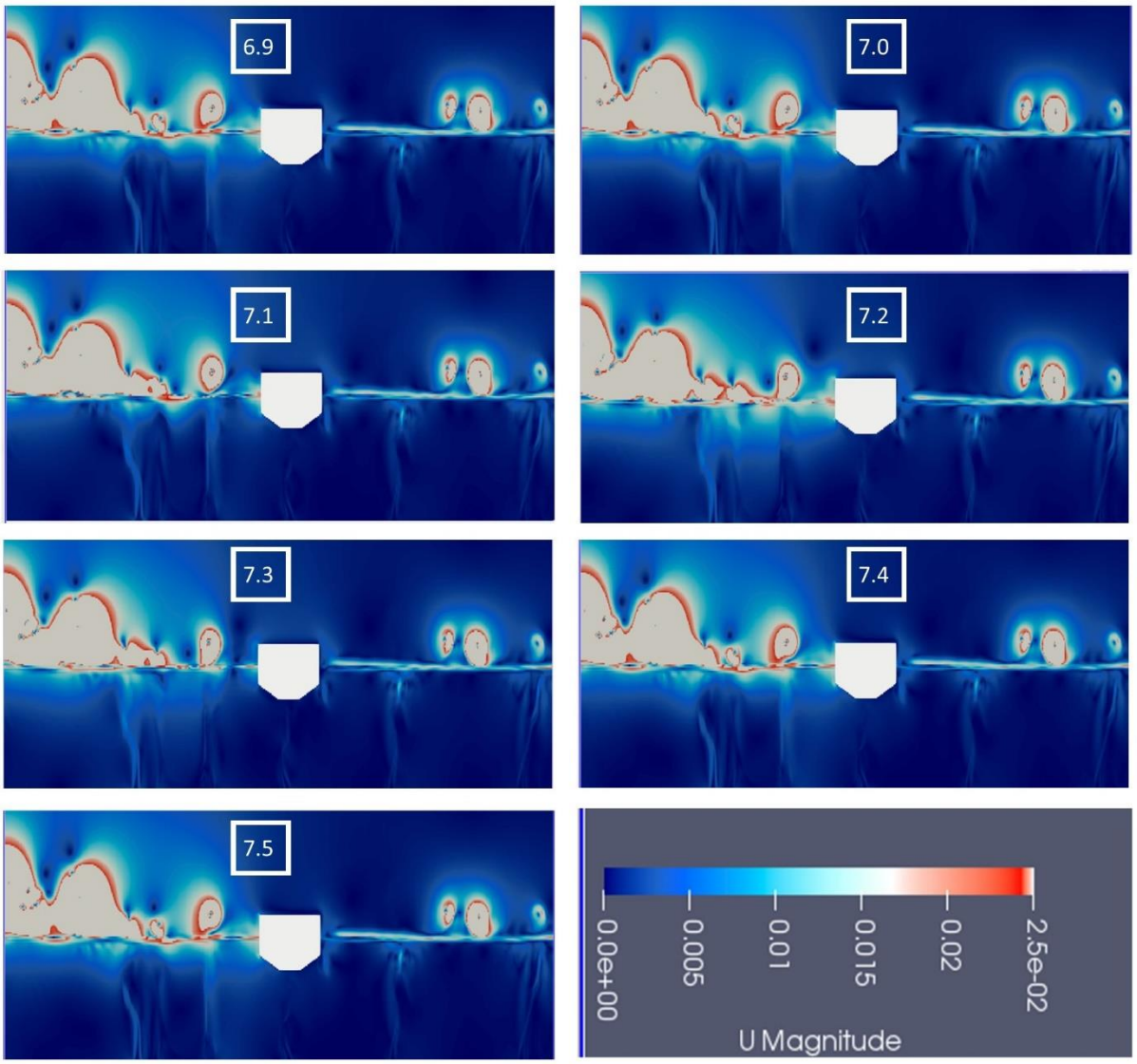

Figure 57 - Velocity Field plot of cage in fixed condition

Across all plots in Figure 57, viewing the lower halves (where the water is present) there are vertical lines of a lighter shade. This shows that water is moving, fastest at these points, however this also shows that waves are passing beyond the fish cage which is clearly not acting as an impermeable object. This supports the findings which the transmission (on average) for this cage condition was very low, but non-zero. This does also indicate that the colour scaling used when investigating the pressure field was not sensitive enough. Secondly, viewing these lighter lines before the cage, the lines appear to be bunching closer together (particularly 7.0s to 7.1s) compared to after the cage. This implies that something is changing the distance between the wave crests. These lines generally match the low pressure areas in Figure 55. As the tank is flat bottomed, this bunching cannot be caused be any shoaling effects/slopes in the seabed as such this further supports the cage wave reflection hypothesis. This water movement also has implications for the use of fish cages in groups. Cages placed in the shadow of a cage will receive less fluid flow into the cage than that at the front. It would be reasonable to assume that a second cage would further reduce the velocity into a third cage, and so on. As an objective of fish cages is to improve fluid flow through the cages, fixed cages

in groups may not be an option, despite the usefulness of wave reflection/shielding that comes from grouping. .

The vertical lines present in Figure 57 are not present in Figure 58 when the same cage, under the same wave is floating freely. In fact, there is a much faster movement of water moving both toward, under and away from the cage.

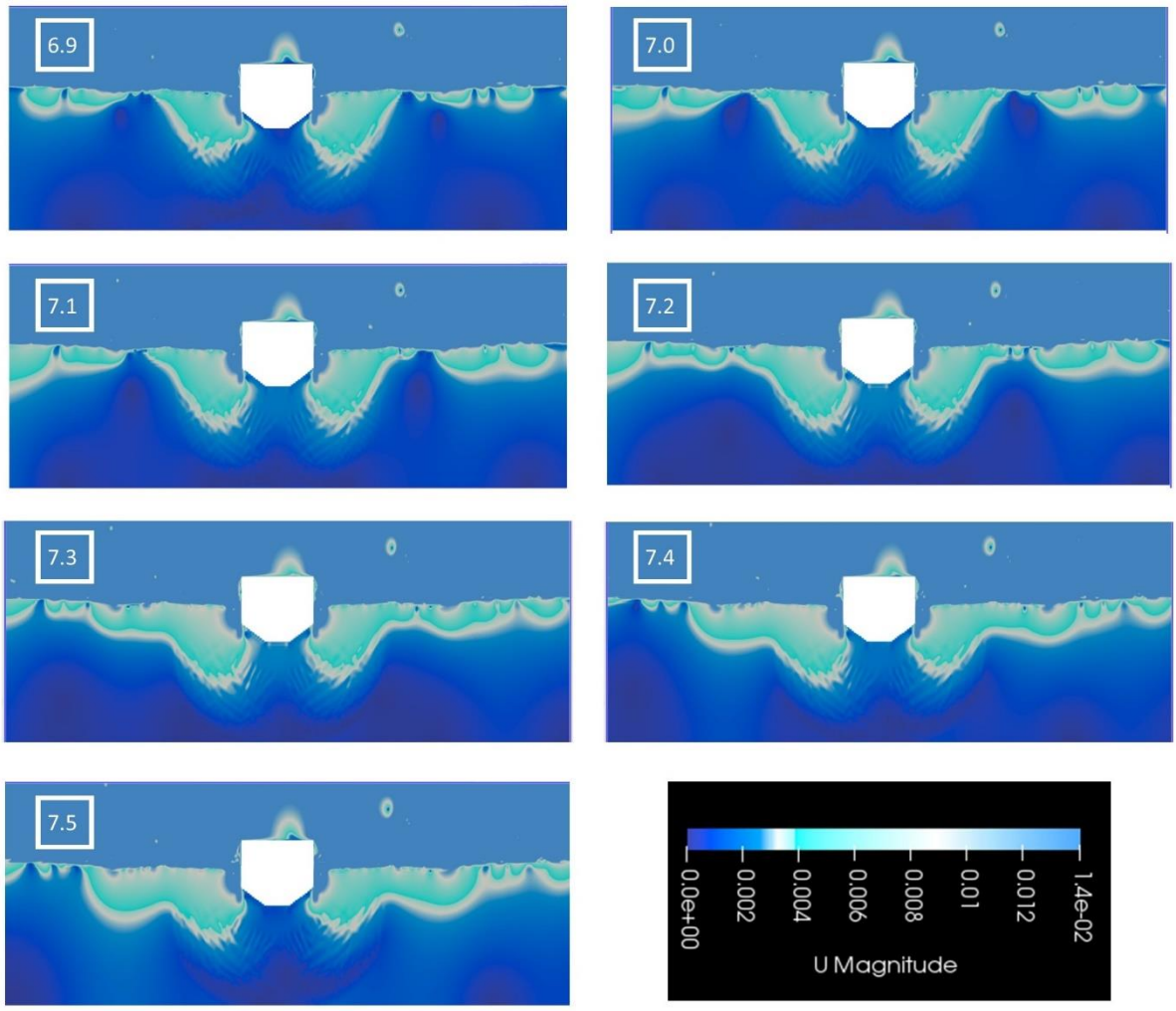

Figure 58 - Velocity field plot of fish cage in floating condition

However, as water passes directly under the cage, it slows. Thus implying the cage is forcing the water to speed up somehow, perhaps due to its heave motion? This consistently fast water may also explain why the pressure plots are a consistent colour beneath the cage. Especially when comparing t =7.1s between Figure 56 and Figure 58. There is a change of pressure beneath the cage, and the largest change of velocity across the period at 7.1s. This further shows that the colour scaling may not be sensitive enough, and for future assessment, smaller areas should be assessed to allow for a more intricate scale.

Interestingly, the water directly adjacent to the sides of the cage has a velocity of near zero. As the cage modelled here is solid and not porous this water is unable to move through the cage. It does however give a positive indication that flow through the cage could be sufficient when nets are modelled. Further to this, though the wave height, and water velocity has been reduced after the

floating cage the velocity is not so significantly reduced it would prevent cages being grouped (to a degree).

Whilst this only scratches the surface of how useful assessment of water velocity can be, it is clear this part of CFD would be of great use to both engineers, and biologists when designing and assessing fish cages.
Understanding where the fast and slow water relative to a cage is allows engineers to determine how the cage may affect other structures near it. These could be other cages, service vessels, or underwater areas of sensitivity, for example. Useful in the design stage. This understanding can also benefit those farming and treating the fish, being able to predict the strength of flow can have an impact on fish health and growth, invaluable in such a rapidly expanding sector.

5.4. Conclusion

This project was undertaken to explore the usefulness of computational fluid dynamics within the aquaculture sector, specifically floating fish-cages. Such an exploration is valuable due to the ever expanding aquaculture sector which is attempting to answer an increasing demand for seafood, particularly fish. The need to understand the motions, forces and fluid behaviors surrounding fish cages stems from benefits found further offshore.

To explore CFD's usefulness within this sector assessment of a cage-like shape within a numerical wave tank with use of the open source software, OpenFoam, was undertaken. A broad spectrum of assessment conditions were applied, including varied wave height, wave period and three different means of restricting the cage's motion – fixed, freely floating and moored. Before any assessment or simulation involving the cage was done, the OpenFoam software model was checked for accuracy, error, and inconsistencies through the creation of a numerical wave tank.
There were 4 checks made of the wave tank model which raised confidence and showed the model to be reliable. The four checks showed acceptable to strong agreement. Firstly, the wave generation within the software was checked for three waves using three different wave theories, ensuring that waves produced could be relied upon to be accurate regardless of theory. The wave reflection within the tank was assessed and reduced to approximately 5% raising confidence that any results produced would operate under the imposed conditions without interference from boundaries not present in the real world. Forces acting on an object were verified by comparison to wave-tank experiments, showing a maximum error of less than 5%. Finally motions of a floating object were again checked against wave-tank experiments which showed a strong agreement with each other. On top of this, a mesh convergence study was undertaken to reduce the computation time as low as possible whilst maintaining accuracy as high as possible.
To firmly seat the simulations in the aquaculture sector, the cage was modelled on a real-world, currently deployed cage which has suffered failure in recent years, an example which may benefit from CFD analysis. The project struggled to model the exact cage due to time requirements, the appropriate meshing couldn't be undertaken, so with dimensions kept broadly similar, cage geometry was modified to be workable.

The objectives of this project were, in broad terms, to study wave interaction with floating fish cages through the use of a Numerical wave tank. The wave tank should allow for floating objects from which forces, and motions could be measured along with the effect the cage has on the fluid

especially in the pressure and velocity fields. Through simulation of the 15 cases, these objectives were achieved.

The simulations yielded some complex results which would certainly benefit from further investigation. Forces across the fixed, floating and moored conditions behaved generally as expected with force increasing as wave-height increased however mooring showed little-to-no difference in comparison to the freely-floating condition, indicating that the mooring tension was perhaps not strong enough/added to the right place in the geometry.
This mooring trend continued when reviewing motions of the cage, few of the motions behaved as expected and it is believed that this is partly caused by reflection from the cage affecting incoming waves, particularly for heave motion. Other motions proved more difficult to explain. For example, the cage pitched in only one direction, though it is unclear if this was due to the geometry of the cage selected, or the mooring. The investigation of the motions would be improved by further study across additional wave conditions and a fine-tuning of mooring to produce a desired stiffness.
Similarly, an area which would also benefit from further investigation would be the pressure throughout the fluid. Here, differences were so slight that review of the field as a whole was difficult, and though assessment did raise multiple points of interest in regards to the deployment of a cage, such as how the pressure behaves before and after the cage, this could certainly be expanded upon by reviewing sections of the cage more closely. Thankfully, review of the velocity field was much clearer demonstrating a clear difference between fixed and floating cages, and indicating that a fixed cage may prove more difficult to deploy within this sector.
The ultimate aim of this project was to show that CFD would be a useful tool for the aquaculture sector and this has been achieved in a number of ways.
Firstly, the recording of forces allows for an accurate understanding of the extremes a cage may face. This allows for proper mooring and structural engineering which would improve the survivability, and economic viability by reducing the risk of asset loss. The motions, pressure, and velocities around the cage can give valuable information to both engineers and those producing the fish. For example, understanding what velocity is moving around a cage allows producers to control how they treat their fish, and monitor which cages may over-stress the fish. Similarly, engineers can make better choices on how to configure a farm layout shielding, or exposing cages dependent on requirements.
This project only scratches the surface in regards to the uses of CFD, with a multitude of work which could be undertaken to further state the case for its use in this sector (explored below). However it clearly shows the incredible potential for CFD's use within modern day aquaculture.

5.5. Future Work and the impact of Covid-19.

Given the current Covid-19 global pandemic situation, this project required modification and trimming in order to produce worthwhile, cohesive work. This was due to the impacts of the restrictions caused by remote working, the reduction in working speed, and problems which arose due to this new way of undertaking work. These problems are summarised below;

- Moving to working from home – As the University moved to distance learning - my advisor arranged for me to be provided with a computer to undertake the simpler parts of the project before moving to the central computing cluster. Unfortunately due to instabilities and incompatibilities with the hardware this initially did not work. Lockdown made it incredibly difficult to have this looked at by my advisor, or any member of the university,

slowing progress immensely. Eventually this had to be abandoned for the health of those involved and progress was set back to square one without access to the relevant software.

- Gaining access to the computer cluster at the University of Dundee, and ensuring required software was successfully operating. This required multiple communications and virtual meetings with the Scientific Computing Officer – Nicholas Dawes who, due to settling in to working from home was, on occasion difficult to get hold of (as we all were).
- Computing cluster going offline 27/06/20 until 01/07/20. This was understandably not immediately fixed due to the social-distancing requirements in place. This sudden offline resulted in the loss of running simulations and bringing progression of project work to a standstill for the best part of 4 days. Further to this, upon restoration of the cluster, demand on resources was much higher resulting in much longer wait times to execute simulations.
- Computer cluster going offline 11/08/2020 until 13/08/20. (Approximately 2 weeks before this project was due for submission). This is when the bulk of results were to be obtained. The sudden offline resulted in the loss of a non-trivial amount of work across 4 running simulations. This also created a higher demand on shared resources, limiting the number of simulations which could be run by any single user at any one time, with a 3 day wait for access to a cluster node, progress was drastically slowed at a crucial point.

These events significantly delayed the computation of final results, at a huge detriment to both the quality and breadth of work, the result analysis, and report writing due to a further compressed timeline.

The modifications which occurred as an impact of Covid-19 have notably reduced the strength of work undertaken.
Firstly - due to the closure of The University of Dundee campus – the wave tank experiments were removed. This removed the ability to validate the tests undertaken within OpenFOAM, or to understand and present the key differences between wave tank experiments and CFD simulation.

Secondly, due to the compressed timescales caused by technical difficulties associated with remote working multiple simulations were removed from the project's contents.
The removal of three-dimensional cases. Due to complications in creating simulation/simulation run-time there was not enough time to cover this subject in a depth which would add to the project. Similarly, investigation of porous media/ porosity effects were removed. Such effects are ultimately three-dimensional and thus relied on the completion of the previous step so investigating these was not possible.
Finally, the correction of mesh for selected fish-cage geometry. Whilst the cage geometry used in the assessment of CFD as a tool for the aquaculture sector was suitable, it was no identical to those found to being used by industry. This was due to meshing difficulties causing bad cells, and if timing allowed could ultimately have been fixed to allow the use of industry geometry. This would have placed the project firmly within the current aquaculture sector, and presented CFD's applicability to the sector clearly and undeniably.

Given the above, there is a multitude of future work which could be undertaken to further show that CFD is an invaluable tool for use in the aquaculture sector.

- Modification of cage geometry to exactly mimic deployed cage – reruns of all simulations could then be undertaken. This would give a clearer understanding of how real-world cages behave and influence the fluid around them.
- Converting the model to three-dimensions – this would allow the inclusion of sway, yaw and roll motions as well as forces in the y direction.

- Addition of Porous effects – A key component missing in the above work is the porous effects. As is obvious, nets used in fish cages are effectively porous materials which allow fluid to pass through them. The inclusion of porous effects would change the motions and forces involving the cage, and distinctly change the pressure and velocity fields. This would give a more accurate representation of the floating fish cage, and a clearer idea as to how fluid passes through the cage, in turn affecting the farmed fish.
- Wave-Tank Experiments – All of the simulations undertaken could then be validated through scale model tests. This would raise confidence in the findings of the CFD model and directly demonstrate that computational fluid dynamics can represent events in the real world.

After all of this future work is undertaken, the applicability of CFD to the problems face by the aquaculture sector would be clear with an obvious route-map for assessing and understand the interactions of non-linear waves with floating fish cages.

6. References

Adria Moreno Miquel, A. K. (2018). Analysis of Different Methods for Wave Generation and Absorption in a CFD-Based Numerical Wave Tank. Journal of Marine Science and Engineering, 6(78).

Anderson Coldebella, A. L. (2017, December 21). Effluents from Fish Farming Ponds: A View from the Perspective of Its Main Components. MDPI.

B Chenari, S. S. (2015). Numerical Modelling of Regular Waves Propagations and Breaking Using Waves2Foam. Journal of Clean Energy Technologies, 3(4), 276 - 282.

Bing Ren, M. H. (2015). Nonlinear simulations of wave-induced motions of a freely floating body using WCSPH method. Applied Ocean Research, 1 - 12.

Christian Windt, J. D. (2019). On the Assessment of Numerical Wave Makers in CFD Simulations. Marine Science and Engineering.

Chun-Woo Lee, Y.-B. K.-H.-Y.-K.-Y. (2008). Dynamic Simulation of a fish cage sustem subjected to currents and waves. Ocean Engineering, 35, 1521-1538.

Coastal Communities Network Scotland. (2020, January 23). Mass escape from Colonsay fish farm after Storm Brendan. (Coastal Communities Network Scotland) Retrieved 08 02, 2020, from https://www.communitiesforseas.scot/mass-escape-from-colonsay-fish-farm-after-storm-brendan/

Comsol. (2017, February 21). Finite Element MEsh Refinement. Retrieved April 02, 2020, from https://www.comsol.com/multiphysics/mesh-refinement

David W. Fredriksson, M. R. (2003). Fish cage and mooring system dynamics using physical and numerical models with field measurements. Aquaculture Engineering, 27, 117-146.

E. Mantzavrakosa, M. K. (2007). Impacts of a marine fish farm in Argolikos Gulf (Greece) on the water column and the sediment. Desalination, 210, 110-124.

FRANK ASCHE, M. F. (2015). Fair Enough? Food Security and the International Trade of Seafood . World Development, 67, 151 - 160.

Guo-Hai Dong, T.-J. X.-P.-C.-K. (2010). Numerical simulation of hydrodynamic behaviour of gravity cage in irregular waves. Aquaculture Engineering, 42, 90-101.

Hideaki Miyata, H. A. (1997). CFD performance prediction simulaton for hull-form design of sailing boats. Marine Science and Technology, 2, 257-267.

Jasak, H. (1996). Error Analysis and Estimation for the Finite Volume Method with Applications to Fluid Flows. London: Imperial College of Science Technology and Medicine.

Josh Davidson, M. C. (2015). Implementation of an OpenFOAm Numerical Wave Tank for Wave Energy Experiments. 11th European Wave and Tidal Energy Conference. Nantes, France.

Kathy Overton, F. O. (2019). Thermal delousing with cold water: Effects on salmon lice removal and salmon welfare. Aquaclture, 505, 41-46.

L.D. Wright, C. F. (2001). Effects of ambient currents and waves on gravity driven sediment transport on continental shelves. Marine Geology, 175, 25-45.

LI Yong, L. M. (2010). Wave-Body Interactions For A Surface Piercing Body in Water Of Finite Depth. Journal of Hydrodynamics, 22(6), 745-752.

Lumb, C. (1989). Self-pollution by Scottish Salmon farms? Marine Pollution Bulletin, 20(8), 375-379.

Masoud Hayatdavooid, R. C. (2015). Wave forces on a submerged horizontal plate - Part II: Solitary and cnoidal waves. Journal of Fluids and Structures, 580-596.

Miguel, J. (2011). Interactive Simulation of Ship Motions in Random Seas Based on Real Wave Spectra., (pp. 235 - 246). Lisbon.

Morgan, G. (2010). Using the rasInterFoam CFD model for wave transformation and coastal modelling. Proceedings of 32nd Conference on Coastal Engineering. Shanghai China.

MOWI. (2019, November). Planning Application Documents 18/02657/MFF. (Argyll and Bute Council) Retrieved 08 01, 2020, from https://publicaccess.argyll-bute.gov.uk/online-applications/applicationDetails.do?activeTab=externalDocuments&keyVal=PJKKFECH0GD00

Pal T. Bore, J. A. (2017). Modelling of hydrodynamic loads on aquaculture net cages by a modified morison model. VII International Conference on Computational Methods in Marine Engineering.

Seifert, D. D. (2015). Active Flow Control Maneuvering System. AIAA .

Skandali, D. (2015). Identification of response amplitude operators for ships based on full scale measurements. Delft: Heerema Marine Contractors.

Sørensen, J. D. (2011). Wind Energy Systems - Optimising Design and Construction for Safe and Reliable Operation. Delft: Woodhead Publishing.

Tahsin Tezdogan, A. I. (2014). Operability assessment of high speed passenger ships based on human comfort criteria. Glasgow: University of Strathclyde.

Wiegel, R. (1959). A presentation of cnoidal wave theory for pracital application. Berkley: University of California.

Yuanchuan Liu, Q. X. (2017). Establishing a fully coupled CFD analysis tool for floating offshore wind turbines. Renewable Energy, 112, 280-301.

Yun-Peng Zhao, X.-D. B.-H.-W. (2019). Deformation and stress distribution of floating collar of net cage in steady current. Ships and Offshore Structures, 14(4), 371-388.

Yun-Peng Zhao, Y.-C. L.-H.-K. (2007). Numerical simulation of the effects of structure size ratioand mesh type on three-dimensional deformationof the fishing-net gravity cage in current. Aquaculture Engineering, 36, 285-301.

7. Appendix 1 – MOWI Fish cage industry drawings (Argyll and Bute planning department)

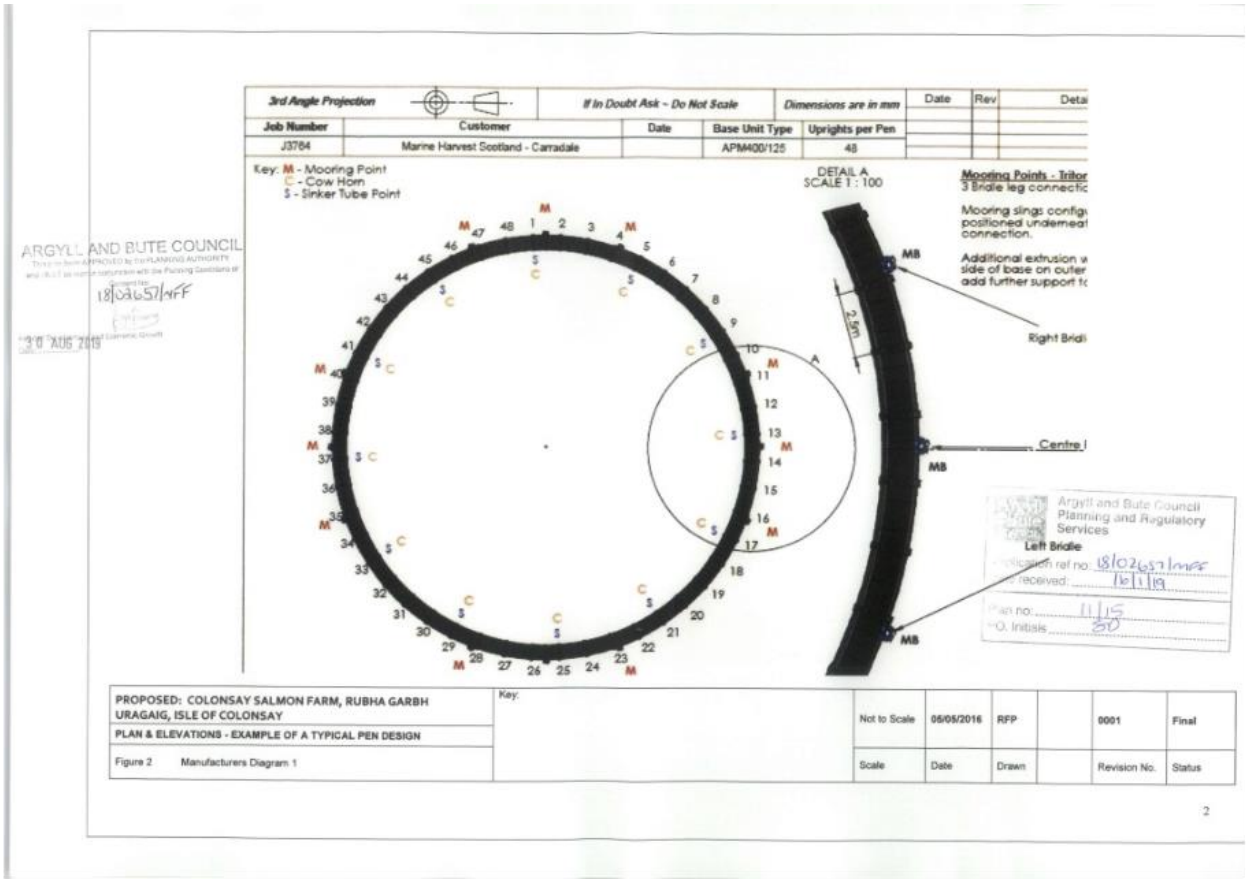

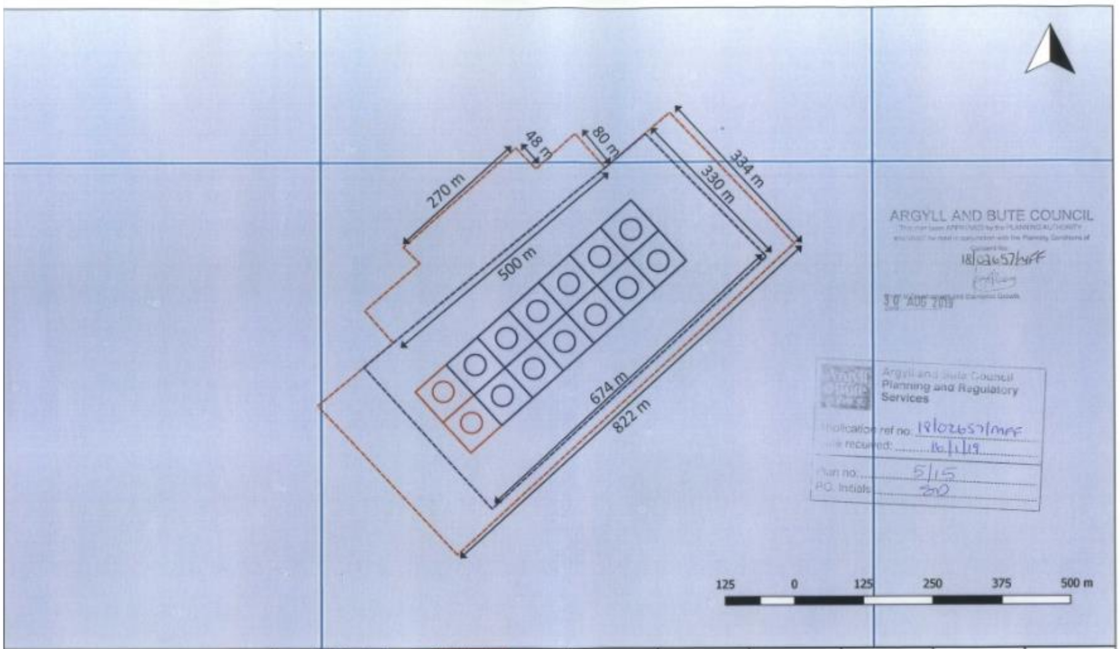

COLONSAY FISH FARM: ISLE OF COLONSAY	Key: Current cages; Proposed cages	1:5,000	07/01/2019	RFP	KW	v3	Final
ORDANACE SURVEY MAP OF SITE LOCATION	Current mooring containment area; Proposed mooring containment area	Scale	Date	Drawn	Checked	Revision No.	Status
Figure 5: Detailed view of Colonsay fish farm. 12 circular plastic cages of 120m circumference and proposed 14 circular plastic cages of 120m circumference.							

COLONSAY FISH FARM: ISLE OF COLONSAY	Key:	1:500,000	07/01/2019	RFP	KW	v3	Final
ORDANACE SURVEY MAP OF SITE LOCATION	ARGYLL AND BUTE COUNCIL	Scale	Date	Drawn	Checked	Revision No.	Status
Figure 1: General view and location of Colonsay.							

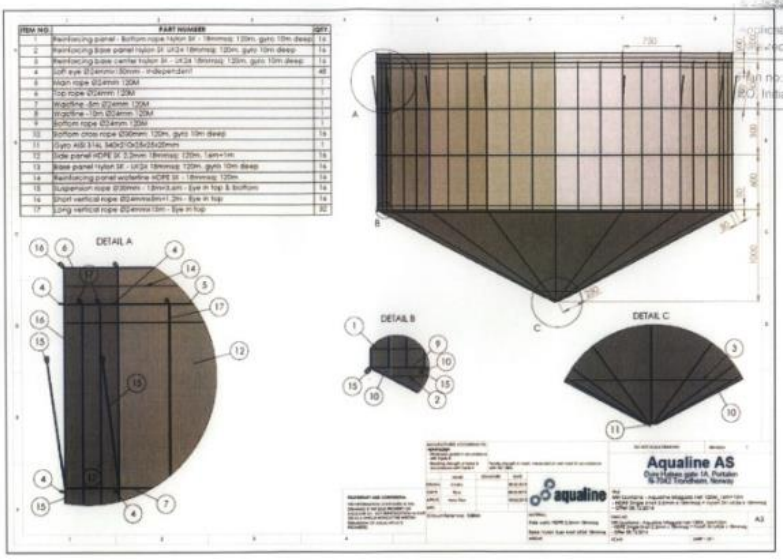

PROPOSED: COLONSAY SALMON FARM, RUBHA GARBH URAGAIG, ISLE OF COLONSAY	Key:	Not to Scale	05/05/2017	RFP		0001	Final
PLAN & ELEVATIONS - EXAMPLE OF A TYPICAL NET DESIGN							
Figure 6 Manufacturers Diagram – Typical Net Design		Scale	Date	Drawn		Revision No.	Status

6

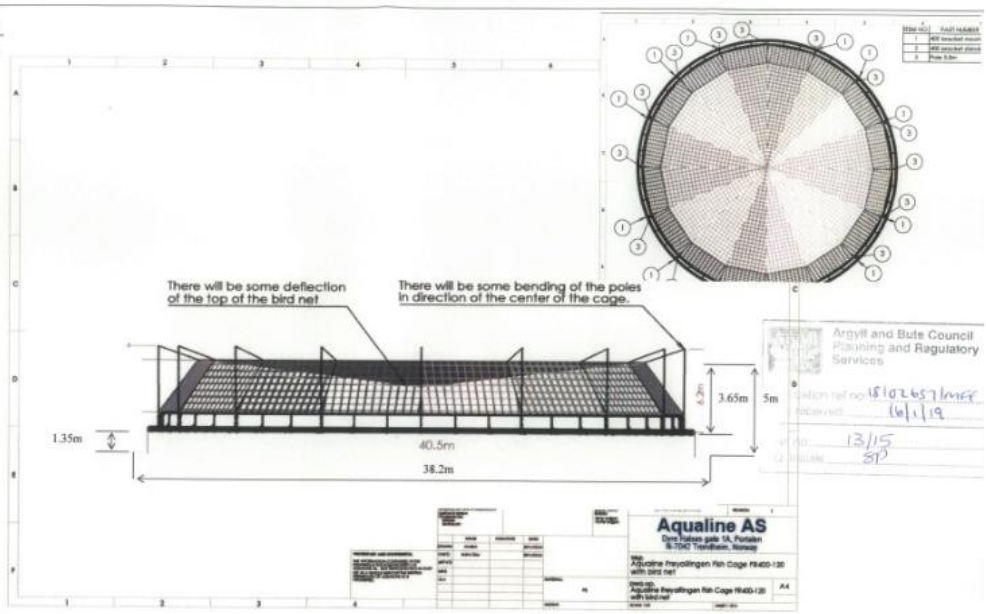

PROPOSED: COLONSAY SALMON FARM, RUBHA GARBH URAGAIG, ISLE OF COLONSAY	Key:	none	05/05/2016	RFP		0001	Final
PLAN & ELEVATIONS - EXAMPLE OF A TYPICAL PEN DESIGN TOP NET SUPPORT OPTION 2							
Figure 4 Top-Net Support Structure	Cage and top net support + net	Scale	Date	Drawn		Revision No.	Status

4

3rd Angle Projection	If In Doubt Ask ~ Do Not Scale	Dimensions are in mm	Date	Rev	Det

Job Number	Customer	Date	Base Pipe Type	Uprights per Pen
	Marine Harvest Scotland - Carradale		400sdr21	48

Note: Overall height of BNSW the same as a standard 30m wheel and not adjusted along with increase to circumference as per customer request

THIS IS A SPECIAL SCENAREO FOR MH CARRADALE

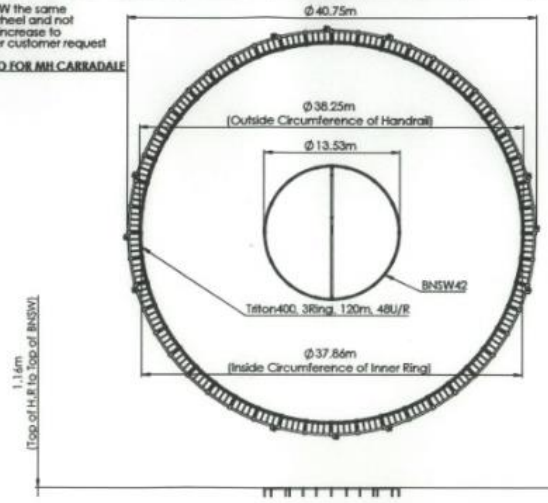

PROPOSED: COLONSAY SALMON FARM, RUBHA GARBH URAGAIG, ISLE OF COLONSAY	Key:	Not to Scale	05/05/2016	RFP		0001	Final
PLAN & ELEVATIONS - EXAMPLE OF A TYPICAL PEN DESIGN TOP NET SUPPORT OPTION 1							
Figure 3 Manufacturers Diagram 2		Scale	Date	Drawn		Revision No.	Status

3

8. Appendix 2 – Force Time Series Plots.

8.1. X direction

The time series plots of forces in the x direction are plotted below.

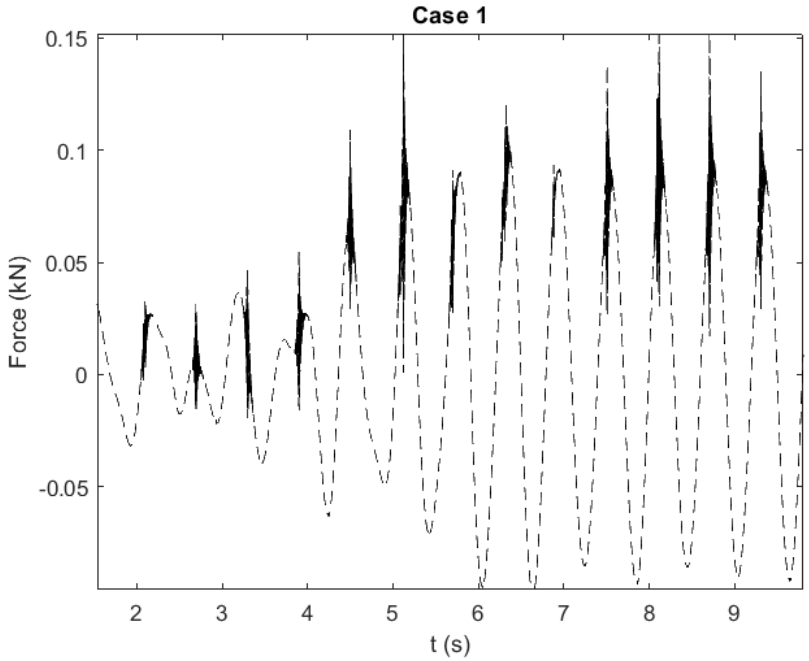

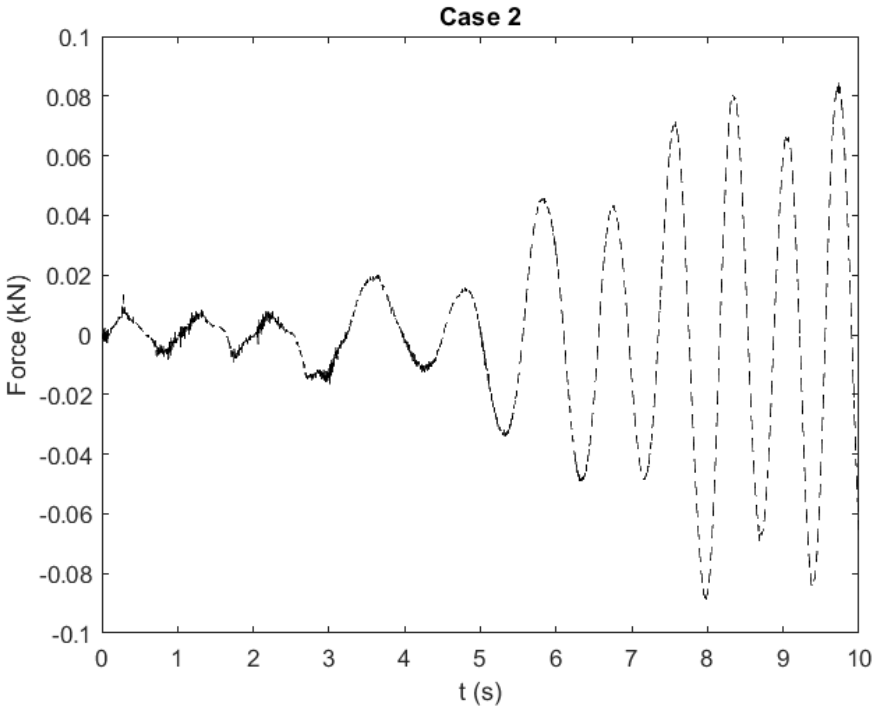

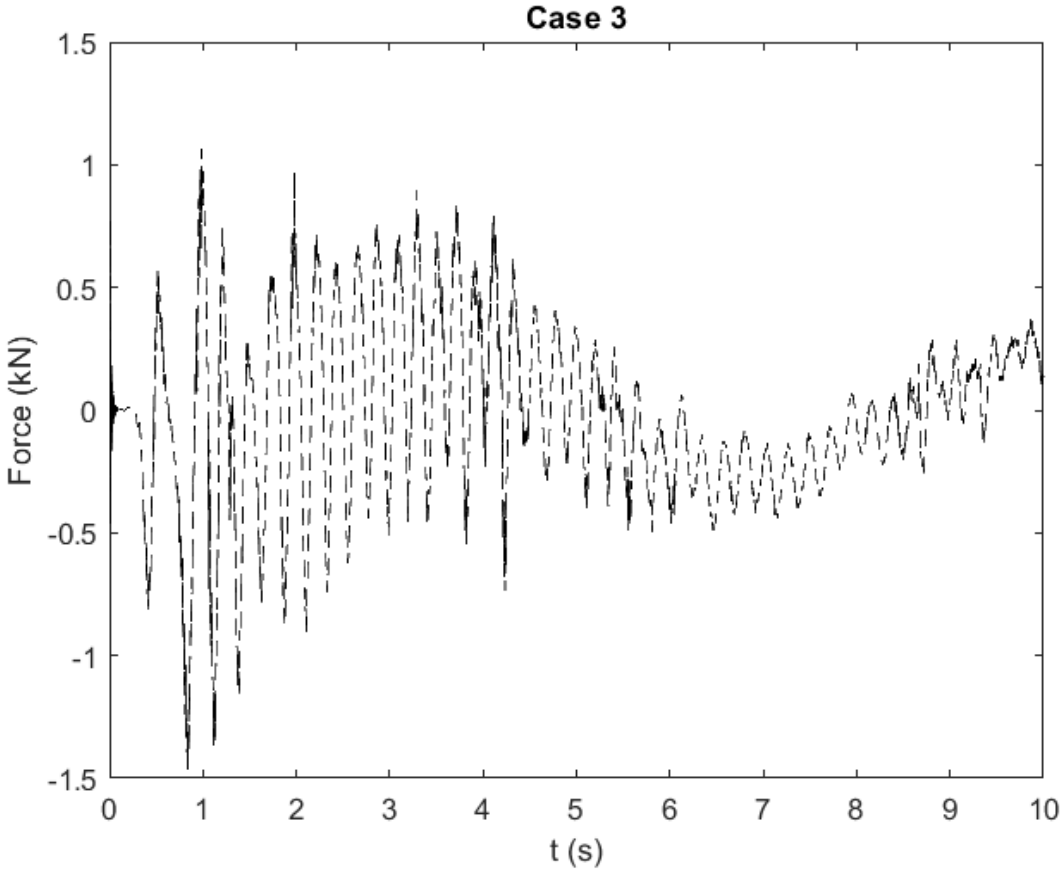
Case 3
Force (kN)
t (s)
1.5
1
0.5
0
-0.5
-1
-1.5
0
1
2
3
4
5
6
7
8
9
10

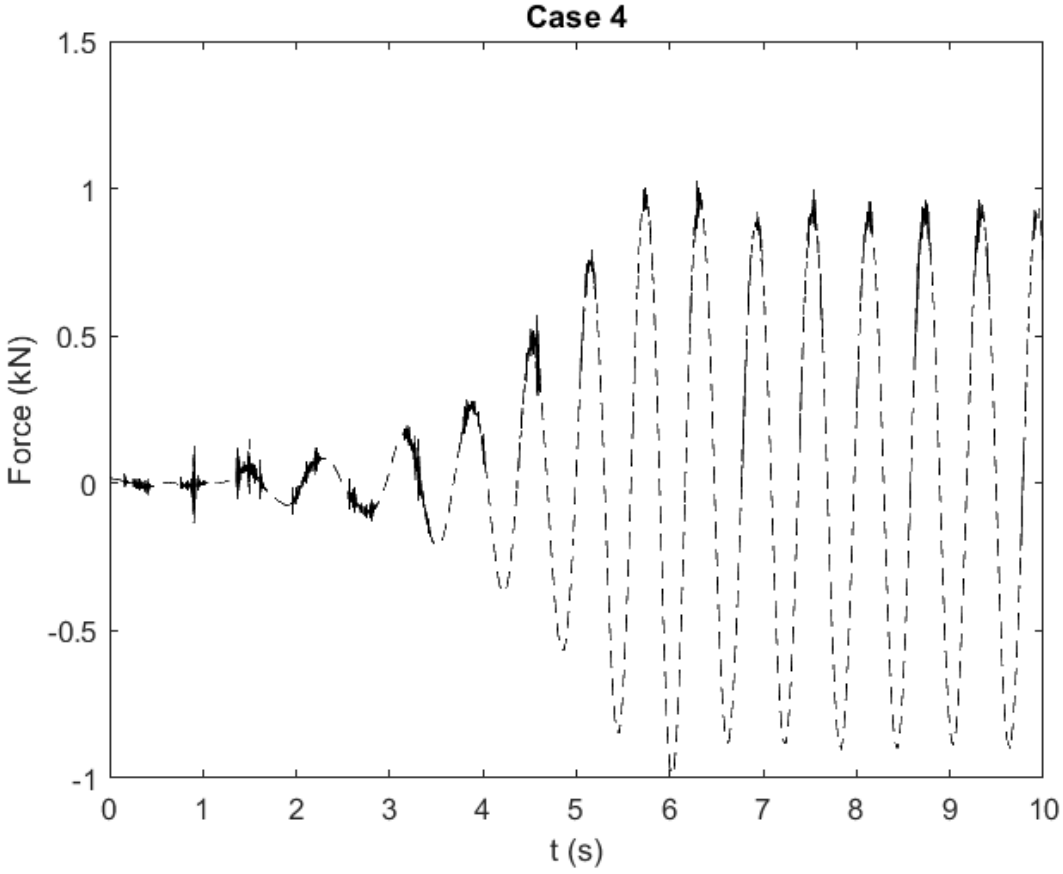
Case 4
Force (kN)
t (s)
1.5
1
0.5
0
-0.5
-1
0
1
2
3
4
5
6
7
8
9
10

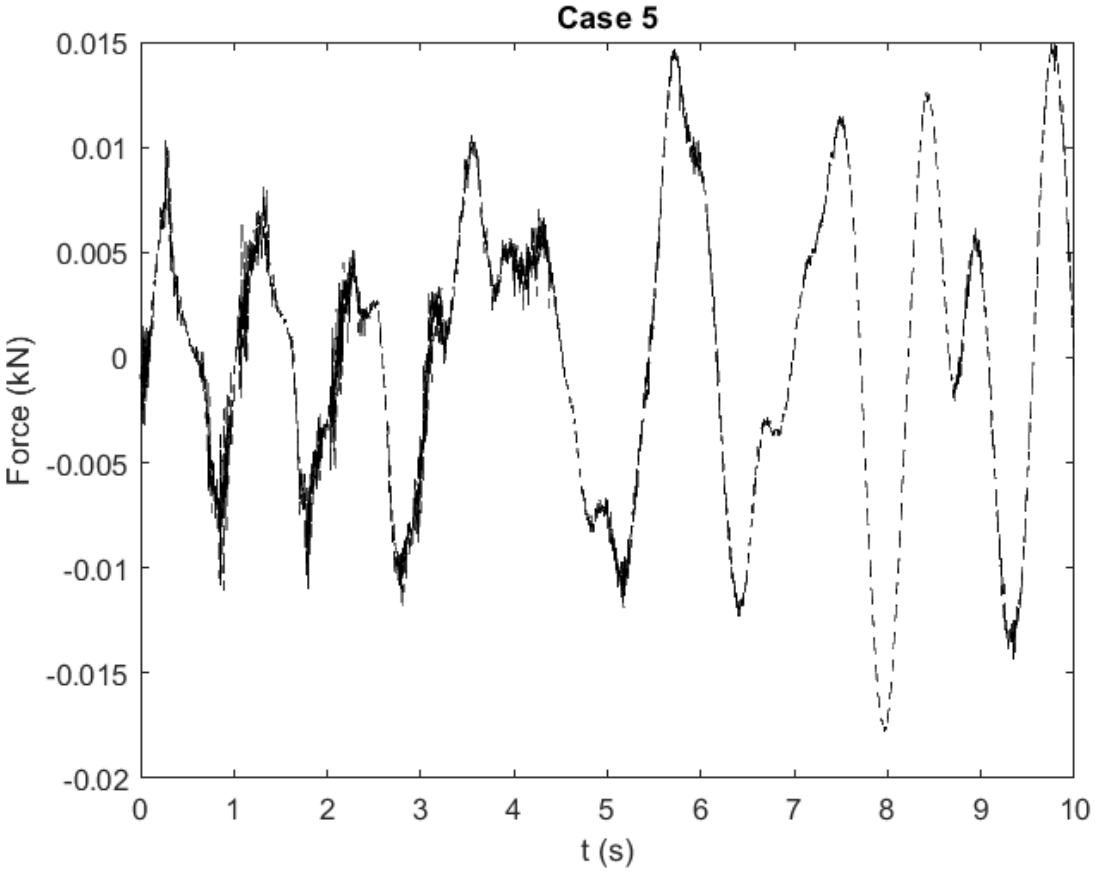
Case 5
0.015
0.01
0.005
0
-0.005
-0.01
-0.015
-0.02
Force (kN)
0
1
2
3
4
5
6
7
8
9
10
t (s)

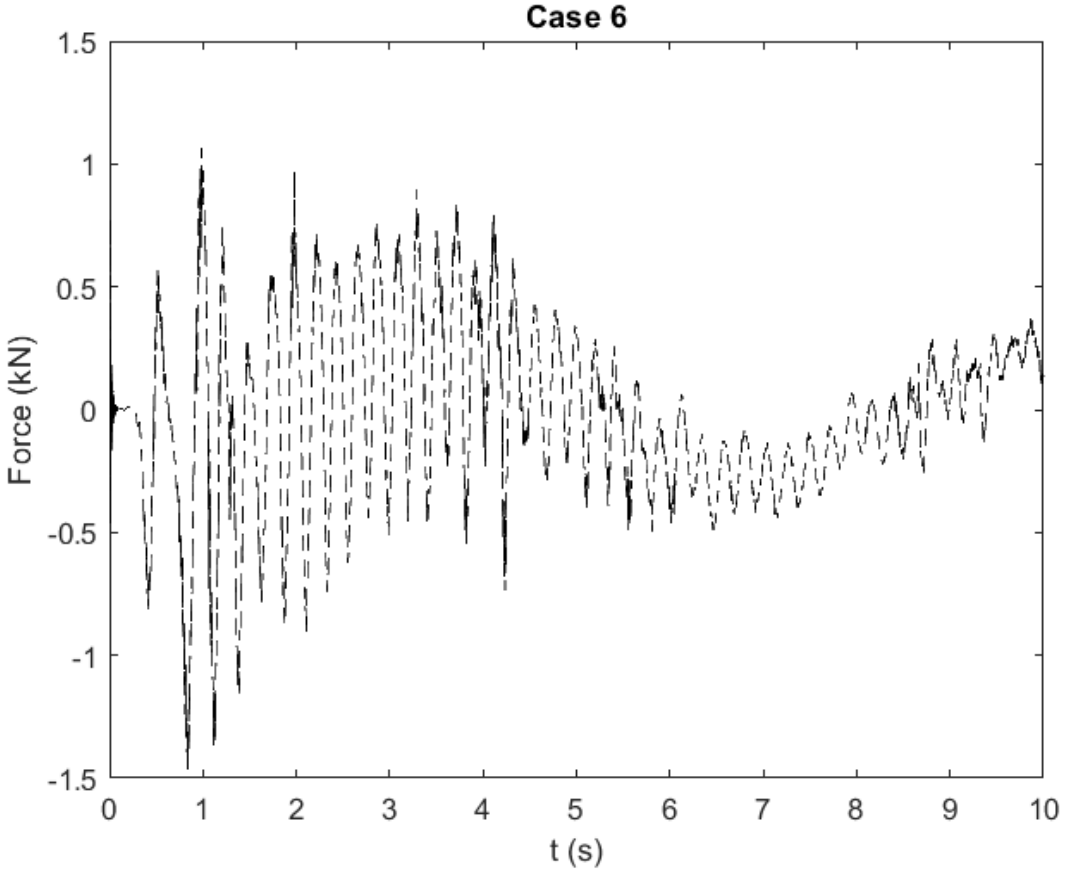
Case 6
1.5
1
0.5
0
-0.5
-1
-1.5
Force (kN)
0
1
2
3
4
5
6
7
8
9
10
t (s)

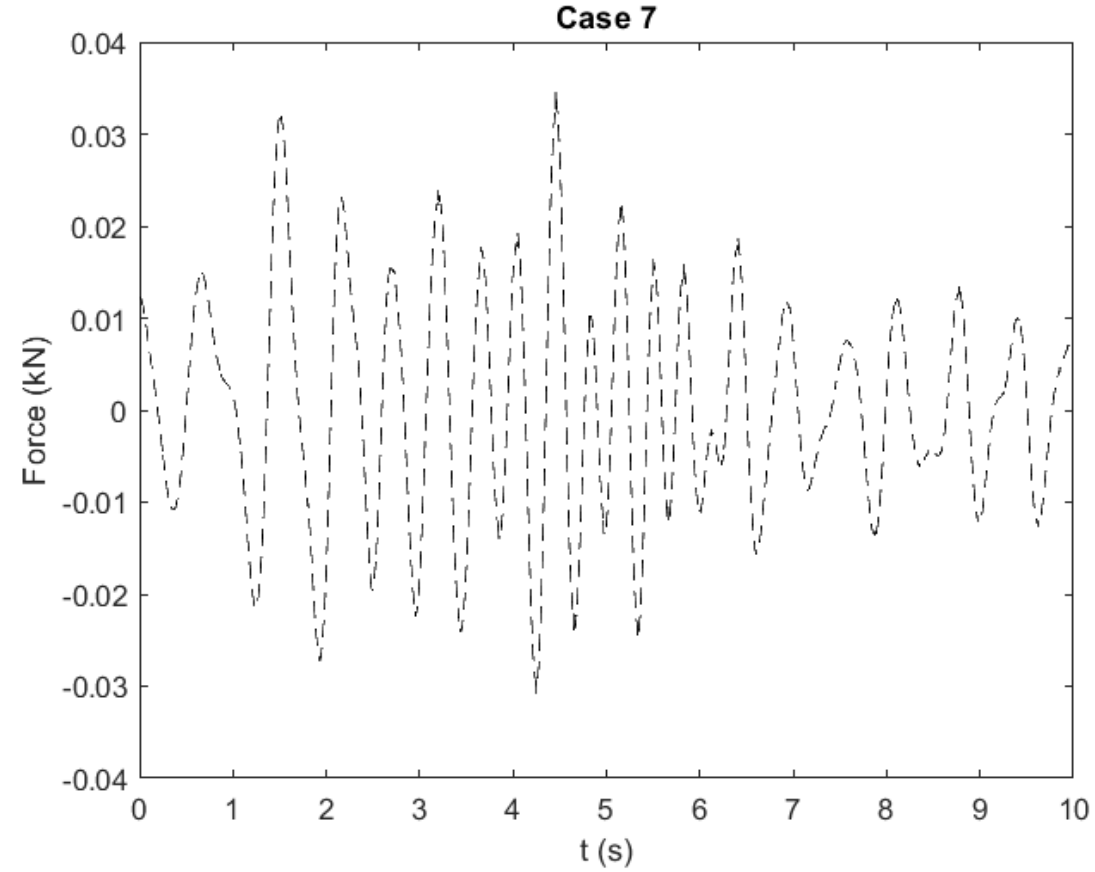
Case 7
Force (kN)
t (s)
0.04
0.03
0.02
0.01
0
-0.01
-0.02
-0.03
-0.04
0
1
2
3
4
5
6
7
8
9
10

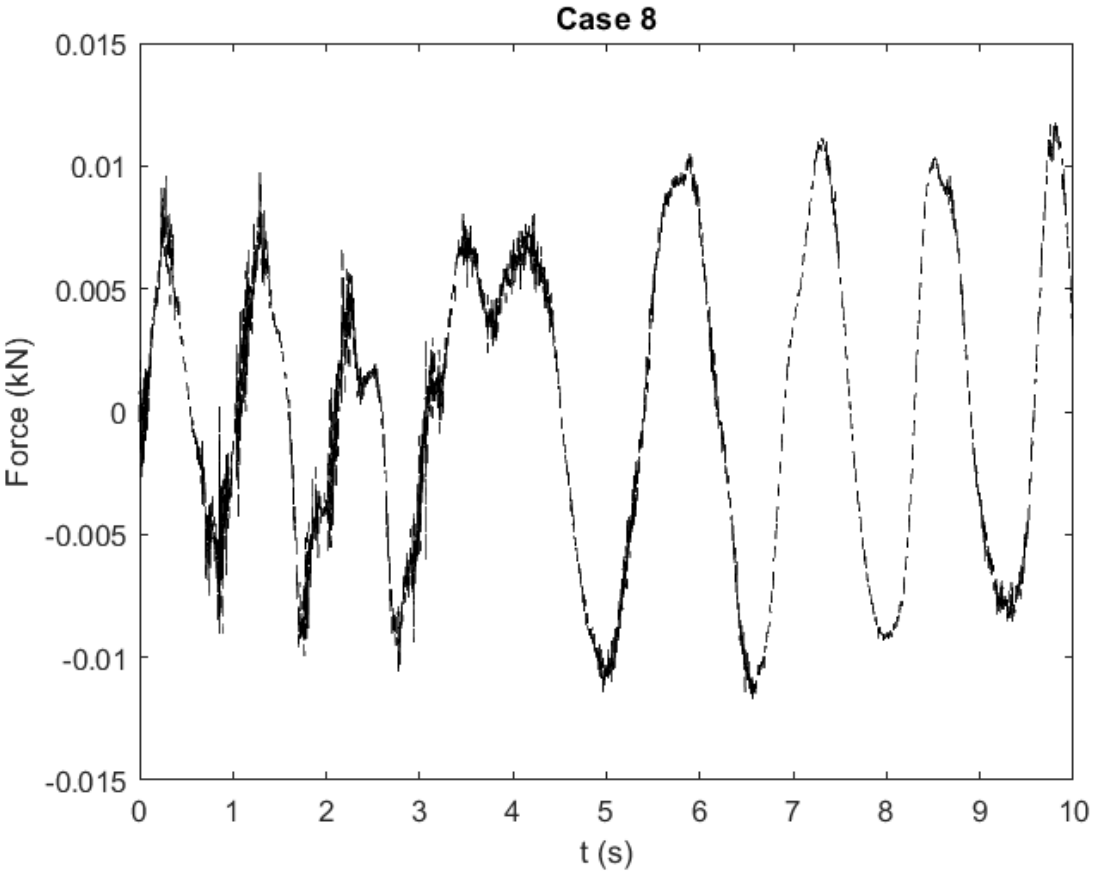
Case 8
Force (kN)
t (s)
0.015
0.01
0.005
0
-0.005
-0.01
-0.015
0
1
2
3
4
5
6
7
8
9
10

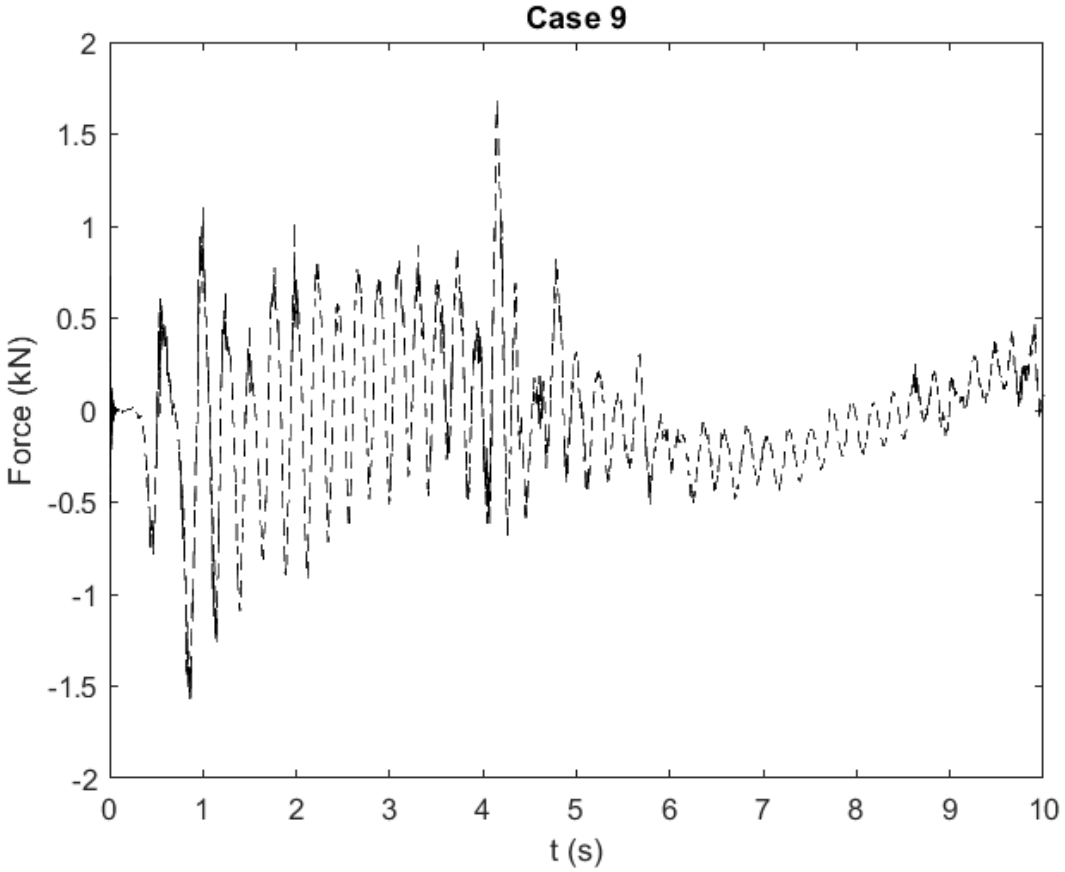
Case 9
Force (kN)
t (s)
2
1.5
1
0.5
0
-0.5
-1
-1.5
-2
0
1
2
3
4
5
6
7
8
9
10

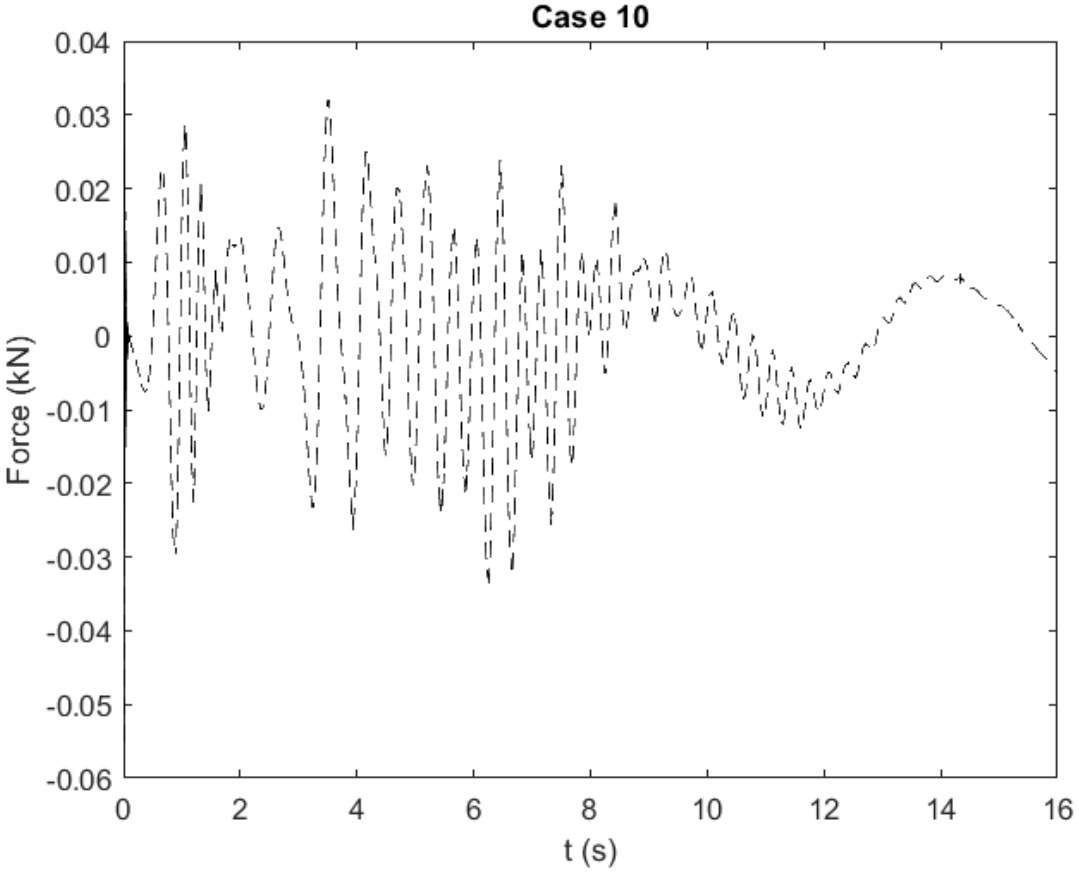
Case 10
Force (kN)
t (s)
0.04
0.03
0.02
0.01
0
-0.01
-0.02
-0.03
-0.04
-0.05
-0.06
0
2
4
6
8
10
12
14
16

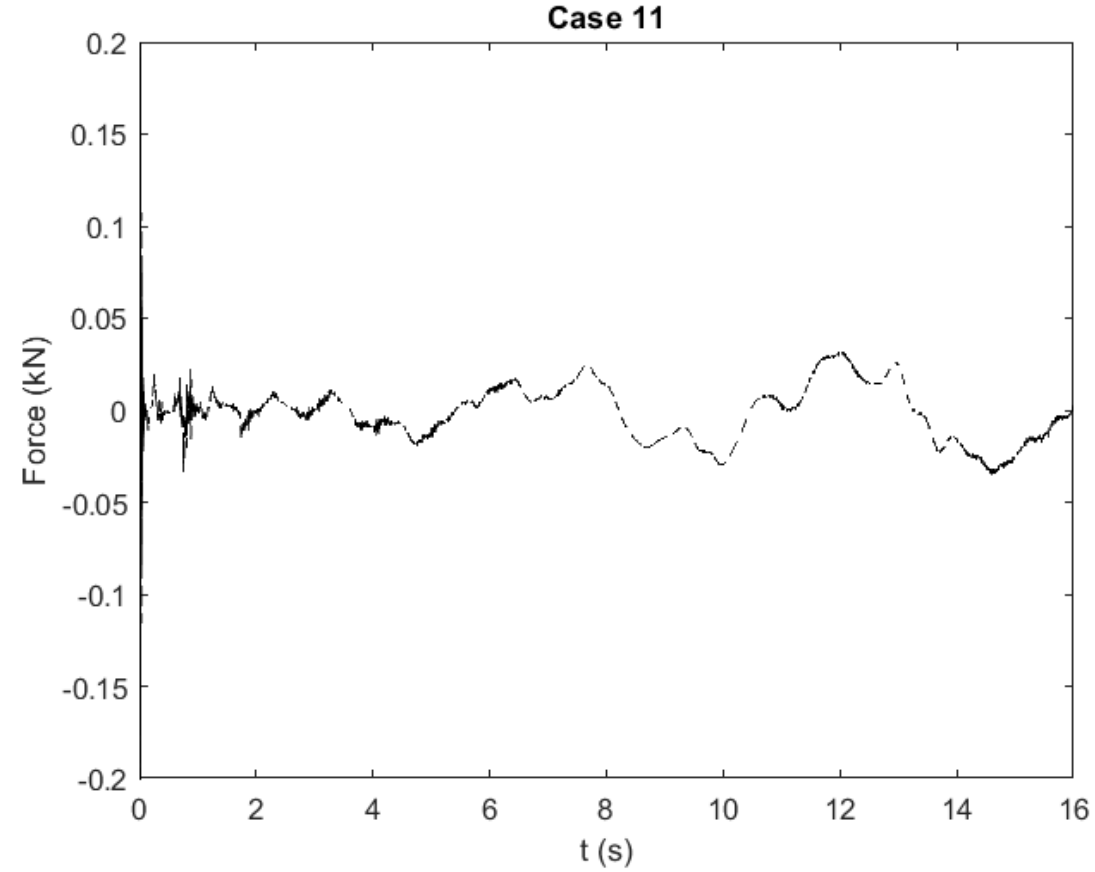
Case 11
Force (kN)
t (s)
0.2
0.15
0.1
0.05
0
-0.05
-0.1
-0.15
-0.2
0
2
4
6
8
10
12
14
16

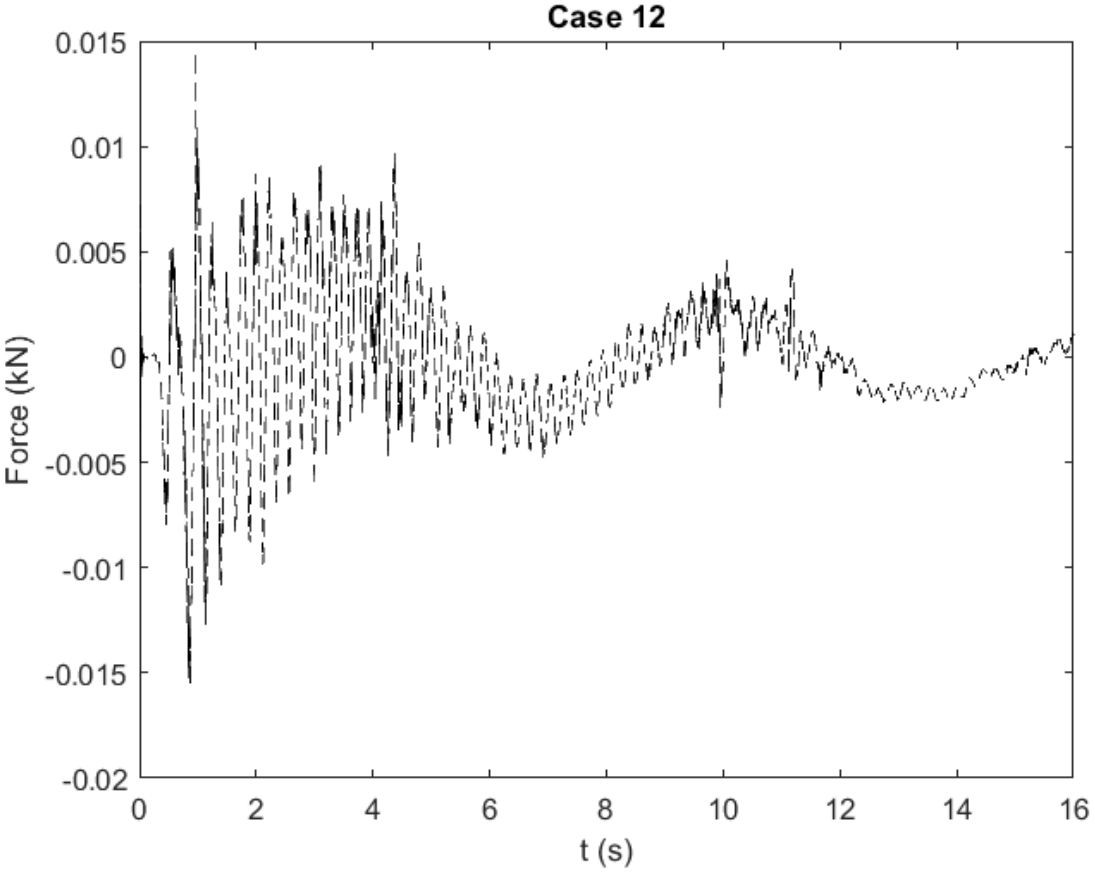
Case 12
Force (kN)
t (s)
0.015
0.01
0.005
0
-0.005
-0.01
-0.015
-0.02
0
2
4
6
8
10
12
14
16

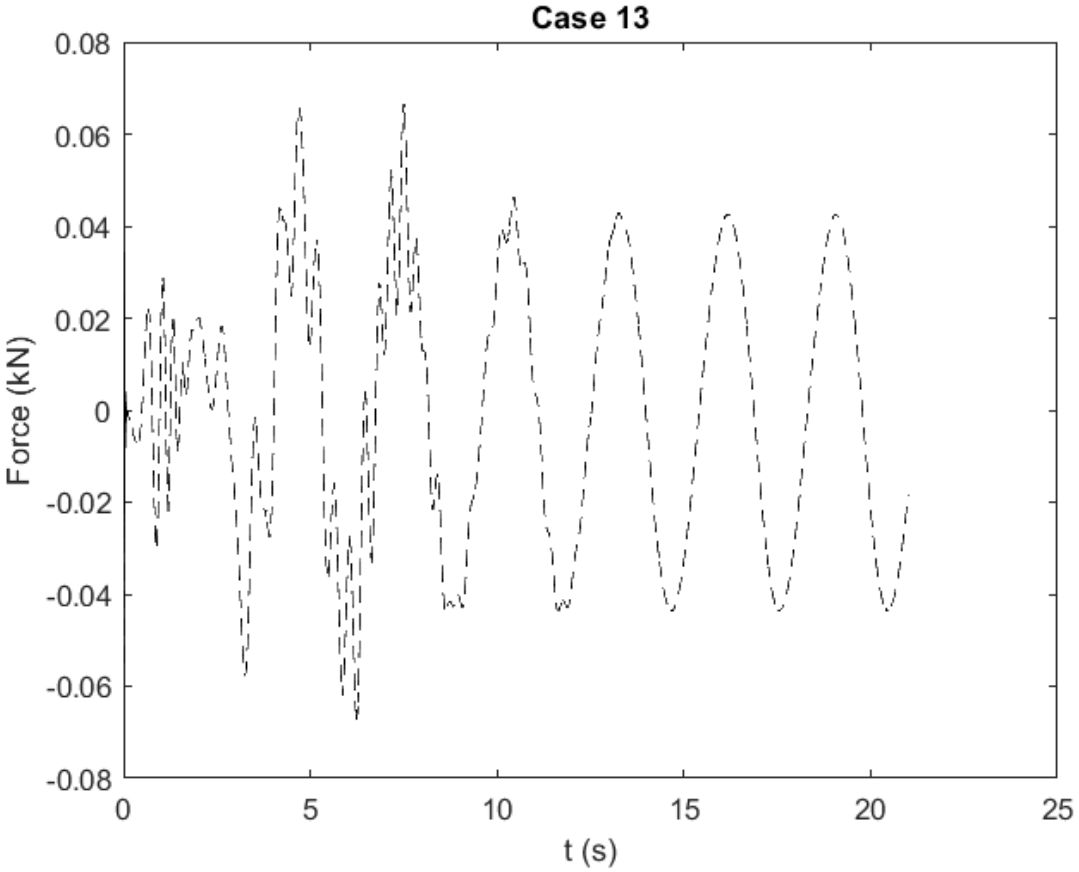
Case 13
0.08
0.06
0.04
0.02
0
-0.02
-0.04
-0.06
-0.08
Force (kN)
0
5
10
15
20
25
t (s)

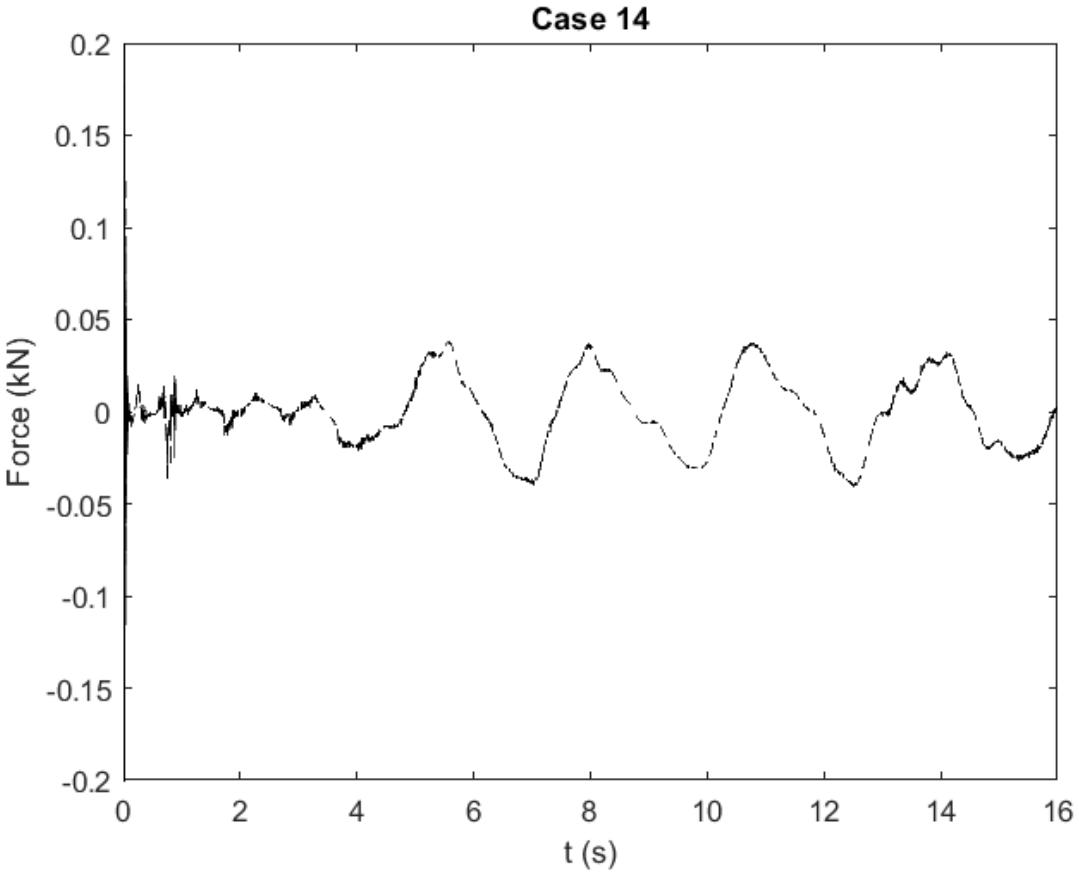
Case 14
0.2
0.15
0.1
0.05
0
-0.05
-0.1
-0.15
-0.2
Force (kN)
0
2
4
6
8
10
12
14
16
t (s)

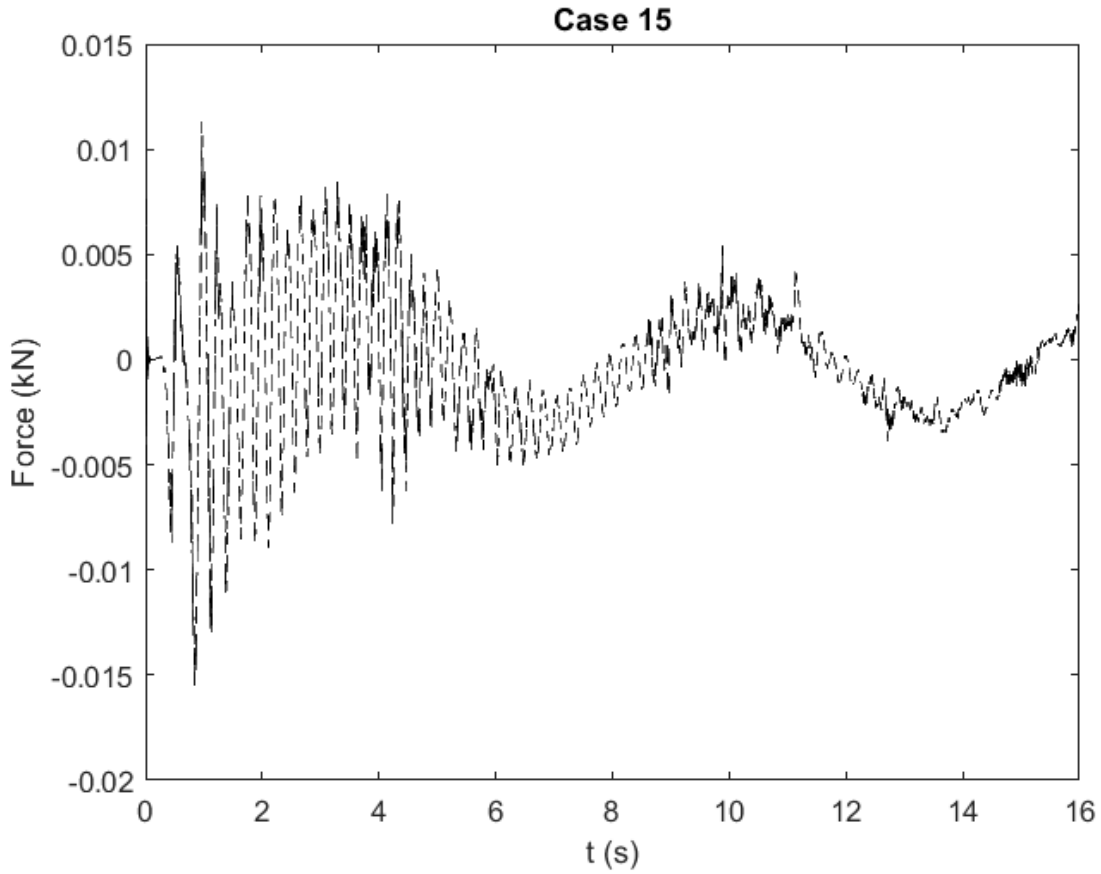

8.2. Z direction

The time series plots of forces in the z direction are plotted below. These have had the buoyancy force removed to indicate the force induced by the wave interaction.

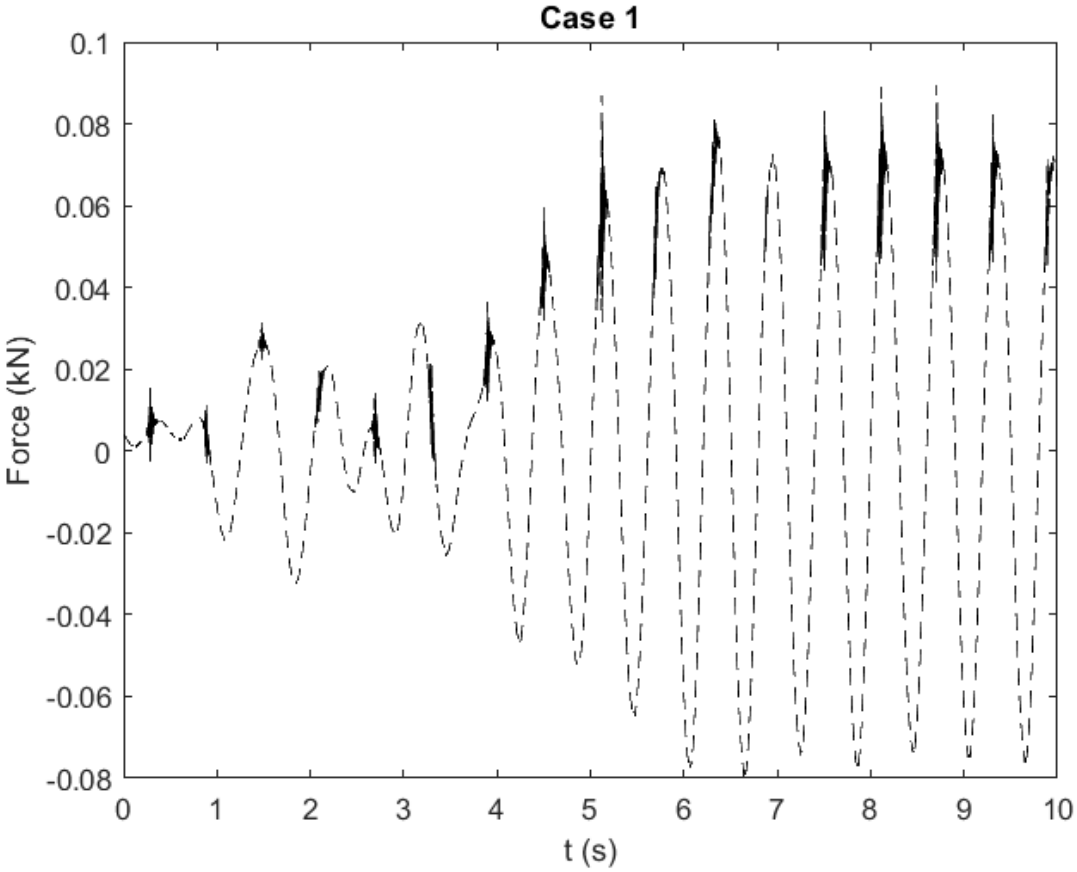
Case 1
Force (kN)
t (s)
0.1
0.08
0.06
0.04
0.02
0
-0.02
-0.04
-0.06
-0.08
0
1
2
3
4
5
6
7
8
9
10

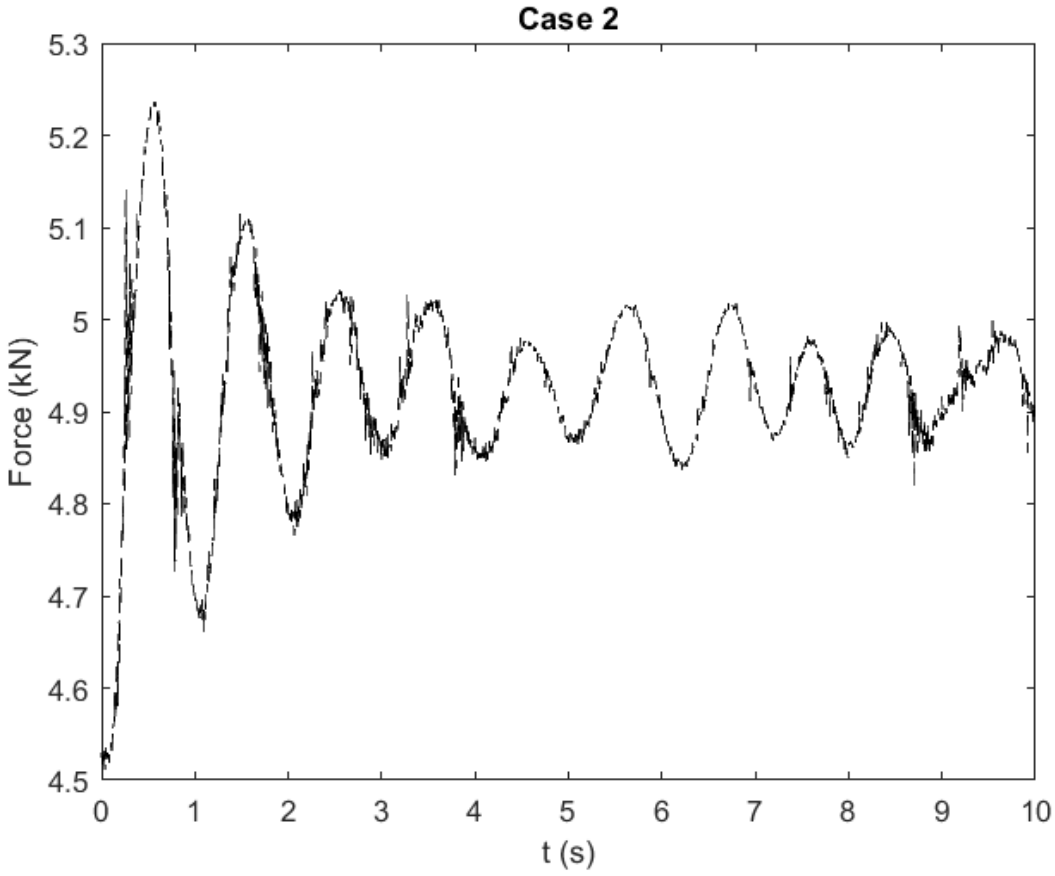
Case 2
Force (kN)
t (s)
5.3
5.2
5.1
5
4.9
4.8
4.7
4.6
4.5
0
1
2
3
4
5
6
7
8
9
10

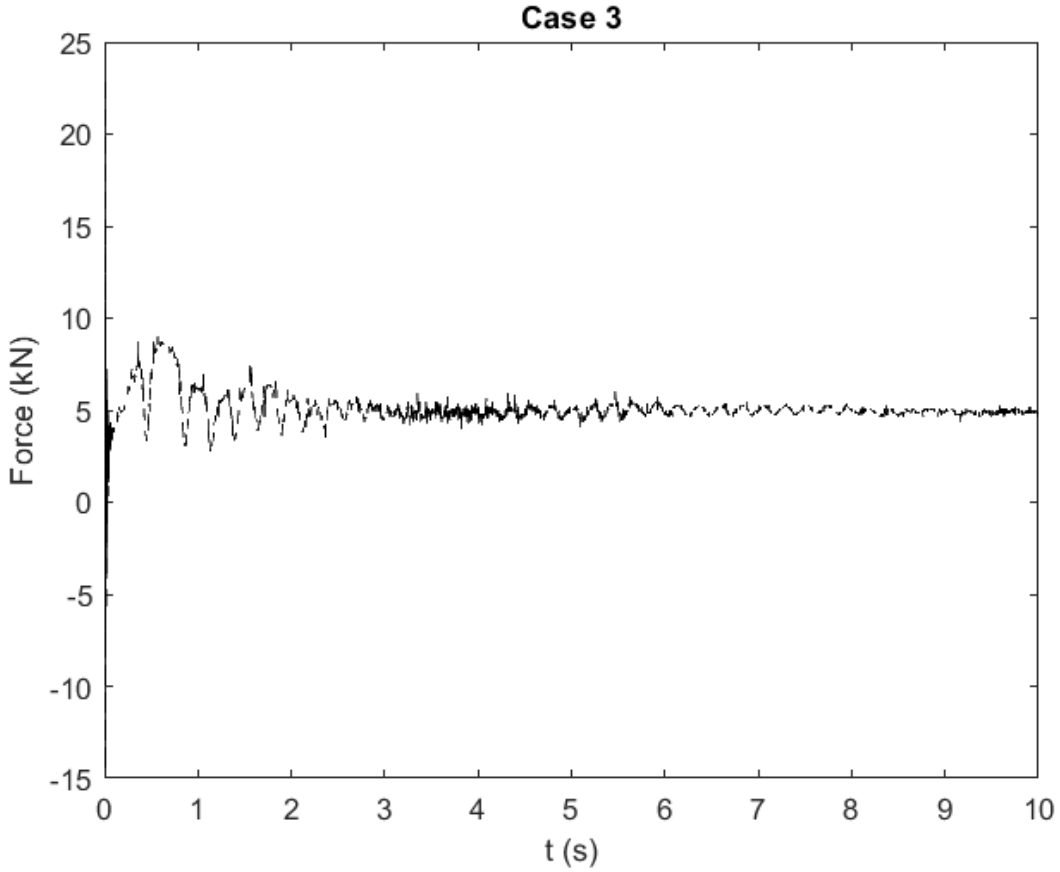
Case 3
Force (kN)
t (s)
25
20
15
10
5
0
-5
-10
-15
0
1
2
3
4
5
6
7
8
9
10

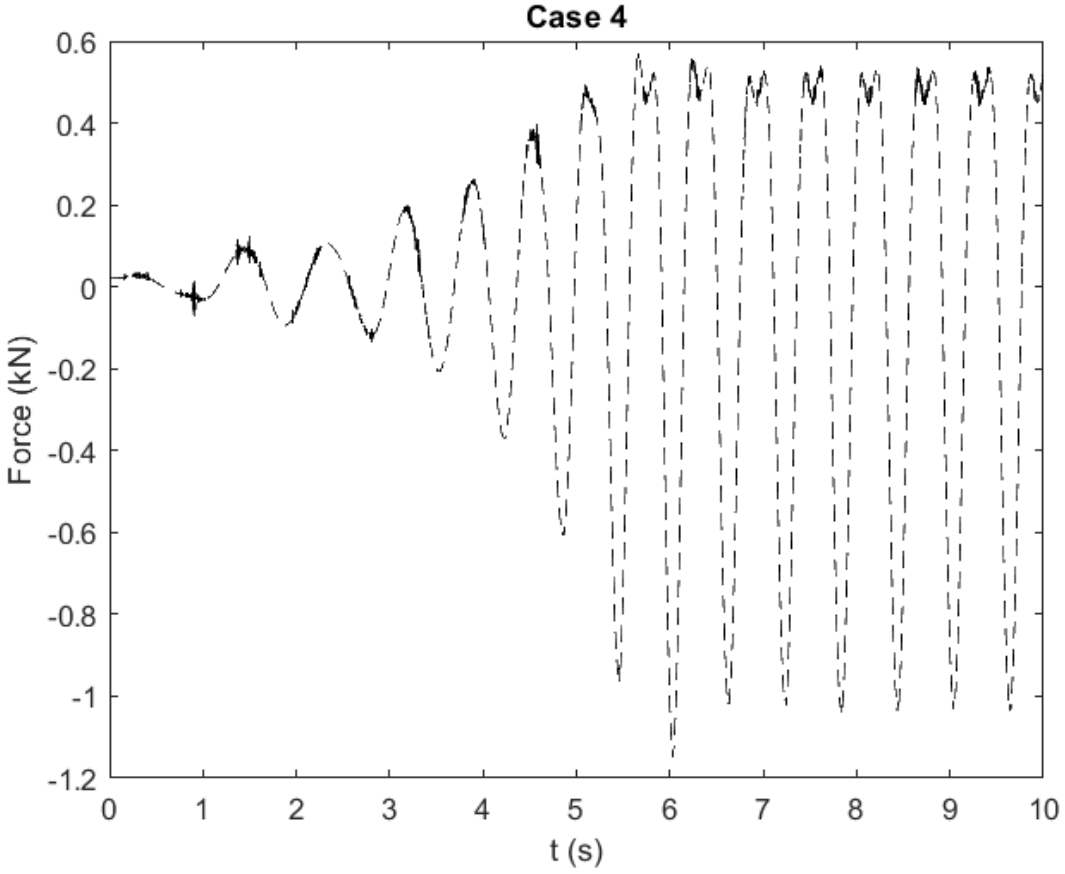
Case 4
Force (kN)
t (s)
0.6
0.4
0.2
0
-0.2
-0.4
-0.6
-0.8
-1
-1.2
0
1
2
3
4
5
6
7
8
9
10

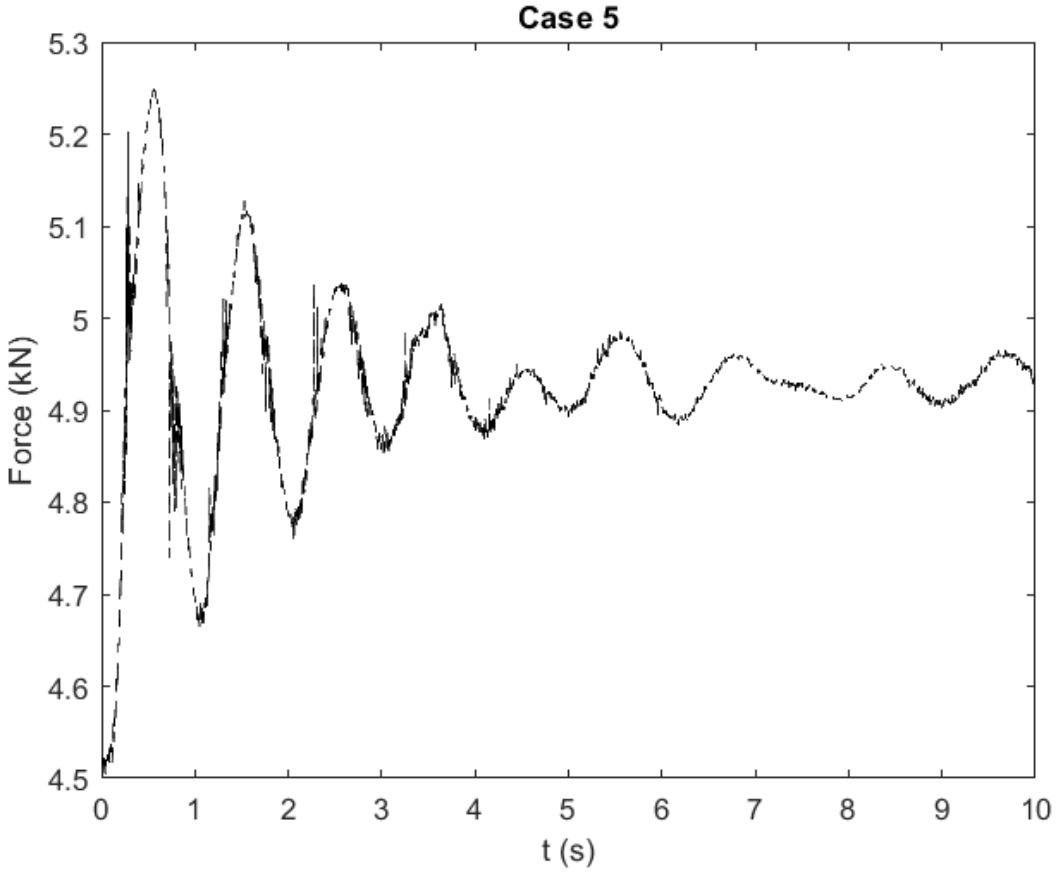
Case 5
Force (kN)
t (s)
5.3
5.2
5.1
5
4.9
4.8
4.7
4.6
4.5
0
1
2
3
4
5
6
7
8
9
10

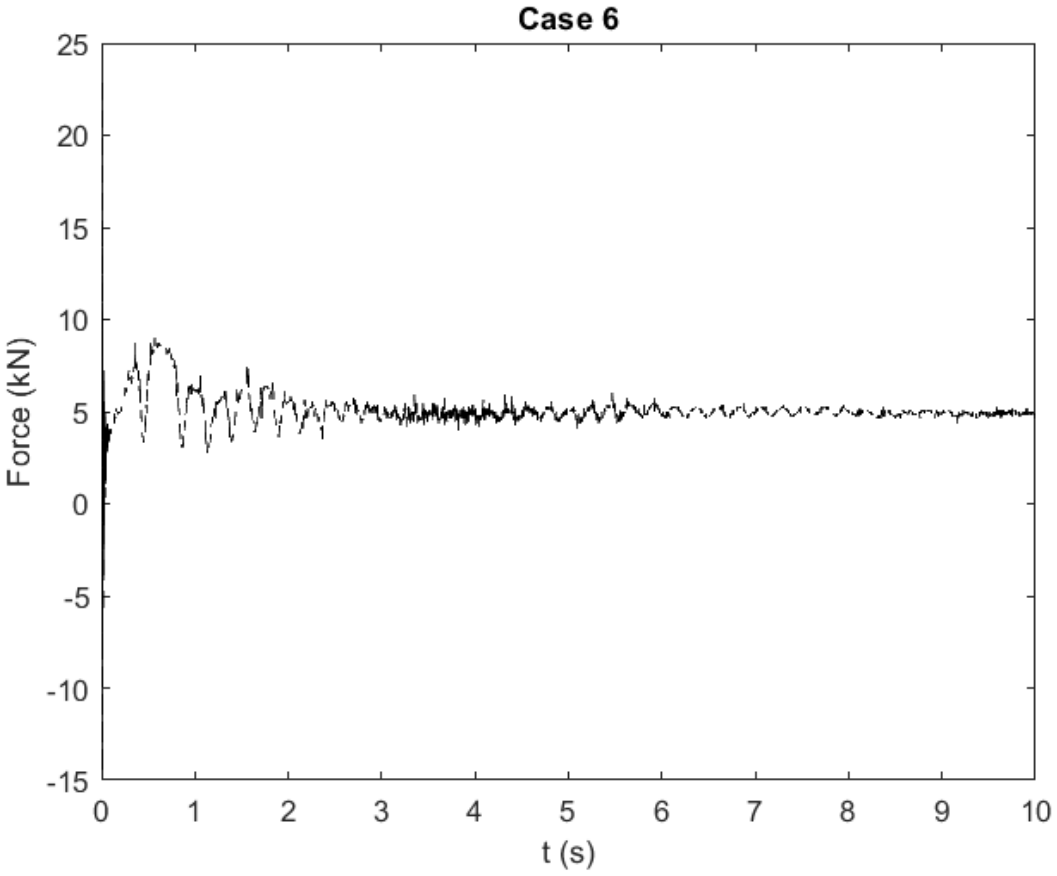
Case 6
Force (kN)
t (s)
25
20
15
10
5
0
-5
-10
-15
0
1
2
3
4
5
6
7
8
9
10

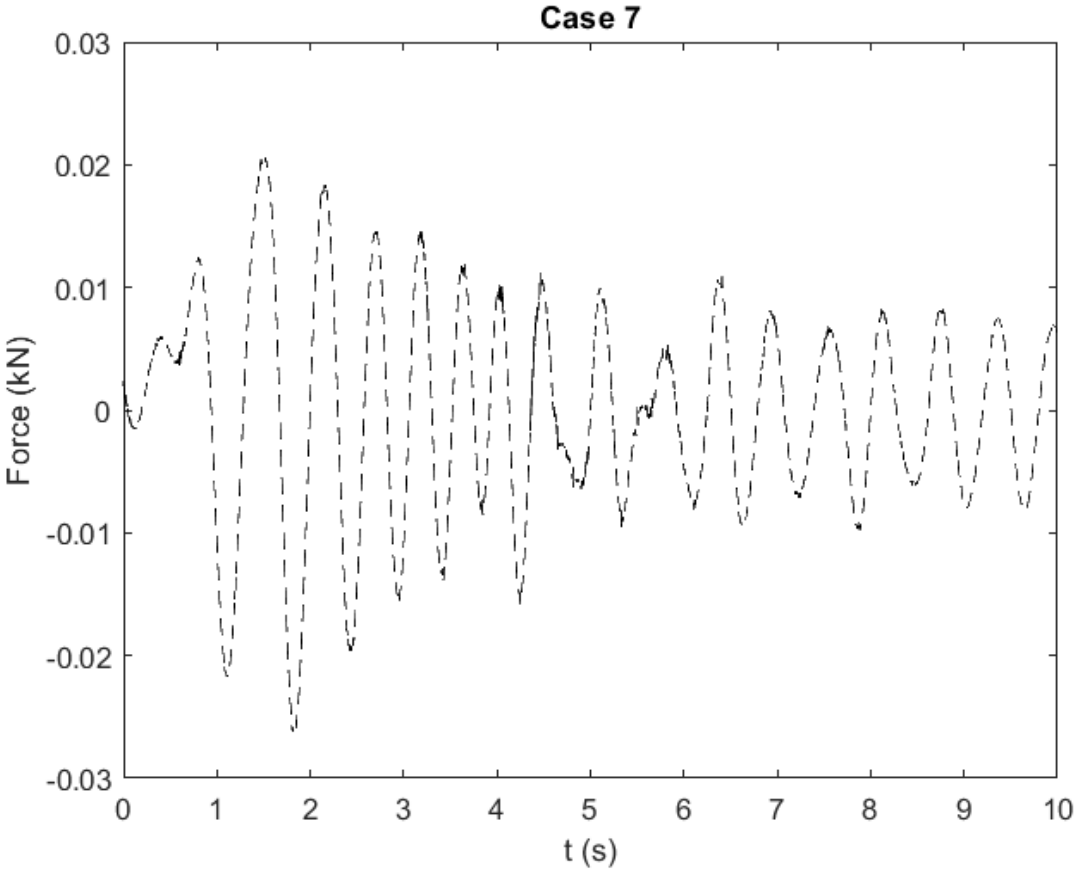
Case 7
0.03
0.02
0.01
0
-0.01
-0.02
-0.03
Force (kN)
0
1
2
3
4
5
6
7
8
9
10
t (s)

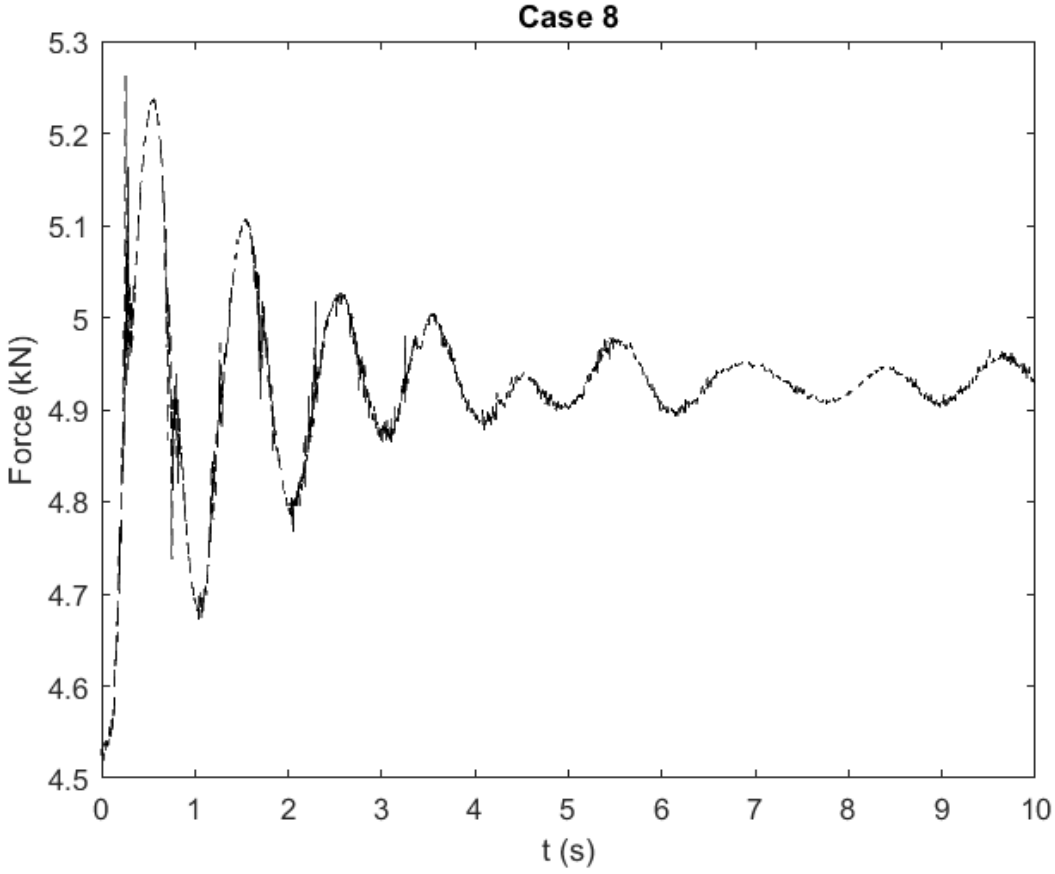
Case 8
5.3
5.2
5.1
5
4.9
4.8
4.7
4.6
4.5
Force (kN)
0
1
2
3
4
5
6
7
8
9
10
t (s)

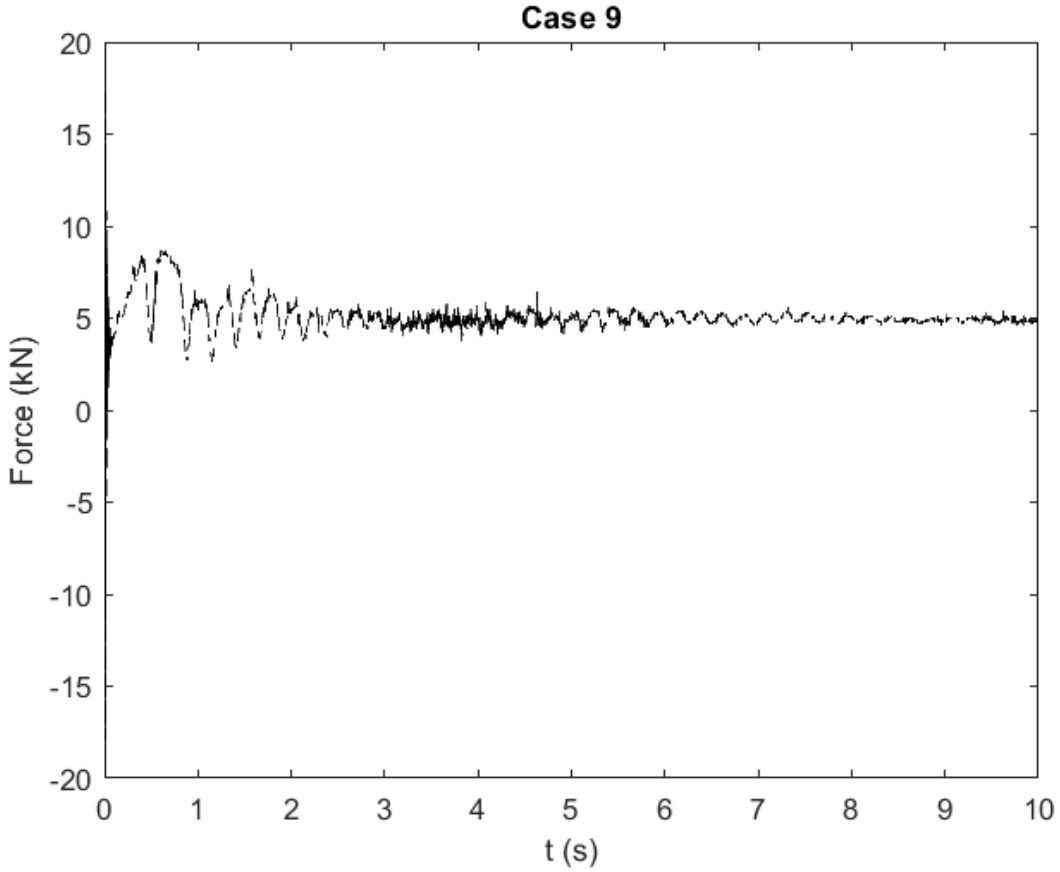
Case 9
Force (kN)
t (s)
20
15
10
5
0
-5
-10
-15
-20
0
1
2
3
4
5
6
7
8
9
10

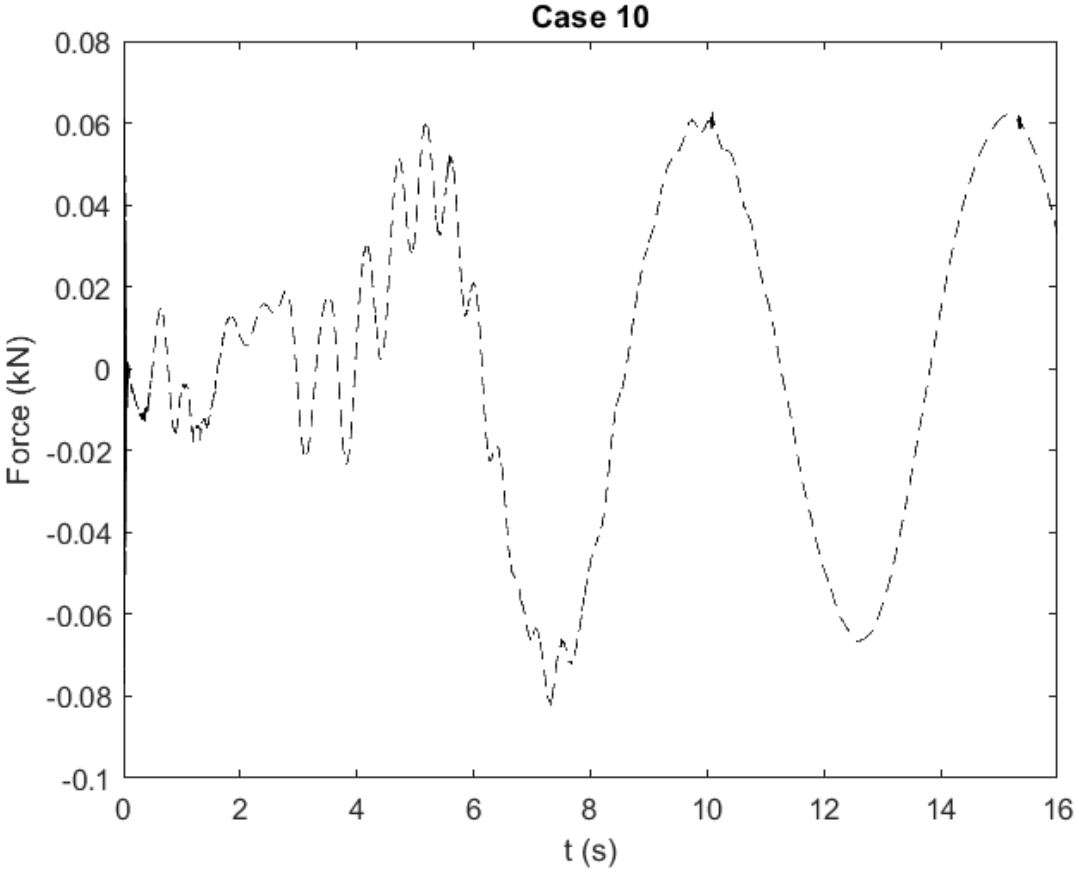
Case 10
Force (kN)
t (s)
0.08
0.06
0.04
0.02
0
-0.02
-0.04
-0.06
-0.08
-0.1
0
2
4
6
8
10
12
14
16

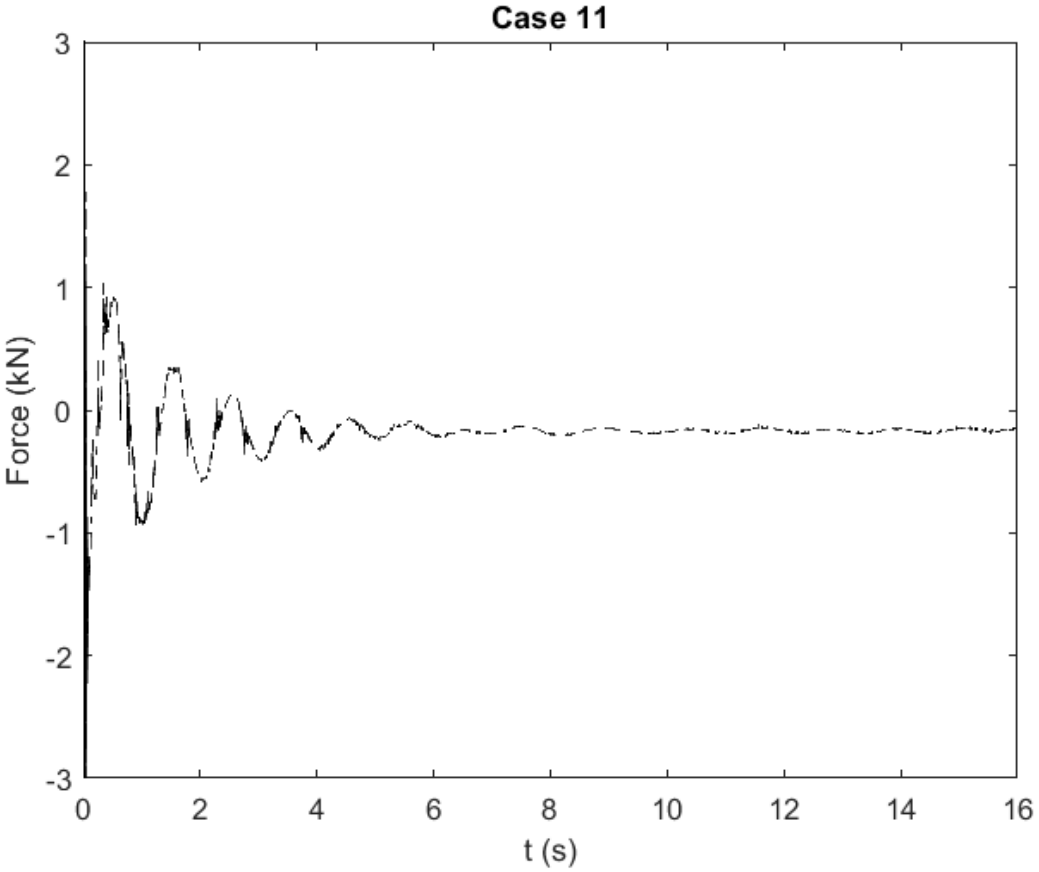
Case 11
Force (kN)
t (s)
3
2
1
0
-1
-2
-3
0
2
4
6
8
10
12
14
16

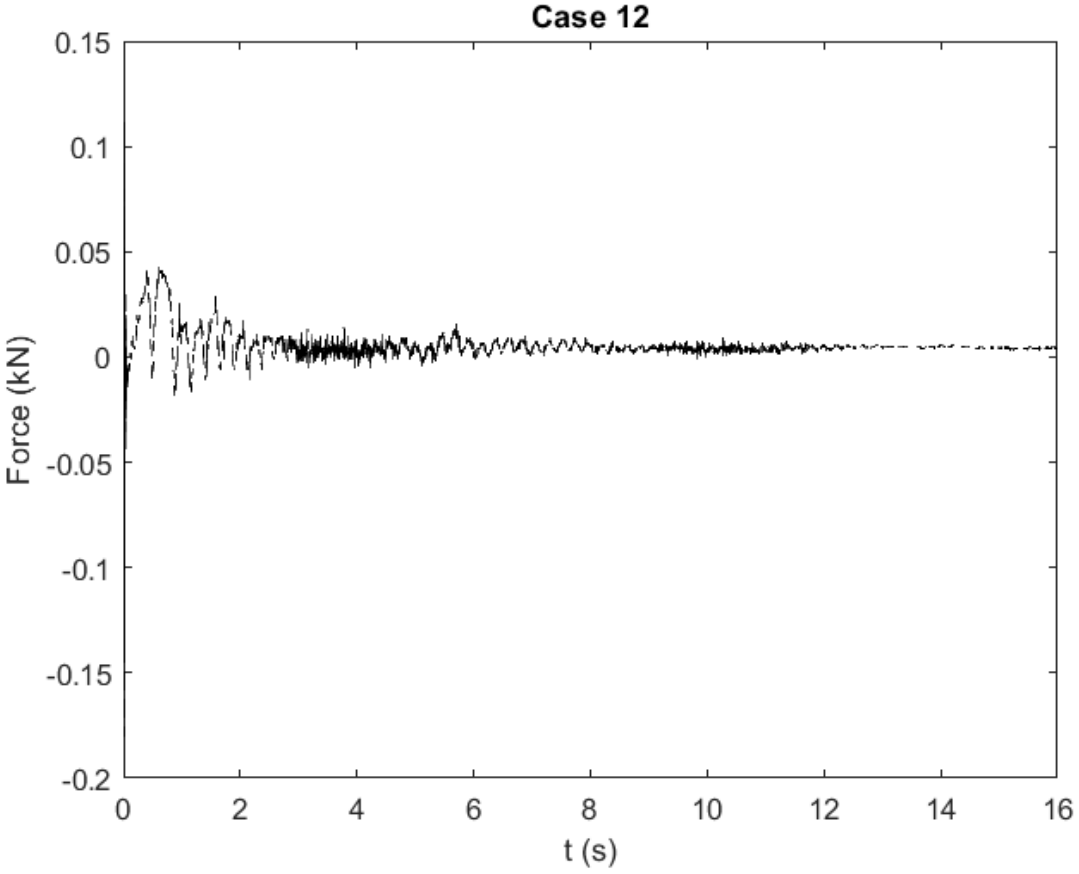
Case 12
Force (kN)
t (s)
0.15
0.1
0.05
0
-0.05
-0.1
-0.15
-0.2
0
2
4
6
8
10
12
14
16

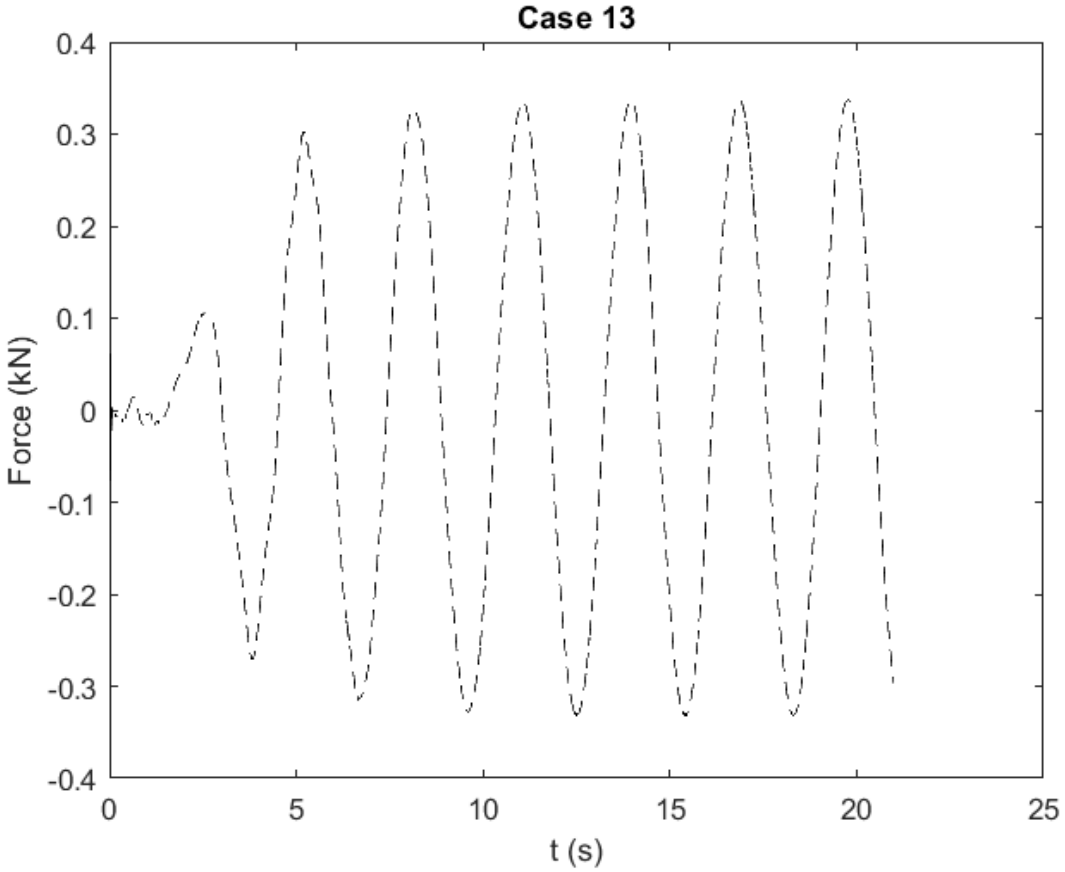
Case 13
Force (kN)
t (s)
0.4
0.3
0.2
0.1
0
-0.1
-0.2
-0.3
-0.4
0
5
10
15
20
25

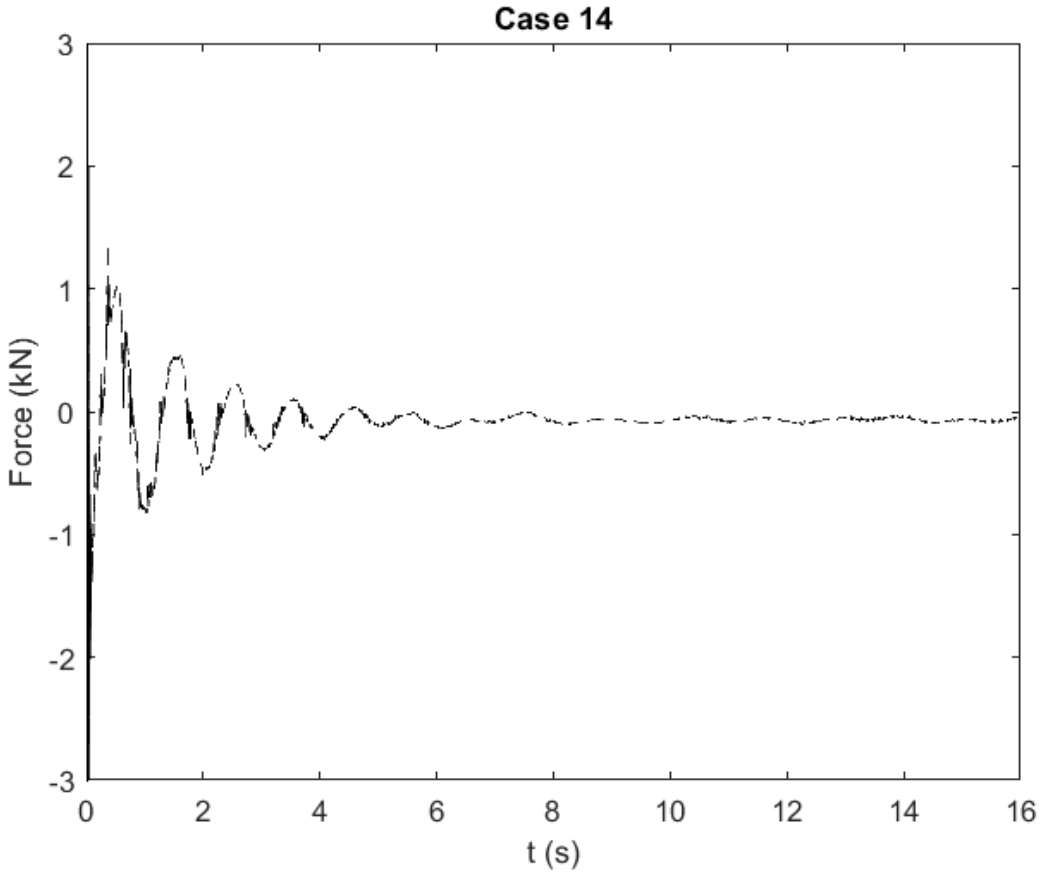
Case 14
Force (kN)
t (s)
3
2
1
0
-1
-2
-3
0
2
4
6
8
10
12
14
16

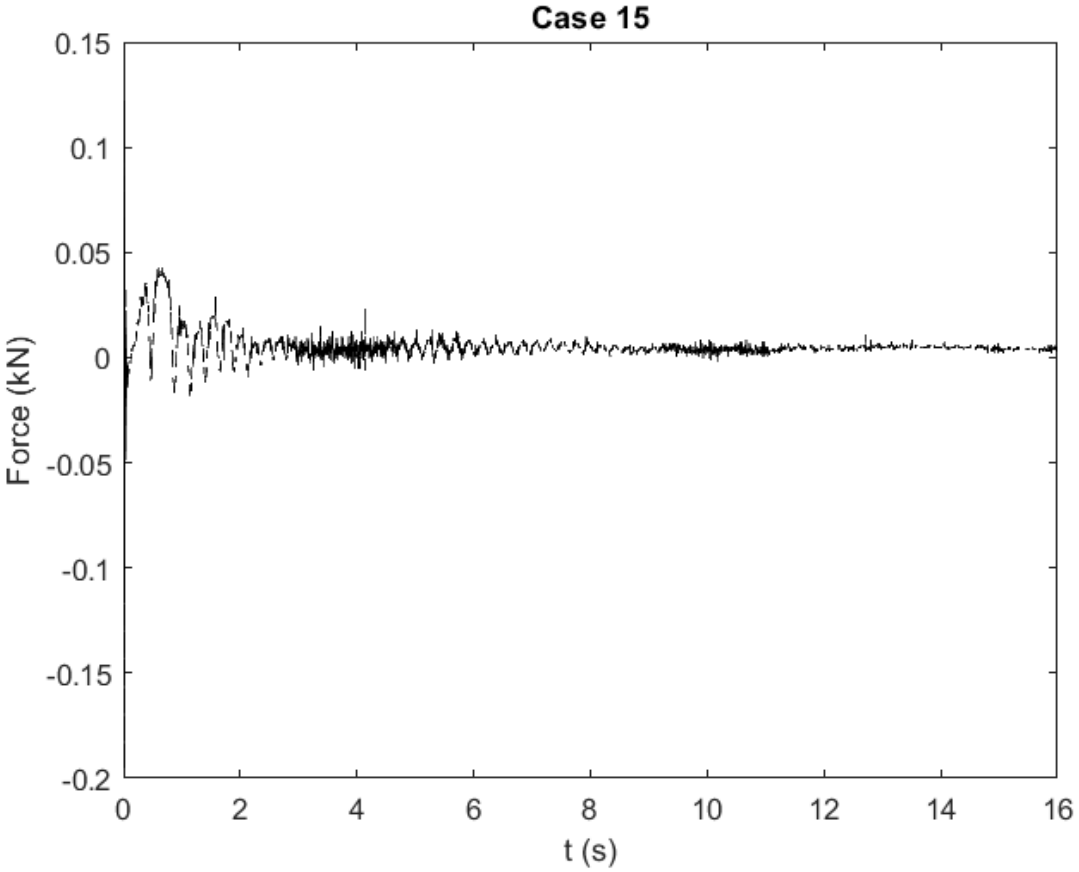
Case 15
0.15
0.1
0.05
0
-0.05
-0.1
-0.15
-0.2
Force (kN)
0
2
4
6
8
10
12
14
16
t (s)

No content after this page